Regulation of synaptic structure and function at the *Drosophila* neuromuscular junction

by

Aline D. Blunk

Dipl. Biol., Freie Universität Berlin (2006)

Submitted to the Department of Brain and Cognitive Sciences
in Partial Fulfillment of the Requirements for the Degree of

Doctorate of Philosophy in Neuroscience

at the

MASSACHUSETTS INSTITUTE OF TECHNOLOGY

September 2013

Author .....
Department of Brain and Cognitive Sciences
August, 2013

Certified by .....
Dr. J. Troy Littleton
Professor of Biology
Thesis Supervisor

Accepted by...
Dr. Matt Wilson
Sherman Fairchild Professor of Neuroscience
Director of the Graduate Program

Regulation of synaptic structure and function at the *Drosophila* neuromuscular junction

by

Aline D. Blunk

Submitted to the Department of Brain and Cognitive Sciences
on August 21, 2013
in Partial Fulfillment of the Requirements for the Degree of

Doctorate of Philosophy in Neuroscience

Abstract

Neuronal communication requires a spatially organized synaptic apparatus to coordinate neurotransmitter release from synaptic vesicles and activation of postsynaptic receptors. Structural remodeling of synaptic connections can strengthen neuronal communication and synaptic efficacy during development and behavioral plasticity. Here, I describe experimental approaches that have revealed how the actin cytoskeleton participates in transynaptic signaling to control synapse assembly. I also describe my studies on how regulation of endocytic trafficking controls synaptic growth during neuronal development.

To identify regulators of synapse assembly, I carried out a large-scale EMS mutagenesis screen of the second chromosome. From this screen I identified a mutation in actin 57B that disrupts synaptic morphology and presynaptic active zone organization. Actin 57B is one of six actin genes in *Drosophila* and is expressed in body wall muscle during larval development. The isolated allele harbors a point mutation disrupting a highly conserved amino acid present throughout the actin family. Homozygous mutant larvae show impaired alignment and spacing of presynaptic active zones. Additionally, disruption of the organization of the postsynaptic density is observed, with mislocalization of the Spectrin cytoskeleton and the PSD-homolog Disc-Large. Phallodin staining reveals a severe disruption of postsynaptic actin surrounding presynaptic boutons, with the formation of aberrant large actin swirls. Based on these results, we hypothesize that the loss of a synaptic interaction mediated by actin 57B

leads to disruption of postsynaptic cytoskeletal organization and dysregulation of signals required to organize presynaptic active zones.

Additionally, I present data that provide new insights into the mechanisms controlling synaptic growth signaling during transit through the endocytic pathway. Nervous Wreck (Nwk) is a presynaptic F-BAR/SH3 protein that regulates synaptic growth signaling in *Drosophila*. Here, I show that Nwk acts through a physical interaction with Sorting Nexin 16 (SNX16). SNX16 promotes synaptic growth signaling by activated BMP receptors, and live imaging in neurons reveals that SNX16-positive early endosomes undergo transient interactions with Nwk-containing recycling endosomes. We identify an alternative signal termination pathway in the absence of Snx16 that is controlled by ESCRT-mediated internalization of receptors into the endosomal lumen. Our results define a presynaptic trafficking pathway mediated by SNX16, NWK and the ESCRT complex that functions to control synaptic growth signaling at the interface between endosomal compartments.

Together, these experiments have expanded our understanding of the molecular mechanisms that control synaptic growth and assembly, highlighting the role of the postsynaptic actin cytoskeleton and the presynaptic endosomal trafficking pathway as key regulators.

Thesis Supervisor: Dr. J. Troy Littleton
Title: Professor of Biology

Table of Content

CHAPTER 1

Introduction

Aline Dorret Blunk[1]

[1]The Picower Institute of Learning and Memory, Department of Brain and Cognitive Sciences

Massachusetts Institute for Technology, Cambridge, MA 02139

1.1 Introduction

The brain consists of a vast network of neurons that are able to communicate and integrate internal and external signals. Information is transmitted between neurons and their target cell at a specialized region, the synapse. The presynaptic terminal contains a pool of synaptic vesicles, filled with neurotransmitter. Upon neuronal activity, these vesicles fuse in a Ca^{2+} dependent manner with specific areas of the presynaptic membrane, the active zone, and release their content into the synaptic cleft. This activates postsynaptic neurotransmitter receptor clusters directly apposed to sites of presynaptic vesicle fusion, leading to opening of ion channels and activation of downstream signaling cascades, thereby transmitting the signal to the postsynaptic target cell. Considering the importance of this precise communication, several questions arise: 1) Which molecules induce and stabilize synaptic contacts? 2) How is the subsequent formation of pre- and post-synaptic specializations regulated? 3) After synapse formation, how can connectivity strength be adjusted to mediate synaptic plasticity? This chapter will address these questions. I will give an overview of key players and introduce regulatory mechanisms involved in these processes. Although many details have been illuminated, how synapse formation and synaptic growth is regulated remains a critical question in Neuroscience and is the subject of my thesis work, using the *Drosophila* neuromuscular junction as a model system.

1.2 The *Drosophila* neuromuscular junction

Although different types of chemical synapses exist, varying for example in their neurotransmitter specificity, the principles of basic synaptic transmission are highly conserved throughout evolution. The *Drosophila* neuromuscular junction (NMJ) is a powerful model system to study synapse formation and growth. At the NMJ, a presynaptic neuron connects with specific muscle fibers in a stereotypical fashion. Whereas mammalian NMJs use acetylcholine (ACh), the *Drosophila* larval NMJ is glutamatergic in nature. It therefore has similarities to vertebrate central glutamatergic synapses and important insights into regulatory processes gained from studies of the *Drosophila* NMJ have been shown to be evolutionarily conserved (Jan and Jan, 1976). As a model system, *Drosophila* is highly amenable to techniques such as microscopy, immunohistochemistry, physiology and live imaging. Most importantly, the power of genetic manipulation is an invaluable tool, with mutant analysis and precise control of gene expression afforded by the fly model broadening our understanding of nervous system development and function.

The fly transitions through three larval stages during which the animal grows significantly in size. The area of the body wall muscles expands ~100 fold, leading to a concomitant activity-dependent expansion of the synaptic arbor and increases in active zone number to ensure appropriate synaptic output (Figure 1.1) (Stewart et al., 1996; Zito et al., 1999). Due to stereotyped muscle innervation, changes in synaptic growth and synapse formation can be easily

identified (Hoang and Chiba, 2001; Choi, 2004). Thus, the *Drosophila* larval neuromuscular junction (NMJ) serves as an excellent model system in which to decipher signaling pathways and to study regulation of synaptic structure and function.

1.3 Which molecules induce and stabilize synaptic contacts?

Before synapse formation occurs, the neuron needs to find its target cell. In both mammals and *Drosophila*, neurons extend axons that grow along a specific path, outlined by target-derived factors such as netrins and semaphorins. These diffusible molecules instruct axonal pathfinding through formation of concentration gradients, mediated by integration of attractive and repulsive cues at the growth cone. The dynamic nature of the filamentous actin (F-actin) cytoskeleton is important to achieve fast reaction to extracellular guidance cues. F-actin localizes to the leading edge of the growth cone, where activated ligand-receptor complexes can influence actin polymerization state through local actin regulators. The growth cone interacts with dendritic filopodia, or in case of the NMJ, with myopodia, and synaptogenesis is initiated (Ziv and Smith, 1996; Jontes and Smith, 2000; Ritzenthaler et al., 2000). Which molecules then induce synapse formation and stabilize synaptic contacts?

1.3.1 Synapse formation

Trans-synaptic coordination has been shown to be essential for synapse assembly, alignment and stabilization. Cell adhesion molecules (CAM) form a

connection between pre- and post-synapse that provides opportunities for transynaptic signaling (Figure 1.2). Multiple CAMs are expressed at synapses in vertebrates and invertebrates, such as members of the Immunoglobulin (Ig) superfamily, Cadherins and Neurexin-Neuroligin. These interactions help shape contact specificity and induction of synapse specialization. Below, I will concentrate on two CAM complexes that have been implicated in synaptogenesis *in vitro*: homophilic SynCAM and heterophilic Neurexin-Neuroligin. A third CAM, Fasciclin II (FasII), will be discussed in section 5 of this chapter.

SynCAM, a Ig superfamily member, has been shown to induce synapse formation *in vitro* [reviewed in (Biederer, 2006a)]. The protein is highly conserved in vertebrates, however no homolog is present in invertebrates (Biederer, 2006b). Expressed throughout the brain, SynCAM forms Ca^{2+}-independent homophilic connections via its extracellular Ig-like domains. This interaction induces synaptogenesis in co-culture assays. When overexpressed in non-neuronal cells co-cultured with hippocampal neurons, SynCAM stimulates formation of functional synapses (Biederer, 2002). However, expression of just the cytoplasmic tail of SynCAM inhibits synapse assembly. These findings highlight the possibility of CAMs mediating more than just cell-cell adhesion.

Another set of CaMs have also been shown to exhibit synaptogenic function *in vitro*. Neuroligin-Neurexin are Ca^{2+}-dependent, heterophilic CAMs present at vertebrate and invertebrate synapses. Neuroligin localizes to the postsynaptic membrane, whereas Neurexin is expressed presynaptically. Similar

to SynCAM, overexpression of Neuroligin in nonneuronal cells triggers synapse formation in contacting axons, which can be blocked by addition of soluble Neurexin (Scheiffele et al., 2000). Overexpression of β-Neurexin has been shown to induce differentiation of excitatory and inhibitory synapses (Graf et al., 2004; Nam and Chen, 2005). However, conclusions from these *in vitro* studies have been complicated by *in vivo* mutant analysis. Despite their suggested synaptogenic function, Neuroligin triple knock-out mice show no change in synapse number or ultrastructure, but instead have impaired synaptic transmission (Varoqueaux et al., 2006). It has therefore been proposed that Neuroligins stabilize transient synaptic contacts in an activity-dependent manner instead of directing initial synapse formation (Chubykin et al., 2007; Sudhof, 2008). Analysis of Neurexin-Neuroligin can be somewhat simplified by using *Drosophila* as a model system. The *Drosophila* genome contains a single Neurexin homolog and four Neuroligin homologs of which two have been characterized so far. Neurexin has been shown to be essential for synapse formation in the CNS (Zeng et al., 2007). Analysis of *nrx* null mutants shows a reduction of synapse number in the larval brain. At the NMJ, *nrx, nlg1* and *nlg2* mutants show reduction in synaptic bouton number, defects in active zone number and defective synaptic transmission (Li et al., 2007; Banovic et al., 2010; Chen et al., 2010; Sun et al., 2011; Chen et al., 2012). Interestingly, the Neurexin-Neuroligin complex also regulates apposition of presynaptic active zones and postsynaptic GluR clusters (Banovic et al., 2010; Mosca et al., 2012).

It has been proposed that Nrx interacts with the presynaptic active zone protein Syd-1, thereby defining the site of active zone assembly via binding to Liprin-α (see section below for details) (Owald et al., 2012). Postsynaptic Neuroligin regulates GluRIIA incorporation, which has been shown to be important in initial PSD assembly (Owald et al., 2012). In summary, the interaction of Neurexin and Neuroligin has been shown to provide an early template for synapse assembly and maturation at *Drosophila* synapses. Their function as initiators of synapse formation, however, remains uncertain. Indeed, NMJs can form in the absence of these CAMs in *Drosophila*, but are undergrown, suggesting redundant pathways are likely to direct early synapse formation events.

Taken together, CAMs not only confer specificity of synaptic contact but are also involved in synaptogenesis. They provide a means of trans-synaptic communication, essential for coordinated assembly of specialized pre- and postsynaptic protein networks.

1.3.2 Synapse stabilization – linking synaptogenesis and AZ assembly

To direct assembly of synaptic components, CAMs must engage downstream signaling components, of which the cytoskeleton is a target. Both microtubules (MT) and actin form pre- and post-synaptic networks, although MTs are excluded from presynaptic release sites and postsynaptic densities. Actin is the main cytoskeletal component at active zones, dendritic spine heads and at the SSR of the NMJ. However, actin has been shown to function through pathways beyond providing simple structural integrity. Instead, actin has been

shown to be essential for axon and dendrite formation, axonal pathfinding, synapse formation and maintenance [reviewed in (Dillon and Goda, 2005; Cingolani and Goda, 2008; Frost et al., 2010; Hotulainen and Hoogenraad, 2010; Svitkina et al., 2010; Dominguez and Holmes, 2011)]. As expected from its importance in a myriad of cellular processes, actin is highly conserved from yeast to humans, as well as a homolog in prokaryotes (van den Ent et al., 2001). Monomeric actin (G-actin) bound to ATP can polymerize into filaments (F-actin), consisting of two protofilaments in a right-handed double helix. F-actin is an effective ATPase, leading to weakening of the linkage between actin monomers and eventually depolymerization. A wealth of actin regulators control the transition between the two different actin states [reviewed in (Winder, 2003; Dominguez and Holmes, 2011)]. Therefore, the actin cytoskeleton is highly dynamic in nature and can quickly adapt to various intra- and extracellular cues, which is especially important for axonal pathfinding and growth cone motility.

The actin cytoskeleton is known to localize both pre- and postsynaptically. Presynaptically, it is associated with the reserve pool of synaptic vesicles, but has also been shown to form a ring around the active zone (Hirokawa et al., 1989; Morales et al., 2000; Phillips et al., 2001; Shupliakov et al., 2002; Bloom et al., 2003). Localization of actin to the active zone, and its interaction with CAMs, place actin at an ideal position to influence synapse formation. Indeed, F-actin has been shown to be essential for synaptogenesis *in vitro* (Zhang and Benson, 2001). Application of the actin depolymerization agent latrunculin A to young

hippocampal cultures leads to a reduction of synapse number. As the synapse matures and the synaptic protein network stabilizes, this dependency is lost. Similarly, presynaptic F-actin is involved in active zone assembly *in vivo* (Chia et al., 2012). Injection of latrunculin A into *C. elegans* disrupts HSN synapse formation in the early fourth larval (L4) stage, coinciding with HSN synapse formation. No effect was observed when applied in the later L4 stage. Here, the actin cytoskeleton is thought to provide a link between CAMs and active zone organizing proteins (Chia et al., 2012). The presynaptic CAM SYG-1 and its postsynaptic partner SYG-2 are essential for presynaptic F-actin assembly, as loss of either CAM impairs F-actin accumulation. The actin-binding protein Neurabin (NAB-1) acts downstream of SYG-1, providing a link between the actin cytoskeleton and regulators of active zone assembly. Synaptic stability has also been shown to dependent on the presynaptic actin cytoskeleton *in vivo*. Loss of the actin binding proteins α- and β-Spectrin using nerve-specific RNAi knock-down, results in retraction of synaptic boutons at the *Drosophila* NMJ (Pielage et al., 2005). Spectrins were first described in erythrocytes (Marchesi and Steers, 1968; Tillack et al., 1970). In this cell, they are part of a plasma membrane associated protein network, the Spectrin cytoskeleton, that confers cell stability. Both α- and β-Spectrin feature a set of Spectrin repeats that mediate the formation of antiparallel heterodimers. However, only β-Spectrin has an actin binding domain at its N-terminus. Association of Spectrin dimers into heterotetramers results in the final conformation with an actin binding domain at

either end. This enables Spectrin to cross-link short actin filaments into a lattice beneath the plasma membrane (Figure 1.3A). Loss of the Spectrin-Actin cytoskeleton impairs synaptic stability and leads to retraction of synaptic boutons (Pielage et al., 2005). Here, the postsynaptic compartment is apposed to boutons lacking presynaptic markers such as Synapsin and BRP. Together, these studies illustrate the importance of the presynaptic actin cytoskeleton for synapse formation and stabilization.

Within the postsynaptic compartment, actin not only localizes to dendritic filopodia and spines, but also forms a dense network around the bouton at *Drosophila* NMJs (Coyle et al., 2004; Ramachandran et al., 2009). Similar to spine heads, this area is devoid of microtubules (Ruiz-Canada et al., 2004). The boundary between the two regions is regulated by the interplay of the known actin regulatory protein Baz/Par-3, atypical protein kinase C (aPKC) and the phosphatase PTEN (Ramachandran et al., 2009). aPKC and Baz/Par-3 form a complex localizing to the boundary between the actin and MT regions. aPKC phosphorylates Baz/Par-3, which leads to complex dissociation and translocation of Baz/Par-3 to the actin-rich area. There phosphatase PTEN is thought to dephosphorylate Baz/Par-3, leading to retention of the actin regulator. In agreement with this model, downregulation of either of the three proteins leads to a significant reduction in the postsynaptic actin halo in *Drosophila* (Ramachandran et al., 2009). Reciprocally, an enlarged actin region is seen after overexpression of a constitutively active form of aPKC in muscle (Ruiz-Canada et

al., 2004). The actin-rich area coincides with the subsynaptic reticulum (SSR). The SSR consists of layers of membrane folds enriched in Glutamate receptor clusters. Interestingly, actin polymerization has been shown to influence receptor localization through its interaction with the Spectrin network components of the 4.1 protein family (Allison et al., 1998; Shen et al., 2000; Baines et al., 2001; Coleman et al., 2003). Indeed, Spectrin, as well as the *Drosophila* 4.1 protein Coracle (Cora), localize to the SSR at the NMJ (Chen et al., 2005; Pielage et al., 2006; Bogdanik et al., 2008). *Cora* mutants show a reduction of the GluRIIA subunit, and this is phenocopied by actin depolymerization using latrunculin A (Chen et al., 2005). Muscle-specific knock-down of Spectrin disrupts the SSR and leads to an increase in GluR cluster size (Pielage et al., 2006). Interestingly, presynaptic phenotypes are also observed upon loss of postsynaptic Spectrin. Ultrastructural and light level analysis revealed an increase in active zone size and BRP density. As the Spectrin-actin network forms a lattice underlying the postsynaptic plasma membrane, Pielage et al. propose a model that this matrix not only organizes GluR clusters, but also influences presynaptic active zone size and spacing via trans-synaptic signaling, possibly mediated by CAMs (Figure 1.3B).1

In summary, the actin cytoskeleton serves key functions in the organization of the presynaptic and postsynaptic compartment. By linking to CAMs, it influences presynaptic active zone assembly and stability.

Postsynaptically, it forms a network organizing glutamate receptor clusters and CAMs that align presynaptic active zones with postsynaptic receptor fields.

1.4 How is the formation of pre- and postsynaptic specializations regulated?

As discussed above, formation of synaptic specializations is dependent on trans-synaptic communication as pre- and post-synapse have to mature in a coordinated manner to achieve alignment of the release machinery with receptor fields, permitting successful synaptic transmission. After innervation, neurotransmitter receptors cluster opposite the presynaptic terminal. On the presynaptic side, an extensive protein network, the cytomatrix at the active zone (CAZ), has been described that ensures appropriate localization and interaction of components critical for synaptic vesicle release. This section summarizes important insights into these assembly processes.

1.4.1 Postsynaptic receptor clustering at the NMJ

At the mammalian NMJ, one of the best-studied secreted signaling molecules involved in synaptogenesis is the proteoglycan Agrin. First described in the Torpedo electric organ (Godfrey et al., 2002), Agrin has been shown to be a key organizer of the mammalian NMJ, important for maintaining synapse-specific ACh receptor (AChR) clusters. Aneural AChR clusters form in myofibers, a process called prepatterning. Interestingly this has been shown to be activity independent, occurring before muscle innervation (Lin et al., 2001). Axonal

contact, however, is required to maintain specialized postsynaptic densities (PSD) apposed to the presynaptic terminal (Flanagan-Steet, 2005; Panzer et al., 2005). Two nerve-derived molecules are needed to achieve dispersal of aneural AChR clusters and maintain synapse specific clusters. Release of ACh from the incoming nerve inhibits AChR transcription and induces endocytosis of existing aggregates. To ensure synapse specific receptor clustering, concomitant neuronal release of Agrin inhibits ACh induced receptor dispersal opposite the presynaptic terminal [reviewed in (Kummer et al., 2006)]. Mutant analysis reveals the importance of both steps of synapse initiation. Choline acetyltransferase (ChAT) mutants are unable to synthesize ACh and NMJs are therefore silent. Interestingly, muscle fibers were often innervated by multiple axons and the AChR clusters size was increased (Misgeld et al., 2002). Agrin mutant mice show transient formation of postsynaptic specializations, but without stabilization these disappear before birth (Lin et al., 2001). How is the function of Agrin mediated at the postsynapse? Activation of muscle-specific kinase (MuSK) has been known to be essential for Agrin activity. MuSK mutant mice show loss of muscle prepatterning, and Agrin release is unable to inhibit synaptic AChR dispersal (DeChiara et al., 1996; Glass et al., 1996; Lin et al., 2001; Yang et al., 2001). How Agrin and MuSK regulate AChR clustering was unknown until recently, as direct interaction between the two proteins could not be shown. Current studies indicate Agrin interacts with the transmembrane protein Lrp4, which in turn activates the tyrosine kinase MuSK (Bin Zhang et al., 2008; Kim et al., 2008;

Ghazanfari et al., 2011; Daniels, 2012). MuSK activates several downstream signaling cascades, which have been reviewed extensively and will not be further discussed (Ghazanfari et al., 2011). One signaling component, however, has been shown to be essential for MuSK-mediated AChR clustering. Rapsyn is a scaffolding protein associated with the plasma membrane, linking AChR to the cytoskeleton. Loss of Rapsyn leads to absent AChR clustering although receptor transcription is unaffected (Gautam et al., 1995). In summary, nerve-derived ACh and Agrin are essential organizers of postsynaptic specialization at the mammalian NMJ that ensure synapse-specific AChR clustering and mediate dispersal of extrasynaptic receptor aggregates.

So far, no agrin homolog has been described in *Drosophila* and the mechanisms controlling GluR clustering are not yet fully understood [reviewed in (Prokop and Meinertzhagen, 2006; Van Epps and Jin, 2006; Thomas and Sigrist, 2012)]. Glutamate receptors at the *Drosophila* NMJ are heterotetramers, consisting of GluRIID, GluRIIE, GluRIII (also named GluRIIC) and either GluRIIA or GluRIIB (Marrus, 2004; Qin, 2005). Similar to the vertebrate NMJ, active transcription of receptor subunits in muscle cells can be detected before innervation and are localized homogeneously throughout the muscle membrane (Broadie and Bate, 1993a; Currie et al., 1995). Synaptic GluR clustering, however, is dependent on synaptic activity. Upon innervation, GluR subunit expression is upregulated and clusters form opposite the presynaptic terminal (Broadie and Bate, 1993b; Saitoe et al., 1997). How presynaptic activity controls postsynaptic

GluR clustering is still unclear. Non-vesicular release of glutamate has been shown to negatively regulate receptor field size. The inverse relationship has been shown by genetically altering presynaptic glutamate levels (Featherstone et al., 2002). Interestingly, this regulatory pathway seems to be independent of synaptic vesicle release as block of vesicle exocytosis did not affect receptor field size (Featherstone et al., 2002). In addition, mutants of the single known vesicular glutamate transporter (DVGLUT) in *Drosophila* still possess postsynaptic GluR clusters (Daniels et al., 2006). Loss of DVGLUT impairs filling of vesicles with glutamate, leading to absent spontaneous release. However, application of glutamate shows no difference in evoked postsynaptic responses, indicating functional GluR fields. In summary, although no pathway similar to the agrin dependent AChR clustering at the vertebrate NMJ has been found at the *Drosophila* NMJ, presynaptic activity is necessary for proper GluR clustering. Elucidating the regulatory mechanisms is still an active field of research.

1.4.2 Presynaptic assembly of the active zone

Membrane regions specialized for synaptic vesicle exocytosis and neurotransmitter release assemble directly apposed to postsynaptic receptor fields. These two membrane regions appear as electron-dense structures in electron microscopy (EM) images. Early studies showed cone-shaped particles at the mammalian active zone (Gray, 1963; Pfenninger et al., 1972; Phillips et al., 2001). Recently published 3D reconstructions give a more detailed picture of SV localization at active zones, interconnected by a network of filaments (Siksou et

al., 2007). The electron-dense regions and projections are not exclusive to mammals, as they have been described for example in frog, fruit fly and spiders (Meinertzhagen, 1996; Harlow et al., 2001; Foelix et al., 2002).

Proteins localizing to the cytomatrix at the active zone (CAZ) likely regulate SV localization and release (Figure 1.4). Other than proteins involved in SV release itself, such as SNAREs, a set of proteins has been described that specifically reside at the active zone: RIMs (Rab3-interacting molecule), Munc13, Bassoon, Piccolo, ERC/CAST and liprin-α [reviewed in (Ziv and Garner, 2004; Dresbach et al., 2006; Fejtova and Gundelfinger, 2006; Schoch and Gundelfinger, 2006). Except for Bassoon, homologs for these proteins exist at the *Drosophila* NMJ. These proteins have been shown to bind to each other, forming a dense network, and are critically involved in vesicle exocytosis, for example during docking, priming and fusion.

The vertebrate genome contains four RIM genes, in contrast to a single gene in invertebrates. Although it was originally found as a Rab3 interacting protein, it is now known to bind many AZ proteins including liprin-α and Munc13. Mutant analyses in *C. elegans, Drosophila* and mice implicate RIM as a regulator of vesicle priming. Similarly, its interactor Munc13 also functions at this SV exocytosis step. The SNARE protein localized to the plasma membrane, syntaxin, has an open and a closed conformation. Munc13 is thought to stabilize syntaxin in its open state, thereby promoting the formation of the loose SNARE complex. This is a key step in vesicle exocytosis as SNARE complex formation and

subsequent complex zippering drives fusion of the vesicle with the plasma membrane. Bassoon and Piccolo are the largest proteins in the active zone network. Until recently they were thought be exclusively expressed in vertebrates. However, a Piccolo homolog has now been found in *Drosophila* and other invertebrates (Bruckner et al., 2012). Both Piccolo and Bassoon act as scaffolding proteins at the active zone. As an example, Bassoon is essential for photoreceptor ribbon synapses in the retina. Here, Bassoon acts as an anchor, connecting the ribbon to the plasma membrane. Upon loss of this scaffolding protein, free-floating ribbons can be observed in the cytoplasm. ERC/CAST also has scaffolding function, interacting with Piccolo and Bassoon as well as RIM and Liprin-α. Its homolog in *Drosophila,* Bruchpilot (BRP), has been shown to be a component of the T-bar and cluster Ca^{2+} channels via a direct interaction between its N terminus and the Ca^{2+} channel subunit Cacophony. Liprin-α is conserved in vertebrates and invertebrates. It binds to RIM and ERC/CAST, as well as the receptor tyrosine phosphatase LAR. In *Drosophila* and *C. elegans*, Liprin-α has been shown to be important for active zone assembly and synaptic vesicle clustering.

How is this network of proteins assembled? In vertebrates it had been proposed that specialized vesicles containing preassembled complexes could provide the building blocks for CAZ assembly (Ahmari et al., 2000; Zhai et al., 2001; Shapira et al., 2003). Dense-core vesicles with a uniform size of 80 nm have been shown at nascent synapses and contain several of the CAZ proteins

including Piccolo and Basson. They have therefore been named Piccolo-Bassoon transport vesicles (PTV). These specialized vesicles are thought to form at the Golgi as preformed active zone building blocks and then travel along axons of hippocampal neurons. Two to three PTVs are sufficient to deliver the CAZ proteins of one active zone.

The mechanisms controlling active zone assembly at the *Drosophila* NMJ are still not entirely understood. However, there is evidence of delivery of active zone components along axons [reviewed in (Goldstein et al., 2008)]. Loss of the Kinesin-3 family member of microtubule motor proteins Immaculate connections (Imac) leads to a reduction of BRP in boutons (Pack-Chung et al., 2007). Additional motor proteins and passive diffusion could suffice for correct targeting of residual BRP observed at *imac* NMJs. Regulation of transport of active zone components is crucial to prevent ectopic active zone formation in axons. Loss of the SR protein kinase SRPK79D leads to accumulation of BRP in axons (Johnson et al., 2009; Nieratschker et al., 2009). Interestingly, ultrastructural analysis shows axonal ribbon-like projections similar to the dense bodies described at synaptic active zones. These studies support the hypothesis that axonal transport of active zone components is not restricted to vertebrate synapses, but also found at the *Drosophila* NMJ.

1.5 How is connectivity strength adjusted to mediate synaptic plasticity

This section will provide an overview of how connectivity strength can be adjusted after initial synapse formation. First, I will describe underlying molecular mechanisms of activity dependent synaptic plasticity. As this depends on release of a retrograde signal to induce presynaptic changes, I will then focus on a well-known retrograde signaling cascade regulating synaptic growth, the BMP/TGF-β pathway. Additionally, I will give insights into how synaptic growth is controlled by the Wnt pathway. Lastly, regulation of these signaling cascades through endosomal trafficking is a key aspect and will be discussed below.

1.5.1 Activity- dependent synaptic plasticity

To ensure appropriate innervation of the muscle, the NMJ expands in size through addition of synaptic boutons (see section 2 of this chapter). Notably, neuronal activity in response to larval locomotion, seizure activity or hyperexcitability, has been shown to modulate this form of structural plasticity (Budnik et al., 1990; Sigrist et al., 2003; Guan et al., 2005). For instance, loss of two voltage gated K^+ channels in the *shaker (sh); ether a go-go (eag)* double mutant leads to increased neuronal activity as well as synaptic overgrowth (Budnik et al., 1990). How does synaptic activity regulate synaptic growth? Increased neuronal activity leads to postsynaptic Ca^{2+} influx through activated glutamate receptors. Synaptotagmin 4 (Syt4) functions as a postsynaptic Ca^{2+} sensor to detect activity and trigger release of retrograde signals that regulate presynaptic cAMP concentration (Yoshihara, 2005; Barber et al., 2009).

Mutations that alter presynaptic cAMP levels show synaptic growth phenotypes similar to that observed in hyperexcitability mutants (Zhong et al., 1992). Loss of the phosphodiesterase Dunce (dnc) increases cAMP levels and NMJ expansion (Zhong et al., 1992). Additional loss of the adenylate cyclase subunit Rutabaga (rut) in the *dnc* mutant background suppresses this overgrowth phenotype. Despite the fact that single *eag* or *sh* mutants show no growth phenotype, added loss of *dnc* in either mutant background reveals a significant increase in synapse expansion (Zhong et al., 1992). This argues that the activity-dependent synaptic plasticity in hyperexcitability mutants is dependent on a presynaptic cAMP pathway. Levels of the CAM FasII are reduced in these mutants, and overexpression of FasII can suppress the overgrowth phenotype (Schuster et al., 1996a). Fasciclin II (FasII) is a cell adhesion molecule localized to the pre- and the post-synaptic membrane, and is an essential regulator of synaptic growth at the NMJ. As suggested by the involvement in activity-dependent synaptic plasticity, control of synaptic growth by FasII is dependent on expression level (Schuster et al., 1996b; 1996a; Packard, 2003). Reduction of FasII to 10% of wild-type levels leads to a reduction in synaptic boutons. However reducing Fas2 levels by 50% leads to an increase in bouton number. This suggests that synapses fail to be stabilized when FasII expression is below a certain threshold. However, reduction of FasII to a threshold level is necessary to allow for bouton sprouting. Regulation of FasII expression is therefore critical to ensure appropriate synaptic growth. As mentioned, this regulation has been shown to be

dependent on neuronal activity and cAMP levels (Davis et al., 1996; Schuster et al., 1996a). Clustering of FasII at the membrane, and thereby stabilization of the synapse, is mediated by the PDZ-containing protein Disc Large (DLG) in an activity dependent manner (Thomas et al., 1997). On the other hand, reduction of FasII clustering, and thereby enhancement of synapse expansion, is mediated by Ca^{2+}/ calmodulin protein kinase II (CAMKII) dependent phosphorylation of DLG (Koh et al., 1999). In summary, increased neuronal plasticity leads to Syt4 dependent release of a retrograde signal. This increases presynaptic cAMP levels, initiating Fas2 downregulation and subsequent synaptic expansion.

Two well characterized retrograde signaling pathways at the *Drosophila* NMJ are BMP/TGF-β and Wnt. Both have been studied extensively and are known to regulate synaptic NMJ growth [reviewed in (Packard et al., 2003; Marqués, 2005)]. Both pathways also control a wide variety of physiological events in many other tissue types, regulating cell patterning and proliferation throughout development. Interestingly, endocytic trafficking has been shown to regulate synaptic growth signaling by facilitating binding of activated receptor-ligand complexes to downstream signaling components, recycling of receptors back to the plasma membrane and downregulation of signaling through lysosomal degradation. Below I provide an overview of both TGF-β and Wnt signaling, as well as endocytic trafficking.

1.5.2 BMP signaling

The TGF-β signaling pathway has also been found to be important in synaptic growth (Figure 1.5). Mutations in the ligand, receptor or downstream second messengers of the TGF-β pathway show a reduction in bouton size and aberrant bouton morphology (Aberle et al., 2002; MCCABE, 2003). The TGF-β ligand superfamily consists of TGF-β, the bone morphogenic protein (BMP) and the Activin subfamilies. In *Drosophila* there are several type I and II receptors (Thickveins, Tkv; Saxophone, Sax; Baboon, Babo; Punt, Put; Wishful Thinking, Wit), as well as two regulatory (Mothers against Dpp, Mad; dSmad2), one common (Medea, Med) and one inhibitory Smad (daughters against Dpp, Dad), which regulate the signaling cascade. Tkv, Sax and Wit are localized presynaptically and mediate retrograde BMP signaling, whereas the postsynaptic receptors Babo and Put mediate anterograde Activin signaling upstream of the presynaptic cascade (Ellis et al., 2010). The ligand, glass bottom boat (Gbb), binds to presynaptic Wit/Tkv/Sax receptors, leading to phosphorylation and activation of the type I receptor. The activated ligand-receptor-complex is internalized into the synaptic bouton, forming an early endosomal (EE) compartment. SARA (Smad Anchor for Receptor Activation) serves as a binding site for the receptor-regulated Smad Mad, which is activated through phosphorylation by the type I receptor (Di Guglielmo et al., 2003). The active R-Smad binds to a common Smad or Co-Smad, and the complex enters the nucleus where it serves as a transcriptional activator. Prolonged signaling due to

impaired downregulation leads to excessive synaptic growth. Spinster is a transmembrane protein of the lysosomal compartment and required for terminating Gbb signaling, as *spin* mutants show synaptic overgrowth and elevated levels of phosphorylated SMAD (Sweeney and Davis, 2002). Mutation of the inhibitory Smad, Daughters against Decapentaplegic (Dad), shows a similar overgrowth phenotype (Sweeney and Davis, 2002). These and other studies have placed the BMP pathway as a central signaling module for retrograde regulation of synaptic growth at the *Drosophila* NMJ.

1.5.3 Wnt signaling

The *Drosophila* Wnt protein Wingless (Wg) has been shown to be important for coordinated pre- and postsynaptic growth (Figure 1.6) (Packard et al., 2002). *Wg* mutants show a decrease in bouton number at the neuromuscular junction in proportion to muscle size, as well as abnormalities in the morphology of the pre- and post-synaptic compartment. Upon synaptic activation, the ligand Wg is secreted by the presynaptic terminal and binds to dFrizzled receptors from the Frizzled receptor family (Packard et al., 2002; Ataman, 2008). Interestingly, dFrizzled has been localized pre- as well as post-synaptically, and secreted Wg can activate signaling cascades on both sides of the synapse [reviewed in (Korkut and Budnik, 2009)].

Presynaptically, a variant of the canonical Wg signaling pathway has been suggested, as the *Drosophila* homolog of beta-catenin, Armadillo, has not been detected in synaptic boutons (Miech et al., 2008). Wg binding to presynaptic

dFrizzled is thought to activate the phosphoprotein Dishevelled, which in turn inhibits the *Drosophila* homolog of glycogen synthase kinase 3β (Gsk3β), Shaggy (Sgg). Sgg phosphorylates presynaptic Futsch, a protein important for microtubule loop stabilization in boutons and synaptic growth (Hummel et al., 2000; Roos et al., 2000; Franco, 2004). Presynaptic expression of dominant-negative Sgg shows an increase in microtubule loops and bouton number. In *Wg* mutants, on the other hand, a decrease in microtubule loops has been described, as well as an increase in unbundled microtubules (Packard et al., 2002). Unlike the canonical Wg pathway, this variant is therefore transcription independent and regulates synaptic growth locally through changes to the microtubule cytoskeleton.

Postsynaptically, a novel signaling cascade downstream of dFrizzled has been described (Packard et al., 2002; Mathew et al., 2005; Ataman et al., 2006). The activated receptor is internalized and trafficked to the nucleus along microtubules. Interestingly, the C-terminal of dFrizzled is then cleaved and imported into the nucleus where is activates transcription (Mathew et al., 2005). Translocation and import into the nucleus has been shown to be dependent on the PDZ protein dGRIP (Ataman et al., 2006). Together with the BMP pathway, Wnt signaling provides a primary mechanism for regulating structural plasticity at the *Drosophila* NMJ.

1.5.4 Endocytic regulation of growth signals

Endocytic processes are highly important for synaptic growth pathways (Figure 1.7). After binding of the ligand to the receptor, activated ligand/ receptor complexes undergo clathrin- and dynamin-mediated endocytosis. Subsequently the newly formed vesicle can enter a complex system of endosomal compartments, for which Rab GTPases serve as recognition molecules by recruiting proteins that form an endosome-specific scaffold. Rab5, for example, forms a scaffold localized at the early endosome, recruiting phosphatidylinositol-3 (PI3)-kinases. This leads to an enrichment of phosphatidylinositol-3-phosphate (PI3P) in this compartment, which serves as docking site for FYVE domain containing proteins such as the Rab5 effector protein EEA1. Both Rab5 and EEA1 are involved in targeting and fusion of newly formed vesicles with the early endosome after internalization. From the early endosome, receptor/ligand complexes can be trafficked in an active signaling state through early and late endosomal compartments to the lysosome where they are degraded (Di Fiore and De Camilli, 2001; McPherson et al., 2001). However, it has also been proposed that multivesicular bodies (MVB) containing several signaling endosomes with their corresponding second messengers function as a means for transportation to the cell body (Weible and Hendry, 2003). This would supply a snapshot of the active signaling cascades in the synapse to the nucleus and lead to activation of responsive genes even over long distances.

For Wg signaling, it has been shown that uptake of the activated receptor and endosomal transport are essential for signaling (Seto, 2006). Knockdown of dynamin or Rab5 respectively, results in reduced Wg signaling. Additionally, endosomal trafficking has been shown to regulate both Wg and TGF-β signaling through the action of Nervous Wreck (Nwk), a conserved protein belonging to the pombe Cdc15 homology (PCH) protein family. Members of this family, such as CIP4 and FBP17, share an extended FCH (EFC) domain (also called the F-BAR domain) consisting of a FCH and a coiled-coil domain. This domain has been shown to be involved in membrane invagination and tubulation (Itoh et al., 2005; Tsujita, 2006). PCH family members are also able to bind to the Arp2/3 complex activator Wasp and the GTPase dynamin via their SH3 domain(s), thereby linking membrane traffic to the actin cytoskeleton. This link can provide movement either based on unconventional myosin motor proteins (Wu et al., 2000) or on so-called actin comet tails, which use the force generated by growth of actin filaments to propel structures through the cytoplasm (Merrifield et al., 1999). Considering the connection of endosomal trafficking and synaptic growth, it is very interesting that *nwk* mutants show overgrowth of the neuromuscular junction, as well as formation of small satellite boutons that hyperproliferate off of terminal synaptic boutons (Coyle et al., 2004). Double mutants in *wasp* and *nwk* show an even more pronounced increase in bouton size, although available *wasp* mutants retain some residual protein. This result suggests that Wasp and Nwk interact to regulate synaptic growth and that Nwk is required for Wasp function. In fact, Nwk

acts as an activator of Wasp in *in vitro* actin polymerization assays (Rodal et al., 2008). The *nwk* mutant phenotype is not due to an impairment of the endocytic invagination process in general, since mutants exhibit normal endocytosis of synaptic vesicles (Coyle et al., 2004). In contrast, the observed overgrowth is dependent on Wg and TGF-β signaling (O'Connor-Giles et al., 2008; Rodal et al., 2008). As mentioned above, *wit* and *gbb* single mutants exhibit synaptic undergrowth. Loss of either wit or gbb in the sensitized *nwk* mutant background suppresses the *nwk* overgrowth phenotype, suggesting Nwk constrains TGF- β mediated synaptic growth.

In this thesis, I will characterize a binding partner of Nwk, Sorting Nexin 16 (SNX16), which was discovered in a yeast-two-hybrid screen using a Nwk fragment as bait. Interestingly, binding of PCH family members to sorting nexins may be conserved, since it also has been shown that FBP17 binds to SNX2 (Fuchs et al., 2001). The sorting nexin protein family (SNXs) has been shown to be involved in endosomal trafficking (Worby and Dixon, 2002; Carlton and Cullen, 2005; Carlton et al., 2005; Seet and Hong, 2006). Members of this family are characterized by a Phox (PX) domain, which is a phosphoinositol (PI)-binding module (Ellson et al., 2002; Seet and Hong, 2006). It has been shown that the PX domain preferentially binds to PI-(3)-triphosphate (PI3P) but individual members of this family can also bind to other PIs, thereby targeting the corresponding protein to different endosomal compartments. The secondary structure, consisting of three β-sheets and three α-helices forming a PI-binding

pocket, is well conserved although the primary sequences show substantial differences between PX domain containing proteins. SNXs can either be grouped according to their domain structure or to their primary sequence similarity, summarized in the phylogenetic tree (Seet and Hong, 2006). The first identified SNX, SNX1, was found to interact with the cytoplasmic domain of the epidermal growth factor receptor (EGFR) in a yeast-two-hybrid assay and to regulate its degradation by sorting into lysosomes (Kurten et al., 1996). An interaction with receptor serine/threonine kinases was also characterized, when SNX6 was shown to bind to members of the TGF-β receptor family (Parks, 2001). How SNX16 and Nwk regulate trafficking and degradation of signaling receptors through the endosomal system in synaptic boutons will be discussed in Chapter 3 of this thesis.

A

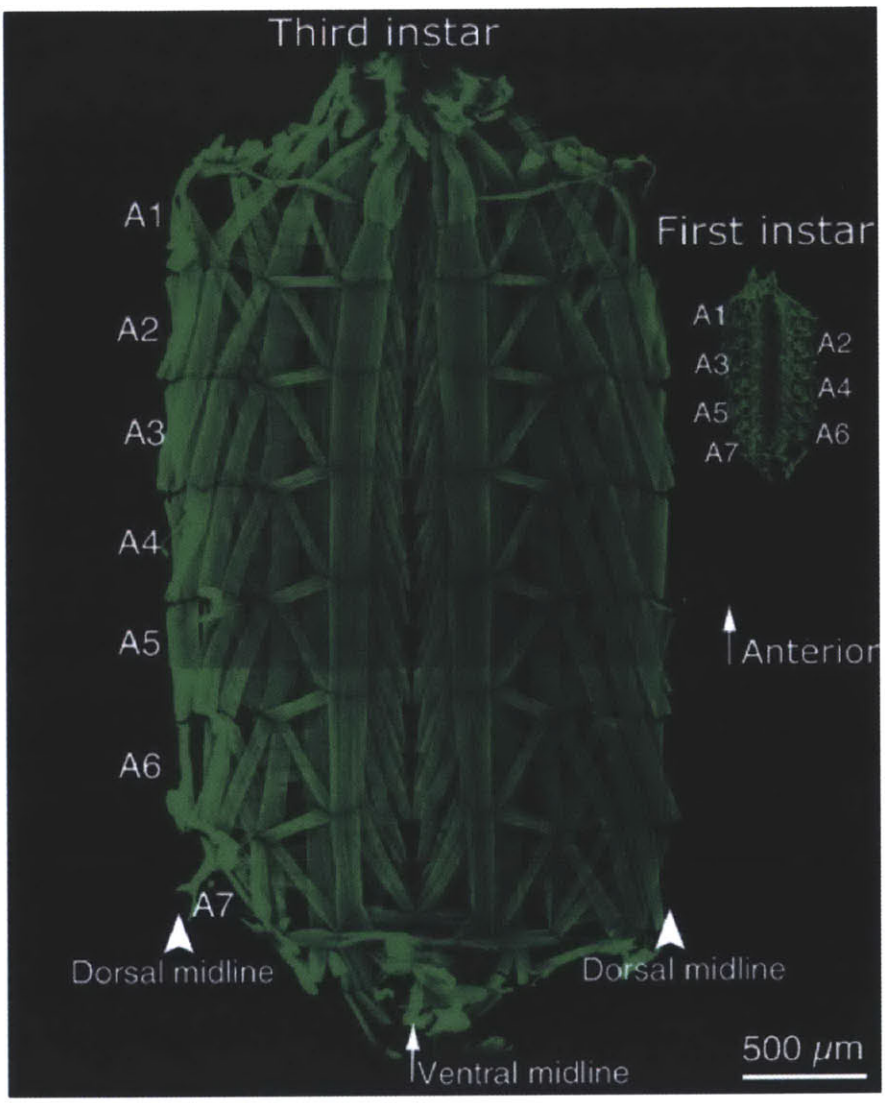

B

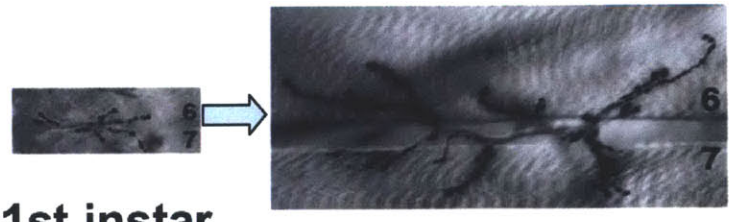

1st instar

3rd instar

Figure 1.1: *During the three larval stages, Drosophila larvae grow significantly in size.*

A, Dissections of a first and third instar larva. Staining with green FITC-Phalloidin labels actin, revealing the body wall muscles. Comparison of the two larval stages highlights the significant increase in muscle size. **B**, Concomitant with the growing muscle, activity- dependent expansion of the larval NMJ ensures appropriate muscle depolarization. [Adapted from (Budnik and Ruiz-Canada, 2006). Reproduced with permission from Elsevier]

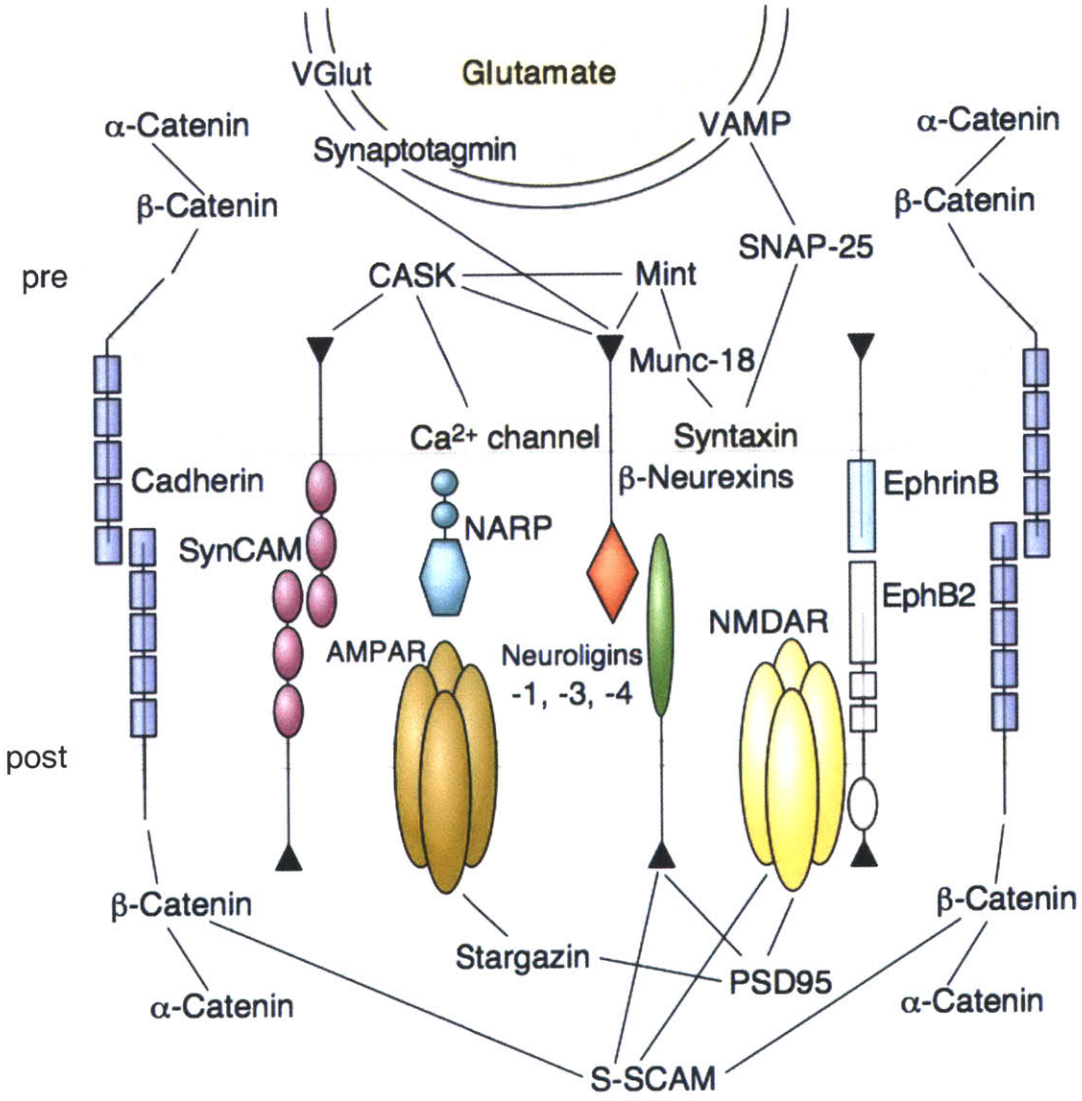
VGlut
Glutamate
α-Catenin
Synaptotagmin
VAMP
α-Catenin
β-Catenin
β-Catenin
SNAP-25
pre
CASK
Mint
Munc-18
Ca2+ channel
Syntaxin
β-Neurexins
Cadherin
EphrinB
NARP
SynCAM
EphB2
NMDAR
AMPAR
Neuroligins
-1, -3, -4
post
β-Catenin
β-Catenin
Stargazin
PSD95
α-Catenin
α-Catenin
S-SCAM

Figure 1.2: *Cell adhesion molecules at the glutamatergic synapse.*

Homo- and heterophilic cell adhesion molecules (CAMs) mediate the connection between the presynaptic terminal (pre) and the postsynapse (post). Notably, these are not just passive connections, but interaction of CAM intracellular domains with downstream binding partners enables trans-synaptic communication. SynCAM and the Neurexin-Neuroligin have been shown to induce synapse formation *in vitro* and are discussed in more detail in section 1.3.1. [Adapted from (Craig et al., 2006). Reproduced with permission from Elsevier]

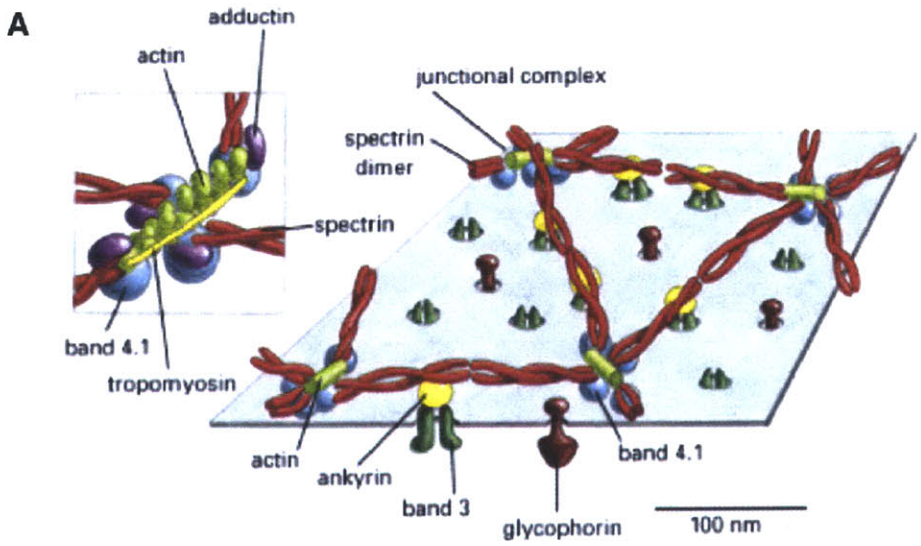
A
adductin
actin
junctional complex
spectrin
dimer
spectrin
band 4.1
tropomyosin
actin
ankyrin
band 3
glycophorin
band 4.1
100 nm

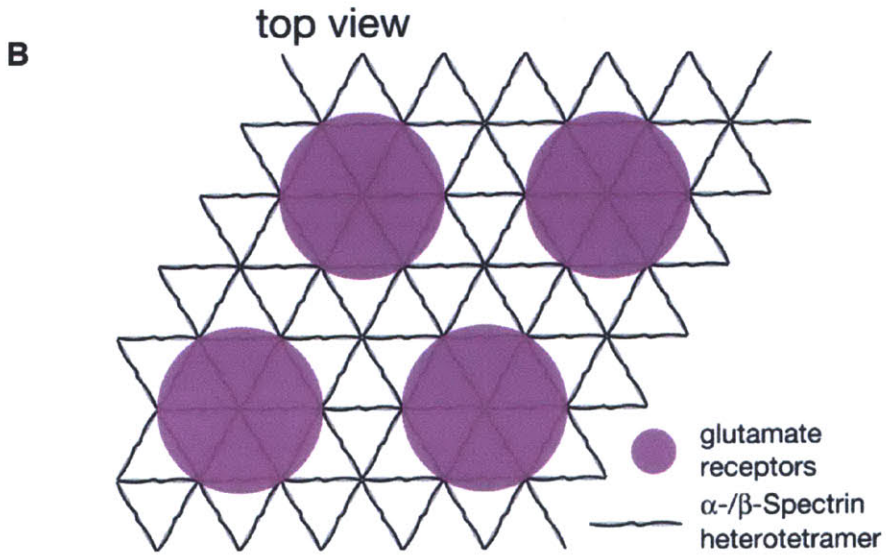
B
top view
glutamate
receptors
α-/β-Spectrin
heterotetramer

Figure 1.3: *The postsynaptic actin- spectrin network could provide a guide for GluR cluster spacing.*

A, Spectrin forms heterotetramers that can cross-link short, Adducin- capped actin filaments, forming a regular lattice. This network is linked to the plasma membrane via Ankyrin, Band 4.1 proteins as well as phospholipid interaction of α-Spectrin. [Adapted from (Alberts et al., 2002)] **B**, Actin and Spectrin form a hexagonal network that has been proposed to provide a guide for postsynaptic GluR cluster spacing at the NMJ of *Drosophila*. [Adapted from (Pielage et al., 2006)]

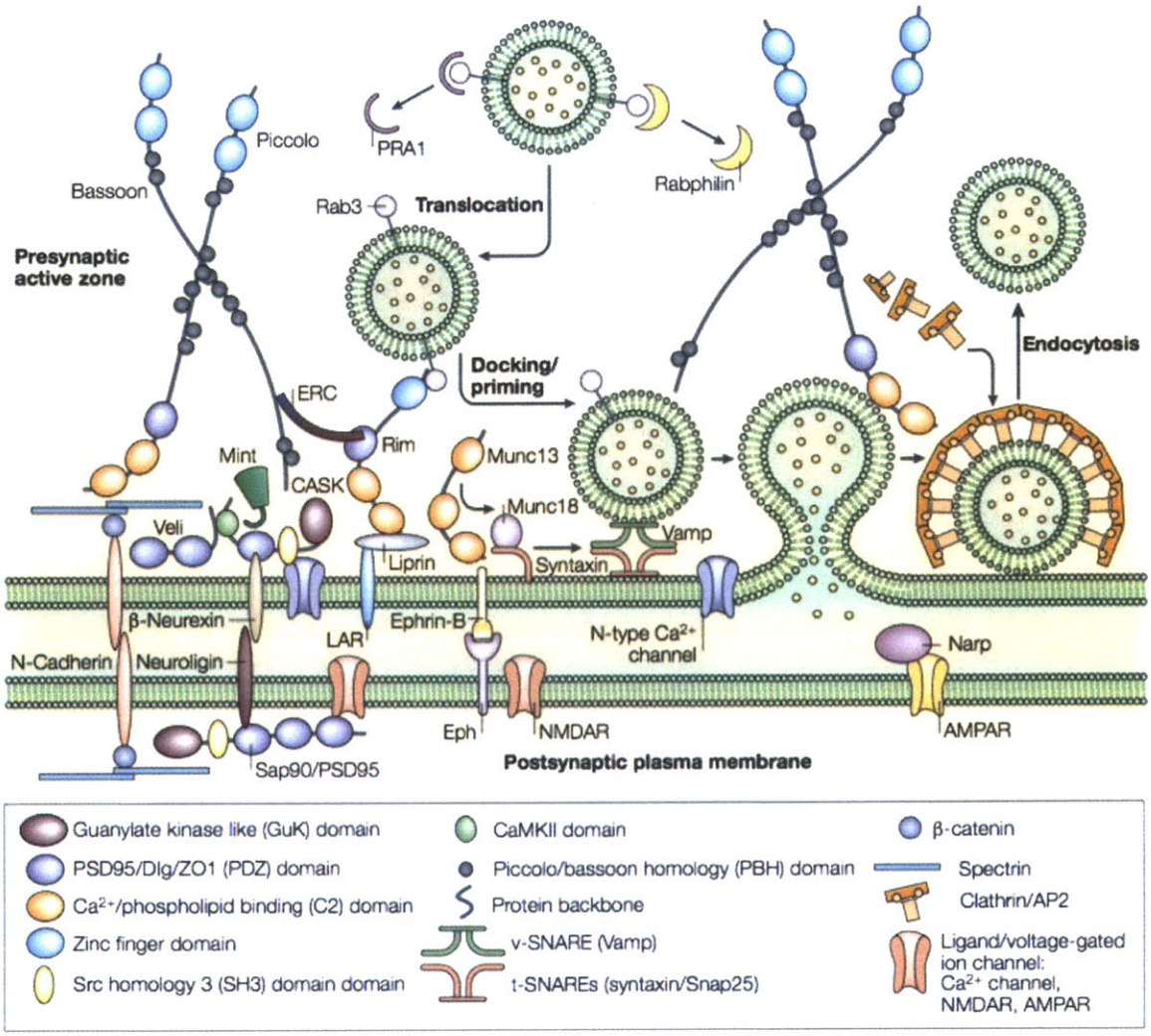
Piccolo
PRA1
Bassoon
Rab3
Translocation
Rabphilin
Presynaptic active zone
Docking/ priming
Endocytosis
ERC
Rim
Mint
CASK
Munc13
Munc18
Veli
Vamp
Liprin
Syntaxin
β-Neurexin
Ephrin-B
LAR
N-type Ca2+ channel
Narp
N-Cadherin
Neuroligin
Eph
NMDAR
AMPAR
Sap90/PSD95
Postsynaptic plasma membrane
Guanylate kinase like (GuK) domain
PSD95/Dlg/ZO1 (PDZ) domain
Ca2+/phospholipid binding (C2) domain
Zinc finger domain
Src homology 3 (SH3) domain domain
CaMKII domain
Piccolo/bassoon homology (PBH) domain
Protein backbone
v-SNARE (Vamp)
t-SNAREs (syntaxin/Snap25)
β-catenin
Spectrin
Clathrin/AP2
Ligand/voltage-gated ion channel: Ca2+ channel, NMDAR, AMPAR

Figure 1.4: *Organization of the cytomatrix at the active zone (CAZ).*

Piccolo, Bassoon, RIM, Munc13 and ERC/CAST are proteins residing at the active zone and are thought to regulate steps of the synaptic vesicle (SV) cycle. Through connections to CAMs, presynaptic voltage-gated Ca^{2+} channels and SV proteins, CAZ proteins organize efficient neurotransmitter release into the synaptic cleft. (Ziv and Garner, 2004. Reproduced with permission from Nature Publishing Group)

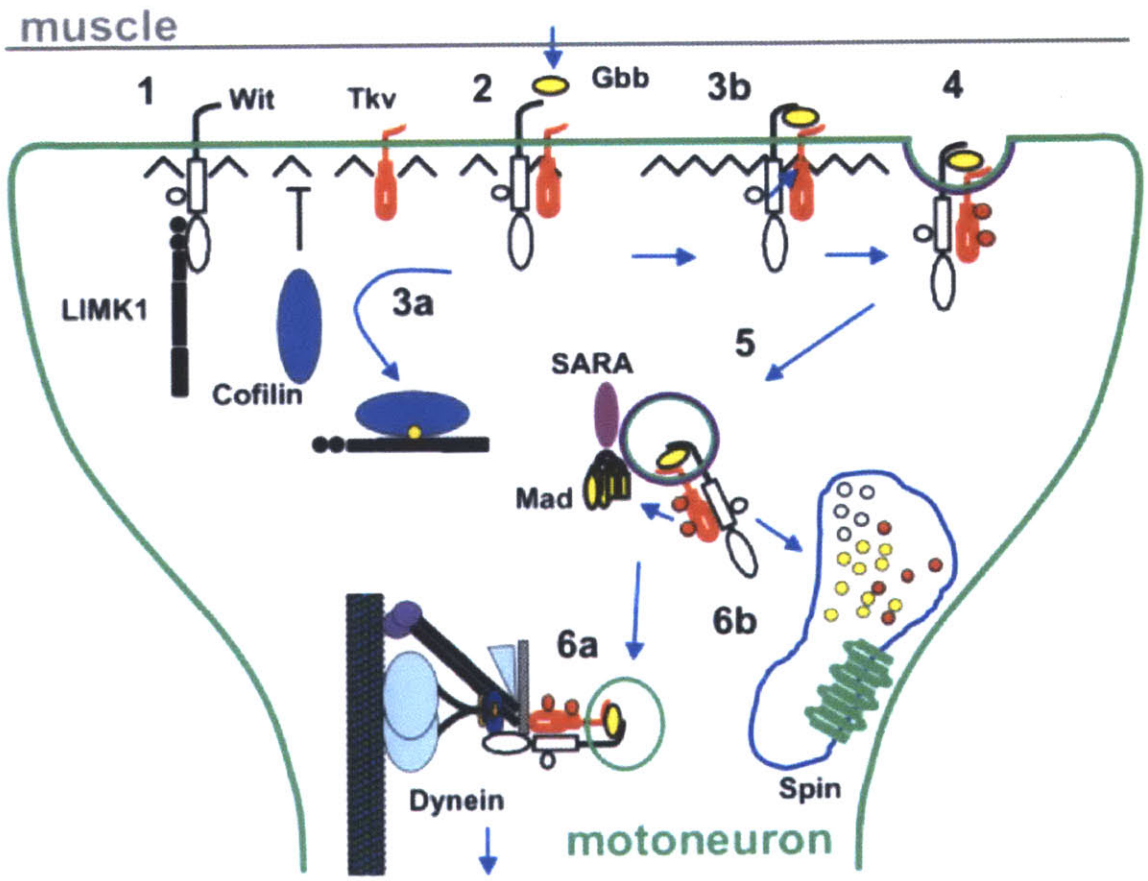
muscle
1
Wit
Tkv
2
Gbb
3b
4
LIMK1
Cofilin
3a
5
SARA
Mad
6b
6a
Dynein
Spin
motoneuron

Figure 2

Figure 1.5: *BMP/ TGF-β signaling at the Drosophila NMJ.*

Retrograde BMP/ TGF-β signaling regulates synaptic growth at the fly NMJ. The ligand Glass bottom boat (Gbb) is released from the muscle and binds to the type I and type II receptors Wishful thinking (Wit) and Thickveins (Tkv). This activates a downstream Smad signaling cascade that eventually leads to changes in transcription. Activated ligand- receptor complexes can be downregulated via the lysosmal pathway, thereby terminating signaling. (Marqués, 2005. Reproduced with permission from Wiley)

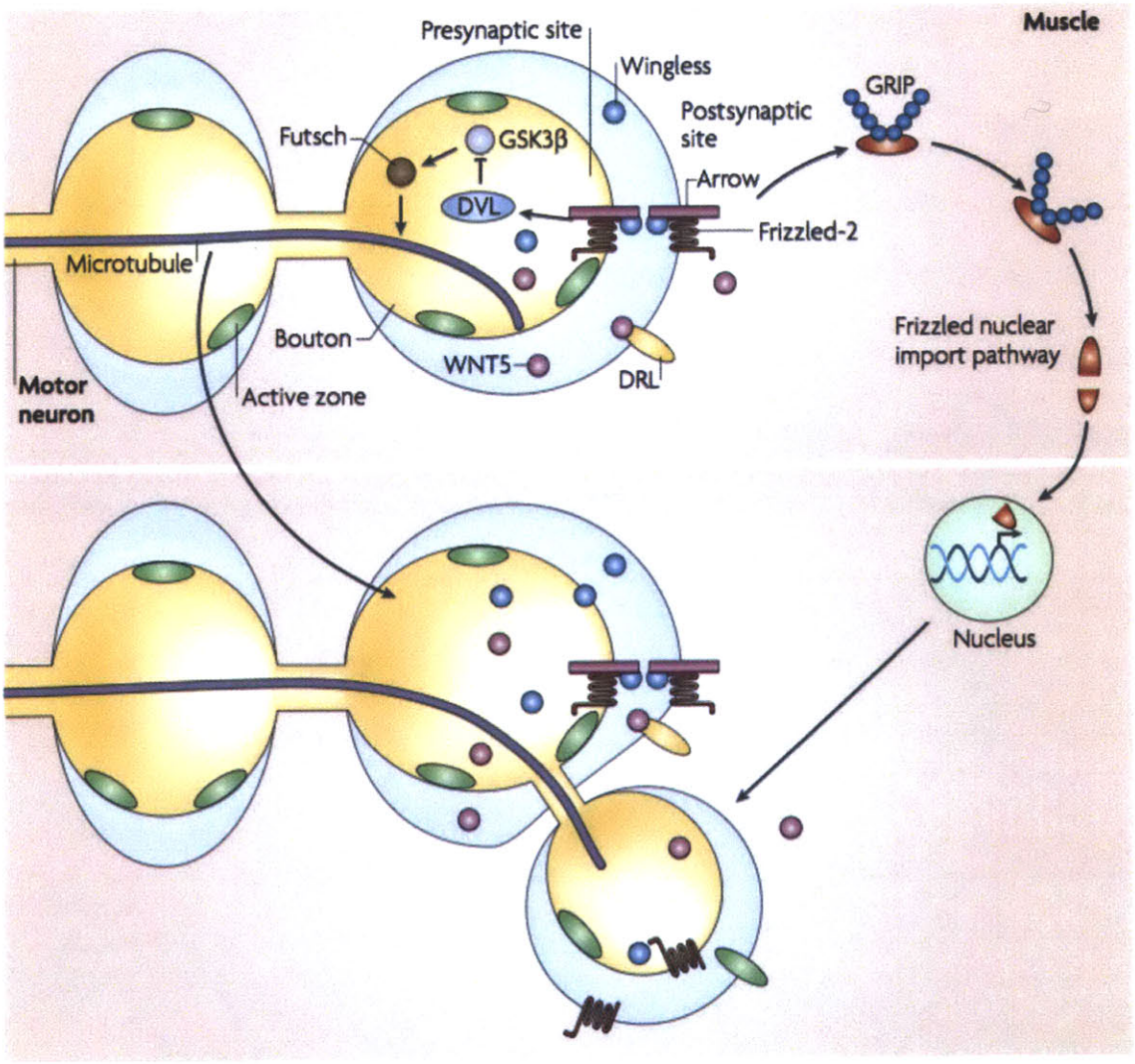
Muscle
Presynaptic site
Wingless
GRIP
Postsynaptic site
Futsch
GSK3β
Arrow
DVL
Frizzled-2
Microtubule
Bouton
WNT5
DRL
Frizzled nuclear import pathway
Motor neuron
Active zone
Nucleus

Figure 1.6: *Wnt signaling at the Drosophila NMJ.*

Wnt signaling regulates synaptic growth at the NMJ. The ligand Wingless is secreted by the presynaptic terminal and binds to its receptors Frizzled-2 and Arrow pre- as well as postsynaptically. In the bouton, this activates a divergent canonical Wnt signaling cascade. This local, transcription independent pathway regulates synaptic growth through changes of the microtubule cytoskeleton. In the muscle, activated Frizzled-2 is internalized and trafficked to the nucleus in a GRIP-dependent manner. Frizzled-2 is then cleaved and imported into the nucleus, leading to transcriptional changes. (Korkut and Budnik, 2009. Reproduced with permission from Nature Publishing Group)

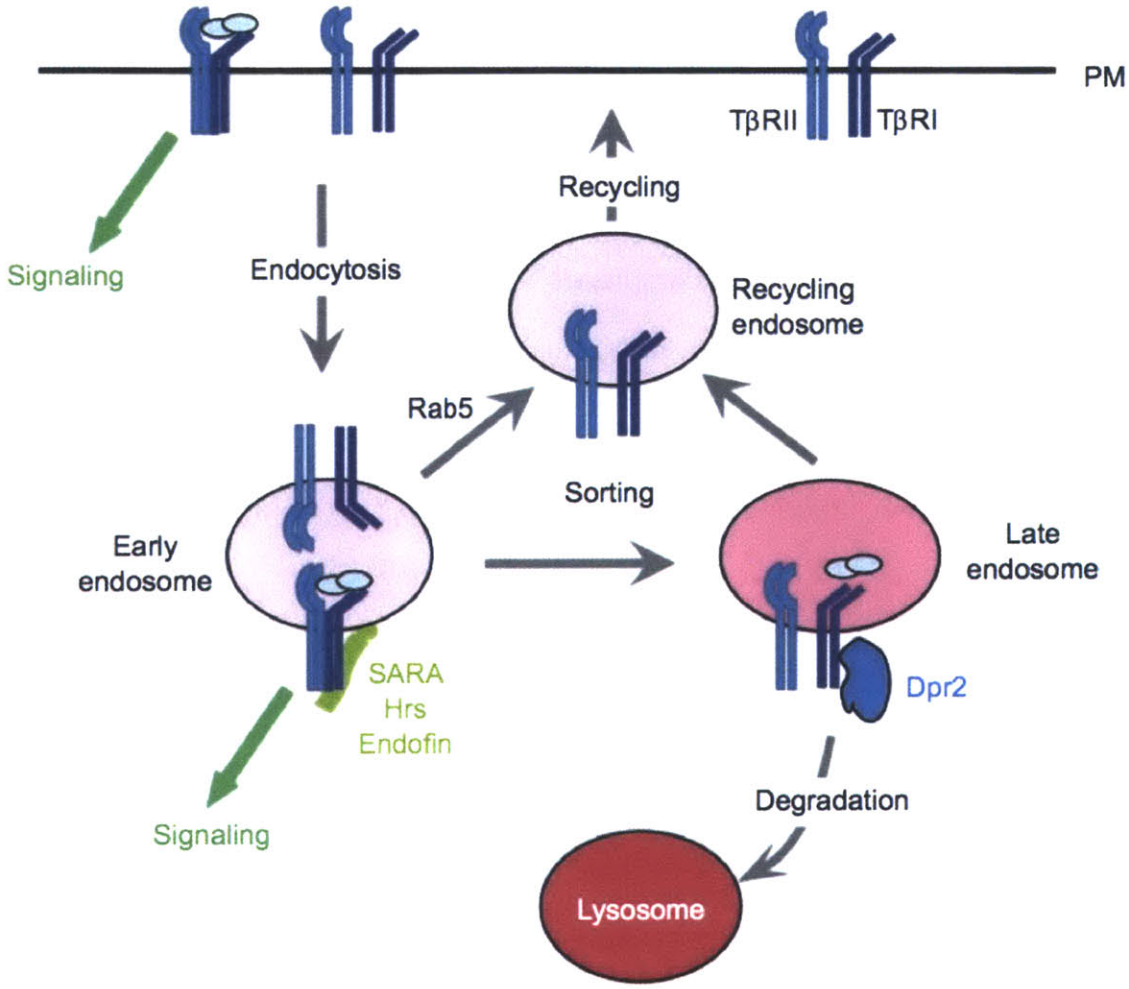
PM
TβRII
TβRI
Recycling
Signaling
Endocytosis
Recycling
endosome
Rab5
Sorting
Early
endosome
Late
endosome
SARA
Hrs
Endofin
Dpr2
Signaling
Degradation
Lysosome

Figure 1.7: *Regulation of signaling through endosomal trafficking, e.g. BMP/TGF-β signaling.*

Synaptic signaling cascades are regulated through endosomal trafficking. Activated ligand- receptor complexes are internalized and interact with downstream binding partners at the early endosome. Receptors can either recycle back to the plasma membrane or they can be degradated in the lysosome. (Chen, 2009. Reproduced with permission from Nature Publishing Group)

References

Aberle H, Haghighi AP, Fetter RD, McCabe BD, Magalhães TR, Goodman CS (2002) wishful thinking encodes a BMP type II receptor that regulates synaptic growth in Drosophila. Neuron 33:545–558.

Ahmari SE, Buchanan J, Smith SJ (2000) Assembly of presynaptic active zones from cytoplasmic transport packets. Nat Neurosci 3:445–451.

Alberts B, Johnson A, Lewis J, Raff M, Roberts K, Walter P (2002) Molecular Biology of the Cell (Lewis J, ed). 4 ed. New York: Garland Science.

Allison DW, Gelfand VI, Spector I, Craig AM (1998) Role of actin in anchoring postsynaptic receptors in cultured hippocampal neurons: differential attachment of NMDA versus AMPA receptors. J Neurosci 18:2423–2436.

Ataman B (2008) Rapid Activity-Dependent Modifications in Synaptic Structure and Function Require Bidirectional Wnt Signaling. Neuron 57:705–718.

Ataman B, Ashley J, Gorczyca D, Gorczyca M, Mathew D, Wichmann C, Sigrist SJ, Budnik V (2006) Nuclear trafficking of Drosophila Frizzled-2 during synapse development requires the PDZ protein dGRIP. Proceedings of the National Academy of Sciences 103:7841–7846.

Baines AJ, Keating L, Phillips GW, Scott C (2001) The postsynaptic spectrin/4.1 membrane protein "accumulation machine". Cell Mol Biol Lett 6:691–702.

Banovic D, Khorramshahi O, Owald D, Wichmann C, Riedt T, Fouquet W, Tian R, Sigrist SJ, Aberle H (2010) Drosophila neuroligin 1 promotes growth and postsynaptic differentiation at glutamatergic neuromuscular junctions. Neuron 66:724–738.

Barber CF, Jorquera RA, Melom JE, Littleton JT (2009) Postsynaptic regulation of synaptic plasticity by synaptotagmin 4 requires both C2 domains. J Cell Biol 187:295–310.

Biederer T (2002) SynCAM, a Synaptic Adhesion Molecule That Drives Synapse Assembly. Science 297:1525–1531.

Biederer T (2006a) SynCAM in Formation and Function of Synaptic Specializations. :125–135.

Biederer T (2006b) Bioinformatic characterization of the SynCAM family of immunoglobulin-like domain-containing adhesion molecules. Genomics 87:139–150.

Bin Zhang, Luo S, Wang Q, Suzuki T, Xiong WC, Mei L (2008) LRP4 Serves as a Coreceptor of Agrin. Neuron 60:285–297.

Bloom O, Evergren E, Tomilin N, Kjaerulff O, Low P, Brodin L, Pieribone VA, Greengard P, Shupliakov O (2003) Colocalization of synapsin and actin during synaptic vesicle recycling. J Cell Biol 161:737–747.

Bogdanik L, Framery B, Frölich A, Franco B, Mornet D, Bockaert J, Sigrist SJ,

Grau Y, Parmentier M-L (2008) Muscle Dystroglycan Organizes the Postsynapse and Regulates Presynaptic Neurotransmitter Release at the Drosophila Neuromuscular Junction Andreu AL, ed. PLoS ONE 3:e2084.

Broadie K, Bate M (1993a) Activity-dependent development of the neuromuscular synapse during Drosophila embryogenesis. Neuron 11:607–619.

Broadie K, Bate M (1993b) Innervation directs receptor synthesis and localization in Drosophila embryo synaptogenesis. Nature 361:350–353.

Bruckner JJ, Gratz SJ, Slind JK, Geske RR, Cummings AM, Galindo SE, Donohue LK, O'Connor-Giles KM (2012) Fife, a Drosophila Piccolo-RIM Homolog, Promotes Active Zone Organization and Neurotransmitter Release. Journal of Neuroscience 32:17048–17058.

Budnik V, Ruiz-Canada C (2006) The fly neuromuscular junction: structure and function, 2nd ed. Access Online via Elsevier.

Budnik V, Zhong Y, Wu CF (1990) Morphological Plasticity of Motor Axons in Drosophila Mutants with Altered Excitability. J Neurosci 10:3754–3768.

Carlton J, Bujny M, Rutherford A, Cullen P (2005) Sorting nexins--unifying trends and new perspectives. Traffic 6:75–82.

Carlton J, Cullen P (2005) Sorting nexins. Current Biology 15:R819–R820.

Chen K, Gracheva EO, Yu S-C, Sheng Q, Richmond J, Featherstone DE (2010) Neurexin in Embryonic Drosophila Neuromuscular Junctions Mei L, ed. PLoS ONE 5:e11115.

Chen K, Merino C, Sigrist SJ, Featherstone DE (2005) The 4.1 protein coracle mediates subunit-selective anchoring of Drosophila glutamate receptors to the postsynaptic actin cytoskeleton. J Neurosci 25:6667–6675.

Chen Y-G (2009) Endocytic regulation of TGF-β signaling. Cell Res 19:58–70.

Chen YC, Lin YQ, Banerjee S, Venken K, Li J, Ismat A, Chen K, Duraine L, Bellen HJ, Bhat MA (2012) Drosophila Neuroligin 2 is Required Presynaptically and Postsynaptically for Proper Synaptic Differentiation and Synaptic Transmission. Journal of Neuroscience 32:16018–16030.

Chia PH, Patel MR, Shen K (2012) NAB-1 instructs synapse assembly by linking adhesion molecules and F-actin to active zone proteins. Nat Neurosci.

Choi JC (2004) Electrophysiological and Morphological Characterization of Identified Motor Neurons in the Drosophila Third Instar Larva Central Nervous System. Journal of Neurophysiology 91:2353–2365.

Chubykin AA, Atasoy D, Etherton MR, Brose N, Kavalali ET, Gibson JR, Sudhof TC (2007) Activity-Dependent Validation of Excitatory versus Inhibitory Synapses by Neuroligin-1 versus Neuroligin-2. Neuron 54:919–931.

Cingolani LA, Goda Y (2008) Actin in action: the interplay between the actin cytoskeleton and synaptic efficacy. Nat Rev Neurosci 9:344–356.

Coleman SK, Cai C, Mottershead DG, Haapalahti J-P, Keinänen K (2003) Surface expression of GluR-D AMPA receptor is dependent on an interaction between its C-terminal domain and a 4.1 protein. J Neurosci 23:798–806.

Coyle IP, Koh Y-H, Lee W-CM, Slind J, Fergestad T, Littleton JT, Ganetzky B (2004) Nervous wreck, an SH3 adaptor protein that interacts with Wsp, regulates synaptic growth in Drosophila. Neuron 41:521–534.

Craig AM, Graf ER, Linhoff MW (2006) How to build a central synapse: clues from cell culture. Trends in Neurosciences 29:8–20.

Currie DA, Truman JW, Burden SJ (1995) Drosophila glutamate receptor RNA expression in embryonic and larval muscle fibers. Dev Dyn 203:311–316.

Daniels MP (2012) The role of agrin in synaptic development, plasticity and signaling in the central nervous system. Neurochemistry International 61:848–853.

Daniels RW, Collins CA, Chen K, Gelfand MV, Featherstone DE, DiAntonio A (2006) A Single Vesicular Glutamate Transporter Is Sufficient to Fill a Synaptic Vesicle. Neuron 49:11–16.

Davis GW, Schuster CM, Goodman CS (1996) Genetic dissection of structural and functional components of synaptic plasticity. III. CREB is necessary for presynaptic functional plasticity. Neuron 17:669–679.

DeChiara TM, Bowen DC, Valenzuela DM, Simmons MV, Poueymirou WT, Thomas S, Kinetz E, Compton DL, Rojas E, Park JS, Smith C, DiStefano PS, Glass DJ, Burden SJ, Yancopoulos GD (1996) The receptor tyrosine kinase MuSK is required for neuromuscular junction formation in vivo. Cell 85:501–512.

Di Fiore P, De Camilli P (2001) Endocytosis and Signaling An Inseparable Partnership. Cell.

Dillon C, Goda Y (2005) The actin cytoskeleton: integrating form and function at the synapse. Annu Rev Neurosci 28:25–55.

Dominguez R, Holmes KC (2011) Actin Structure and Function. Annu Rev Biophys 40:169–186.

Dresbach T, Fejtova A, Gundelfinger ED (2006) Assembly of Presynaptic Active Zones. :235–245.

Ellis JE, Parker L, Cho J, Arora K (2010) Developmental Biology. Dev Biol 342:121–133.

Ellson CD, Andrews S, Stephens LR, Hawkins PT (2002) The PX domain: a new phosphoinositide-binding module. J Cell Sci 115:1099–1105.

Featherstone DE, Rushton E, Broadie K (2002) Developmental regulation of glutamate receptor field size by nonvesicular glutamate release. Nat Neurosci 5:141–146.

Fejtova A, Gundelfinger ED (2006) Molecular organization and assembly of the presynaptic active zone of neurotransmitter release. Results Probl Cell Differ 43:49–68.

Flanagan-Steet H (2005) Neuromuscular synapses can form in vivo by incorporation of initially aneural postsynaptic specializations. Development 132:4471–4481.

Foelix R, Troyer D, Igelmund P (2002) Peripheral synapses and giant neurons in whip spiders. Microsc Res Tech 58:272–282.

Franco B (2004) Shaggy, the Homolog of Glycogen Synthase Kinase 3, Controls Neuromuscular Junction Growth in Drosophila. J Neurosci 24:6573–6577.

Frost NA, Kerr JM, Lu HE, Blanpied TA (2010) A network of networks: cytoskeletal control of compartmentalized function within dendritic spines. Current Opinion in Neurobiology 20:578–587.

Fuchs U, Rehkamp G, Haas OA, Slany R, Kōnig M, Bojesen S, Bohle RM, Damm-Welk C, Ludwig WD, Harbott J, Borkhardt A (2001) The human formin-binding protein 17 (FBP17) interacts with sorting nexin, SNX2, and is an MLL-fusion partner in acute myelogeneous leukemia. Proc Natl Acad Sci USA 98:8756–8761.

Gautam M, Noakes PG, Mudd J, Nichol M, Chu GC, Sanes JR, Merlie JP (1995) Failure of postsynaptic specialization to develop at neuromuscular junctions of rapsyn-deficient mice. Nature 377:232–236.

Ghazanfari N, Fernandez KJ, Murata Y, Morsch M, Ngo ST, Reddel SW, Noakes PG, Phillips WD (2011) The International Journal of Biochemistry & Cell Biology. International Journal of Biochemistry and Cell Biology 43:295–298.

Glass DJ, Bowen DC, Stitt TN, Radziejewski C, Bruno J, Ryan TE, Gies DR, Shah S, Mattsson K, Burden SJ (1996) Agrin acts via a MuSK receptor complex. Cell 85:513–523.

Godfrey EW, Nitkin RM, Wallace BG, Rubin LL, McMahan UJ (2002) Components of Torpedo electric organ and muscle that cause aggregation of acetylcholine receptors on cultured muscle cells. J Cell Biol 99:615–627.

Goldstein AY, Wang X, Schwarz TL (2008) Axonal transport and the delivery of pre-synaptic components. Current Opinion in Neurobiology 18:495–503.

Graf ER, Zhang X, Jin S-X, Linhoff MW, Craig AM (2004) Neurexins induce differentiation of GABA and glutamate postsynaptic specializations via neuroligins. Cell 119:1013–1026.

Gray EG (1963) Electron microscopy of presynaptic organelles of the spinal cord. Journal of Anatomy 97:101.

Guan Z, Saraswati S, Adolfsen B, Littleton JT (2005) Genome-Wide Transcriptional Changes Associated with Enhanced Activity in the Drosophila Nervous System. Neuron 48:91–107.

Harlow ML, Ress D, Stoschek A, Marshall RM, McMahan UJ (2001) The architecture of active zone material at the frog's neuromuscular junction. Nature 409:479–484.

Hirokawa N, Sobue K, Kanda K, Harada A, Yorifuji H (1989) The cytoskeletal architecture of the presynaptic terminal and molecular structure of synapsin 1. J Cell Biol 108:111–126.

Hoang B, Chiba A (2001) Single-Cell Analysis of Drosophila Larval Neuromuscular Synapses. Dev Biol 229:55–70.

Hotulainen P, Hoogenraad CC (2010) Actin in dendritic spines: connecting dynamics to function. J Cell Biol 189:619–629.

Hummel T, Krukkert K, Roos J, Davis G, Klämbt C (2000) Drosophila Futsch/22C10 is a MAP1B-like protein required for dendritic and axonal development. Neuron 26:357–370.

Itoh T, Erdmann KS, Roux A, Habermann B, Werner H, De Camilli P (2005) Dynamin and the Actin Cytoskeleton Cooperatively Regulate Plasma Membrane Invagination by BAR and F-BAR Proteins. Dev Cell 9:791–804.

Jan LY, Jan YN (1976) L-glutamate as an excitatory transmitter at the Drosophila larval neuromuscular junction. J Physiol (Lond) 262:215–236.

Johnson EL, Fetter RD, Davis GW (2009) Negative Regulation of Active Zone Assembly by a Newly Identified SR Protein Kinase. PLoS Biol 7:e1000193.

Jontes JD, Smith SJ (2000) Filopodia, spines, and the generation of synaptic diversity. Neuron 27:11.

Kim N, Stiegler AL, Cameron TO, Hallock PT, Gomez AM, Huang JH, Hubbard SR, Dustin ML, Burden SJ (2008) Lrp4 Is a Receptor for Agrinand Forms a Complex with MuSK. Cell 135:334–342.

Koh YH, Popova E, Thomas U, Griffith LC, Budnik V (1999) Regulation of DLG localization at synapses by CaMKII-dependent phosphorylation. Cell 98:353–363.

Korkut C, Budnik V (2009) WNTs tune up the neuromuscular junction. Nat Rev Neurosci 10:627–634.

Kummer TT, Misgeld T, Sanes JR (2006) Assembly of the postsynaptic membrane at the neuromuscular junction: paradigm lost. Current Opinion in Neurobiology 16:74–82.

Kurten RC, Cadena DL, Gill GN (1996) Enhanced degradation of EGF receptors by a sorting nexin, SNX1. Science 272:1008–1010.

Li J, Ashley J, Budnik V, Bhat MA (2007) Crucial Role of Drosophila Neurexin in Proper Active Zone Apposition to Postsynaptic Densities, Synaptic Growth, and Synaptic Transmission. Neuron 55:741–755.

Lin W, Burgess RW, Dominguez B, Pfaff SL, Sanes JR, Lee KF (2001) Distinct

roles of nerve and muscle in postsynaptic differentiation of the neuromuscular synapse. Nature 410:1057–1064.

Marchesi VT, Steers E (1968) Selective solubilization of a protein component of the red cell membrane. Science 159:203–204.

Marqués G (2005) Morphogens and synaptogenesis inDrosophila. J Neurobiol 64:417–434.

Marrus SB (2004) Differential Localization of Glutamate Receptor Subunits at the Drosophila Neuromuscular Junction. Journal of Neuroscience 24:1406–1415.

Mathew D, Ataman B, Chen J, Zhang Y, Cumberledge S, Budnik V (2005) Wingless signaling at synapses is through cleavage and nuclear import of receptor DFrizzled2. Science Signaling 310:1344.

MCCABE B (2003) The BMP Homolog Gbb Provides a Retrograde Signal that Regulates Synaptic Growth at the Drosophila Neuromuscular Junction. Neuron 39:241–254.

McPherson PS, Kay BK, Hussain NK (2001) Signaling on the endocytic pathway. Traffic 2:375–384.

Meinertzhagen IA (1996) Ultrastructure and quantification of synapses in the insect nervous system. Journal of neuroscience methods 69:59–73.

Merrifield CJ, Moss SE, Ballestrem C, Imhof BA, Giese G, Wunderlich I, Almers W (1999) Endocytic vesicles move at the tips of actin tails in cultured mast cells. Nat Cell Biol 1:72–74.

Miech C, Pauer HU, He X, Schwarz TL (2008) Presynaptic Local Signaling by a Canonical Wingless Pathway Regulates Development of the Drosophila Neuromuscular Junction. J Neurosci 28:10875–10884.

Misgeld T, Burgess RW, Lewis RM, Cunningham JM, Lichtman JW, Sanes JR (2002) Roles of neurotransmitter in synapse formation: development of neuromuscular junctions lacking choline acetyltransferase. Neuron 36:635–648.

Morales M, Colicos MA, Goda Y (2000) Actin-dependent regulation of neurotransmitter release at central synapses. Neuron 27:539–550.

Mosca TJ, Hong W, Dani VS, Favaloro V, Luo L (2012) Trans-synaptic Teneurin signalling in neuromuscular synapse organization and target choice. Nature:1–7.

Nam CI, Chen L (2005) Postsynaptic assembly induced by neurexin-neuroligin interaction and neurotransmitter. Proceedings of the National Academy of Sciences 102:6137–6142.

Nieratschker V, Schubert A, Jauch M, Bock N, Bucher D, Dippacher S, Krohne G, Asan E, Buchner S, Buchner E (2009) Bruchpilot in ribbon-like axonal agglomerates, behavioral defects, and early death in SRPK79D kinase mutants of Drosophila. PLoS Genet 5:e1000700.

O'Connor-Giles K, Ho L, Ganetzky B (2008) Nervous Wreck Interacts with Thickveins and the Endocytic Machinery to Attenuate Retrograde BMP Signaling during Synaptic Growth. Neuron 58:507–518.

Owald D, Khorramshahi O, Gupta VK, Banovic D, Depner H, Fouquet W, Wichmann C, Mertel S, Eimer S, Reynolds E, Holt M, Aberle H, Sigrist SJ (2012) Cooperation of Syd-1 with Neurexin synchronizes pre- with postsynaptic assembly. Nat Neurosci.

Pack-Chung E, Kurshan PT, Dickman DK, Schwarz TL (2007) A Drosophila kinesin required for synaptic bouton formation and synaptic vesicle transport. Nat Neurosci 10:980–989.

Packard M (2003) FASt remodeling of synapses in Drosophila. Current Opinion in Neurobiology 13:527–534.

Packard M, Koo ES, Gorczyca M, Sharpe J, Cumberledge S, Budnik V (2002) The Drosophila Wnt, wingless, provides an essential signal for pre- and postsynaptic differentiation. Cell 111:319–330.

Packard M, Mathew D, Budnik V (2003) Wnts and TGFβ in synaptogenesis: old friends signalling at new places. Nat Rev Neurosci 4:113–120.

Panzer JA, Gibbs SM, Dosch R, Wagner D, Mullins MC, Granato M, Balice-Gordon RJ (2005) Neuromuscular synaptogenesis in wild-type and mutant zebrafish. Dev Biol 285:340–357.

Parks WT (2001) Sorting Nexin 6, a Novel SNX, Interacts with the Transforming Growth Factor-beta Family of Receptor Serine-Threonine Kinases. Journal of Biological Chemistry 276:19332–19339.

Pfenninger K, Akert K, Moor H, Sandri C (1972) The fine structure of freeze-fractured presynaptic membranes. J Neurocytol 1:129–149.

Phillips GR, Huang JK, Wang Y, Tanaka H, Shapiro L, Zhang W, Shan W-S, Arndt K, Frank M, Gordon RE (2001) The presynaptic particle web: ultrastructure, composition, dissolution, and reconstitution. Neuron 32:63–77.

Pielage J, Fetter RD, Davis GW (2005) Presynaptic spectrin is essential for synapse stabilization. Curr Biol 15:918–928.

Pielage J, Fetter RD, Davis GW (2006) A postsynaptic spectrin scaffold defines active zone size, spacing, and efficacy at the Drosophila neuromuscular junction. J Cell Biol 175:491–503.

Prokop A, Meinertzhagen I (2006) Development and structure of synaptic contacts in Drosophila. Seminars in Cell & Developmental Biology 17:20–30.

Qin G (2005) Four Different Subunits Are Essential for Expressing the Synaptic Glutamate Receptor at Neuromuscular Junctions of Drosophila. Journal of Neuroscience 25:3209–3218.

Ramachandran P, Barria R, Ashley J, Budnik V (2009) A critical step for postsynaptic F-actin organization: Regulation of Baz/Par-3 localization by

aPKC and PTEN. Devel Neurobio 69:583–602.

Ritzenthaler S, Suzuki E, Chiba A (2000) Postsynaptic filopodia in muscle cells interact with innervating motoneuron axons. Nat Neurosci 3:1012–1017.

Rodal AA, (null), Littleton JT (2008) Nervous wreck and Cdc42 cooperate to regulate endocytic actin assembly during synaptic growth. J Neurosci 28:8316–8325.

Roos J, Hummel T, Ng N, Klämbt C, Davis GW (2000) Drosophila Futsch regulates synaptic microtubule organization and is necessary for synaptic growth. Neuron 26:371–382.

Ruiz-Canada C, Ashley J, Moeckel-Cole S, Drier E, Yin J, Budnik V (2004) New synaptic bouton formation is disrupted by misregulation of microtubule stability in aPKC mutants. Neuron 42:567–580.

Saitoe M, Tanaka S, Takata K, Kidokoro Y (1997) Neural activity affects distribution of glutamate receptors during neuromuscular junction formation in Drosophila embryos. Dev Biol 184:48–60.

Scheiffele P, Fan J, Choih J, Fetter R, Serafini T (2000) Neuroligin expressed in nonneuronal cells triggers presynaptic development in contacting axons. Cell 101:657–669.

Schoch S, Gundelfinger ED (2006) Molecular organization of the presynaptic active zone. Cell and Tissue Research 326:379–391.

Schuster CM, Davis GW, Fetter RD, Goodman CS (1996a) Genetic dissection of structural and functional components of synaptic plasticity. II. Fasciclin II controls presynaptic structural plasticity. Neuron 17:655–667.

Schuster CM, Davis GW, Fetter RD, Goodman CS (1996b) Genetic dissection of structural and functional components of synaptic plasticity. I. Fasciclin II controls synaptic stabilization and growth. Neuron 17:641–654.

Seet L, Hong W (2006) The Phox (PX) domain proteins and membrane traffic. Biochimica et Biophysica Acta (BBA) - Molecular and Cell Biology of Lipids 1761:878–896.

Seto ES (2006) Internalization is required for proper Wingless signaling in Drosophila melanogaster. J Cell Biol 173:95–106.

Shapira M, Zhai RG, Dresbach T, Bresler T, Torres VI, Gundelfinger ED, Ziv NE, Garner CC (2003) Unitary assembly of presynaptic active zones from Piccolo-Bassoon transport vesicles. Neuron 38:237–252.

Shen L, Liang F, Walensky LD, Huganir RL (2000) Regulation of AMPA receptor GluR1 subunit surface expression by a 4. 1N-linked actin cytoskeletal association. J Neurosci 20:7932–7940.

Shupliakov O, Bloom O, Gustafsson JS, Kjaerulff O, Low P, Tomilin N, Pieribone VA, Greengard P, Brodin L (2002) Impaired recycling of synaptic vesicles after acute perturbation of the presynaptic actin cytoskeleton. Proceedings of

the National Academy of Sciences 99:14476–14481.

Sigrist SJ, Reiff DF, Thiel PR, Steinert JR, Schuster CM (2003) Experience-dependent strengthening of Drosophila neuromuscular junctions. Journal of Neuroscience 23:6546–6556.

Siksou L, Rostaing P, Lechaire J-P, Boudier T, Ohtsuka T, Fejtova A, Kao H-T, Greengard P, Gundelfinger ED, Triller A, Marty S (2007) Three-dimensional architecture of presynaptic terminal cytomatrix. Journal of Neuroscience 27:6868–6877.

Stewart BA, Schuster CM, Goodman CS, Atwood HL (1996) Homeostasis of synaptic transmission in Drosophila with genetically altered nerve terminal morphology. J Neurosci 16:3877–3886.

Sudhof TC (2008) Neuroligins and neurexins link synaptic function to cognitive disease. Nature 455:903–911.

Sun M, Xing G, Yuan L, Gan G, Knight D, With SI, He C, Han J, Zeng X, Fang M, Boulianne GL, Xie W (2011) Neuroligin 2 Is Required for Synapse Development and Function at the Drosophila Neuromuscular Junction. J Neurosci 31:687–699.

Svitkina T, Lin WH, Webb DJ, Yasuda R, Wayman GA, Van Aelst L, Soderling SH (2010) Regulation of the Postsynaptic Cytoskeleton: Roles in Development, Plasticity, and Disorders. Journal of Neuroscience 30:14937–14942.

Sweeney ST, Davis GW (2002) Unrestricted synaptic growth in spinster-a late endosomal protein implicated in TGF-beta-mediated synaptic growth regulation. Neuron 36:403–416.

Thomas U, Kim E, Kuhlendahl S, Koh YH, Gundelfinger ED, Sheng M, Garner CC, Budnik V (1997) Synaptic clustering of the cell adhesion molecule fasciclin II by discs-large and its role in the regulation of presynaptic structure. Neuron 19:787–799.

Thomas U, Sigrist SJ (2012) Advances in Experimental Medicine and Biology (Kreutz MR, Sala C, eds). Vienna: Springer Vienna.

Tillack TW, Marchesi SL, Marchesi VT, Steers E (1970) A comparative study of spectrin: a protein isolated from red blood cell membranes. Biochim Biophys Acta 200:125–131.

Tsujita K (2006) Coordination between the actin cytoskeleton and membrane deformation by a novel membrane tubulation domain of PCH proteins is involved in endocytosis. J Cell Biol 172:269–279.

van den Ent F, Amos LA, LoÈwe J (2001) Prokaryotic origin of the actin cytoskeleton. Nature 413:39–44.

Van Epps H, Jin Y (2006) Development of the Drosophila and C. Elegans Neuromuscular Junctions. :43–65.

Varoqueaux F, Aramuni G, Rawson RL, Mohrmann R, Missler M, Gottmann K, Zhang W, Sudhof TC, Brose N (2006) Neuroligins Determine Synapse Maturation and Function. Neuron 51:741–754.

Weible MW, Hendry IA (2003) What is the importance of multivesicular bodies in retrograde axonal transportin vivo? J Neurobiol 58:230–243.

Winder SJ (2003) Structural insights into actin-binding, branching and bundling proteins. Current Opinion in Cell Biology 15:14–22.

Worby CA, Dixon JE (2002) Sorting out the cellular functions of sorting nexins. Nat Rev Mol Cell Biol 3:919–931.

Wu X, Jung G, Hammer JA (2000) Functions of unconventional myosins. Current Opinion in Cell Biology 12:42–51.

Yang X, Arber S, William C, Li L, Tanabe Y, Jessell TM, Birchmeier C, Burden SJ (2001) Patterning of muscle acetylcholine receptor gene expression in the absence of motor innervation. Neuron 30:399–410.

Yoshihara M (2005) Retrograde Signaling by Syt 4 Induces Presynaptic Release and Synapse-Specific Growth. Science 310:858–863.

Zeng X, Sun M, LIU L, CHEN F, WEI L, Xie W (2007) Neurexin-1 is required for synapse formation and larvae associative learning in Drosophila. FEBS Letters 581:2509–2516.

Zhai RG, Vardinon-Friedman H, Cases-Langhoff C, Becker B, Gundelfinger ED, Ziv NE, Garner CC (2001) Assembling the presynaptic active zone: a characterization of an active one precursor vesicle. Neuron 29:131–143.

Zhang W, Benson DL (2001) Stages of synapse development defined by dependence on F-actin. Journal of Neuroscience 21:5169–5181.

Zhong Y, Budnik V, Wu CF (1992) Synaptic Plasticity in Drosophila Memory and Hyperexcitable Mutants - Role of Camp Cascade. J Neurosci 12:644–651.

Zito K, Parnas D, Fetter RD, Isacoff EY, Goodman CS (1999) Watching a synapse grow: noninvasive confocal imaging of synaptic growth in Drosophila. Neuron 22:719–729.

Ziv NE, Garner CC (2004) Cellular and molecular mechanisms of presynaptic assembly. Nat Rev Neurosci 5:385–399.

Ziv NE, Smith SJ (1996) Evidence for a role of dendritic filopodia in synaptogenesis and spine formation. Neuron 17:91–102.

CHAPTER 2

Postsynaptic actin regulates active zone spacing and glutamate receptor apposition at the *Drosophila* neuromuscular junction

Aline D. Blunk[1], Richard W. Cho[1], Yulia Akbergenova[1], Jihye Lee[1,2], Ke Xu[3], Guisheng Zhong[3], Xiaowei Zhuang[3,4] and J. Troy Littleton[1]

[1]The Picower Institute of Learning and Memory, Department of Brain and Cognitive Sciences, Massachusetts Institute for Technology, Cambridge, MA 02139

[2]The Department of Oral Pathology, School of Dentistry, Pusan National University, Korea

[3]Howard Hughes Medical Institute (HHMI), Department of Chemistry and Chemical Biology, Harvard University, Cambridge, MA 02138

[4]Department of Physics, Harvard University, Cambridge, MA 02318

Aline Blunk performed the majority of the work described in this chapter. The EMS screen was done in collaboration with Yulia Akbergenova, Richard Cho and Jihye Lee. EM analysis was performed by Yulia Akbergenova. Electrophysiology was performed by Richard Cho. STORM imaging was performed in collaboration with Ke Xu and Guisheng Zhong.

2.1 Introduction

Neuronal communication requires a spatially organized synaptic apparatus to link neurotransmitter release from synaptic vesicles to activation of postsynaptic receptors. As such, active zone assembly, including spacing, density and alignment with receptor fields, is tightly regulated to guarantee efficient synaptic transmission. Indeed, active zone density at vertebrate and invertebrate neuromuscular junctions (NMJs) remains constant throughout development (Meinertzhagen et al., 1998; Clarke et al., 2012; Nishimune, 2012). Likewise, assembly of pre- and postsynaptic specializations occurs in a coordinated manner, with their alignment mediated by cell adhesion molecules spanning the synaptic cleft [reviewed in (Dalva et al., 2007; Giagtzoglou et al., 2009; Sun and Xie, 2012)]. However, a complete picture of the signaling pathways underlying active zone assembly, spacing and postsynaptic alignment is lacking.

The *Drosophila* NMJ has become a powerful model glutamatergic synapse for identifying novel regulators of synaptic structure and function. Synaptic boutons of the *Drosophila* neuromuscular junction (NMJ) contain 10-40 evenly spaced active zones directly opposite postsynaptic glutamate receptor clusters (Atwood et al., 1993; Petersen et al., 1997). Recent genetic screens in *Drosophila* and *C. elegans* have revealed several positive and negative signaling pathways that modulate active zone assembly [reviewed in (Sigrist and Schmitz, 2011)]. A diverse set of proteins regulate active zone density, ranging from the

endocytosis regulator synaptojanin (Dickman et al., 2006), the synaptic vesicle associated, small GTPase Rab3 (Graf et al., 2009), the serine threonine kinases Unc-51 (Wairkar et al., 2009) to the postsynaptic Spectrin cytoskeleton (Pielage et al., 2006). In addition to these pathways, proper alignment of the pre- and post-synaptic apparatus requires trans-synaptic communication provided by cell adhesion molecules. Here, the Neurexin- Neuroligin complex, as well as the Teneurins, have recently been implicated to function in parallel pathways, organizing coordinated pre- and postsynaptic assembly (Li et al., 2007; Banovic et al., 2010; Mosca et al., 2012). Despite these advances, the interplay between these different signaling pathways remains poorly understood. To identify mechanisms controlling synapse organization, we carried out a large-scale EMS mutagenesis screen of the *Drosophila* second chromosome. Using fluorescently-conjugated antibodies against the presynaptic active zone protein Bruchpilot (BRP) (Wagh et al., 2006) and the postsynaptic glutamate receptor subunit III (GluRIII) (Marrus, 2004) for immunostaining, we performed a screen for mutants displaying abnormalities in active zone size, number, location and apposition to postsynaptic glutamate receptors. From this screen we identified a mutation in actin 57B, one of six actin genes in *Drosophila* (Fyrberg et al., 1980; Tobin et al., 1980), that disrupts normal active zone spacing and pre-postsynaptic alignment.

Here we present a characterization of the isolated allele, a point mutation of glutamate E84 in actin 57B (act^{E84K}), the main actin present in the postsynaptic larval body wall muscle. We find that actin 57B is a key organizer of active zone

assembly, linking several protein networks to ensure coordinated pre- and postsynaptic maturation. In act^{E84K} mutants, organization of the postsynaptic density is perturbed, evident in defective SSR formation and mislocalization of the Spectrin cytoskeleton and PSD-95 homolog DLG. Postsynaptic F-actin structure is severely disrupted in the mutant, as large abnormal actin swirls replace the normal uniform structure of the actin-rich domain surrounding the presynaptic terminal. Furthermore, a disruption of the actin cytoskeleton leads to a reduction in active zone density and an increase in unapposed BRP and GluRIII clusters.

These findings indicate that synaptic interactions disrupted in the actin 57B mutant cause abnormal postsynaptic actin organization and dysregulation of signals required to organize presynaptic active zone alignment and spacing. Further characterization of this partial loss-of-function actin mutant should provide insights in the role of the postsynaptic cytoskeleton in organizing trans-synaptic adhesion and signaling pathways that regulate synapse formation.

2.2 Results

2.2.1 EMS mutagenesis screen for regulators of synaptic growth and organization

The *Drosophila* NMJ provides a powerful model system to study regulation of synaptic organization. During its life cycle, *Drosophila* undergoes 3 larval stages marked by a significant increase in larval size. To ensure efficient muscle contraction, the synaptic NMJ arbor expands ~10 fold during development, adding new synaptic boutons and increasing the number of active zones through an activity-dependent process (Stewart et al., 1996; Zito et al., 1999) . To identify regulators of active zone (AZ) organization, we carried out an unbiased ethyl methanesulfonate (EMS) mutagenesis screen of the second chromosome. Immunostaining with antibodies against the AZ component Bruchpilot (BRP) (Wagh et al., 2006) and the essential Glutamate receptor subunit III (DGluRIII) (Marrus, 2004) reveals a regular distribution of AZs at 3rd instar NMJs of wild-type animals (Fig. 2.1*A*). Synaptic arbors innervating muscle 4 contain ~10 to 20 AZs per bouton, depending on bouton size. Changes in active zone size, distribution and postsynaptic DGluRIII apposition can therefore be easily identified. This strategy has been previously used successfully for identifying new synaptic growth regulators [for example (Graf et al., 2009; Viquez et al., 2009; Wairkar et al., 2009; Valakh et al., 2012; Enneking et al., 2013)]. In addition, the

antibody assay enabled us to recover mutations regulating synaptic growth and stability, as BRP and DGluRIII distribution also outlines NMJ morphology.

To isolate genes located on the second chromosome that are involved in regulation of synaptic organization, males of an isogenized Canton-S line (wild-type, WT) were mutagenized and crossed to females carrying a second chromosome balancer. Single male progeny was backcrossed to the balancer line, isolating the mutagenized chromosome. A total of 691 homozygosed lines were screened at the 3rd instar larval stage and 27 mutant lines were isolated that disrupted the wild-type synaptic pattern at muscle fiber 4. These mutants were categorized into several phenotypic classes: aberrant AZ distribution, AZ apposition defects, DGluRIII clustering defects, synaptic growth defects (Fig. 2.1*B*), and bouton size abnormalities (Fig. 2.1*C*).

2.2.2 Actin 57B mutants show aberrant active zone spacing and density

During development the *Drosophila* NMJ undergoes synaptic expansion while maintaining constant active zone density (Meinertzhagen et al., 1998; Reiff et al., 2002; Sigrist et al., 2002). Recently, several regulators of active zone number and distribution have been identified (Dickman et al., 2006; Pielage et al., 2006; Graf et al., 2009; Wairkar et al., 2009). However, the molecular mechanisms that define AZ number, spacing and density remain largely unknown (reviewed in Clarke et al., 2012). One of the AZ mutants identified in our EMS screen, line 117B, showed abnormal spacing and distribution of BRP puncta in

presynaptic boutons (Fig. 2.3*B*). Given the severity of the phenotype in this line, we proceeded to characterize the mutation in more detail. Mutant larvae very rarely survive to pupation, showing reduced locomotion and larval growth. Meiotic recombination mapping of the lethal phenotype placed the locus between 2-94 and 2-99. Further deficiency mapping indicated that the mutation resides at 57B4-B5, as defined by the breakpoints of deficiencies Df(2R)BSC404 and Df(2R)BSC814. Sequence analysis of the 7 candidate genes that reside in this region revealed a mutation in one of the six *Drosophila* actin genes, Actin 57B (Fyrberg et al., 1980).

Actin is a highly conserved protein, which shows few sequence changes across different species (Fig. 2.2*A*). The six *Drosophila* actin genes are highly conserved, differing in only 27 nucleotides. However, they show spatial- and temporal- specific expression that has been well characterized previously (Fyrberg et al., 1998; Meinertzhagen et al., 1998; Clarke et al., 2012; Nishimune, 2012). Actin 57B is one of four muscle actins and is the main actin present in larval body wall muscle that forms the postsynaptic compartment during our screening developmental window (Fyrberg et al., 1983; Tobin et al., 1990; Kelly et al., 2002; Dalva et al., 2007; Giagtzoglou et al., 2009; Sun and Xie, 2012). The mutation identified in the actin 117B mutant changes the highly conserved glutamate E84 to lysine (act^{E84K}, Fig. 2.2*A*). E84 lies in subdomain 1 of the actin monomer, facing out from the actin filament (Fig. 2.2*B-D*). This actin region has been implicated in binding to members of the Calponin Homology (CH) domain

superfamily, including β-spectrin, α-actinin and dystrophin (residues highlighted in Figure 2.2*B*,*C*) (Atwood et al., 1993; Honts et al., 1994; McGough et al., 1994; Hanein et al., 1997; Hodgkinson et al., 1997; Petersen et al., 1997; Moores et al., 2000; Galkin, 2002; Sutherland-Smith et al., 2003).

The act^{E84K} mutant was isolated based on its abnormal BRP and DGluRIII immunostaining. In wild-type, BRP puncta show a regular distribution throughout synaptic terminals, and are directly apposed to postsynaptic glutamate receptor fields (Fig 2.3*A*). Mutant animals display abnormal NMJ morphology, as well as a severe redistribution of active zones. Instead of the regular spaced distribution, some boutons contain large BRP clusters, whereas others are nearly devoid of BRP puncta (Fig 2.3*B*). Concomitant with the defect in presynaptic active zone distribution, postsynaptic glutamate receptor fields show aberrant localization. At wild-type NMJs, glutamate receptors are clustered into distinct receptor fields directly apposed to presynaptic active zones. DGluRIII cluster shape is abnormal in act^{E84K} and fused receptor fields are evident opposite presynaptic BRP clusters. Homozygous act^{E84K} mutants are significantly smaller than age matched control animals (Fig. 2.3*C*) (control: 36640 ± 1542 μm^2 muscle area, n=15; act^{E84K}: 12550 ± 580.9 μm^2 muscle area, n=33; $p<0.0001$), and total bouton number per muscle area is slightly increased (Fig. 2.3*D*) (control: $1.5 \times 10^{-03} \pm 0.13 \times 10^{-03}$, n=8; act^{E84K}: $1.9 \times 10^{-03} \pm 0.15 \times 10^{-03}$, n=11; p=0.0381). Total active zone number normalized by bouton number shows a reduction compared to wild-type (Fig. 2.3*E*) (control: 7.54 ± 0.24, n=8; act^{E84K}: 6.165 ± 0.34, n=11; p=0.0071).

One possible explanation for reduced active zone number could be a reduction in bouton volume due to the smaller size of mutant animals. However we find that bouton volume is slightly increased compared to wild- type (Fig. 2.3*F*) (control: 7.47 ± 0.35 μm^3, n=416; act^{E84K}: 8.84 ± 0.49 μm^3, n=273; p=0.0189). Interestingly, active zone density has been shown to remain constant at mammalian and *Drosophila* NMJs (Meinertzhagen et al., 1998; Reiff et al., 2002; Chen et al., 2011; Sigrist and Schmitz, 2011). While control animals have around one active zone per μm^3, we observe a significant shift in density towards fewer active zones per volume in act^{E84K} (Fig. 2.3*G*) (control: 1.12 ± 0.02 AZ/μm^3, n=416; act^{E84K}: 0.76 ± 0.34 AZ/μm^3, n=273; p<0.0001). Detailed analysis shows a tight peak around one active zone per μm^3 bouton volume for control, as expected from the regular distribution of BRP at the NMJ. In mutant animals, the frequency distribution shows a broader peak, demonstrating loss of ordered AZ spacing and a distinct shift towards larger bouton volume per AZ. We conclude that Actin 57B is a key organizer of the postsynaptic protein network that instructs presynaptic NMJ morphology and active zone spacing.

Further analysis of act^{E84K} mutants also revealed defects in active zone apposition. To ensure efficient synaptic transmission, active zones assemble directly opposite neurotransmitter receptor clusters. Occasionally, unapposed active zones occur even in control animals, however at a relatively low rate (Fig. 2.3*H*) (5.474 ± 0.3816 %, n=19). In act^{E84K} mutant animals, BRP puncta without a GluRIII counterpart, or vice versa, are more frequent. Quantification reveals a

significant increase of unapposed active zones (Fig. 2.3*H*) (8.983 ± 0.8459 %, n=19; p=0.0006). Thus, the postsynaptic actin cytoskeleton is a key regulator of synapse assembly, ensuring proper alignment of presynaptic release sites with postsynaptic receptor fields.

2.2.3 Postsynaptic actin cytoskeleton assembly is impaired in *act^{E84K}*

In muscle, actin forms the thin filaments of the sarcomere, which interact with myosin thick filaments and are anchored at the Z-disc. Sarcomeres assemble into myofibrils, which connect to the sarcolemma via interaction of actin with the costamere and the dystrophin-dystroglycan complex (Greener and Roberts, 2000; Dickman et al., 2006; Sparrow and Schöck, 2009). Phalloidin selectively binds to F-actin and can be used to visualize sarcomeric and NMJ actin in wild-type animals (Fig. 2.4*A-C*). Bundled myofibrils are evident in larval body wall muscle of controls. F-actin incorporates into sarcomeric units, assembling each myofibril. The sarcomeric I-band pattern of muscle myofibrils is preserved in age matched *act^{E84K}* mutant larvae, indicating the E84K mutation does not disrupt sarcomere assembly (Fig. 2.4*A*). However, aberrant actin filaments are visible outside of the sarcomeric organization, concentrating around the NMJ (Fig. 2.4*A*). F-actin has previously been shown to localize postsynaptically in a halo around boutons (Coyle et al., 2004; Chen et al., 2005; Nunes et al., 2006; Graf et al., 2009; Ramachandran et al., 2009) (Fig. 2.4*B,C*), forming a key component of the postsynaptic Spectrin cytoskeleton of the NMJ (Bennett and Baines, 2001; Dubreuil and Das, 2009; Wairkar et al., 2009).

Instead of the normal homogenous distribution of actin surrounding boutons, large actin swirls are evident in act^{E84K} (Fig. 2.4*C*), reminiscent of actin wisps seen in β-Spectrin mutants (Pielage et al., 2006; Ramachandran et al., 2009). Together with the location of E84 at the CH domain binding site, our data suggests disruption of β-spectrin interaction with actin filaments is likely to result in aberrant postsynaptic cytoskeletal assembly.

Under carful rearing conditions, act^{E84K} third instar larvae can live up to 6 days without entering the pupal stage. During this time, muscle integrity progressively degenerates and larval locomotion decreases (data not shown). In vertebrate muscle, the costamere protein complex localizes at the muscle membrane above the sarcomere Z-disc. It is necessary for muscle stability during contraction as it connects myofibrils with the sarcolemma and connective tissue (Li et al., 2007; Sparrow and Schöck, 2009; Banovic et al., 2010; Mosca et al., 2012). Recently, orthologs of the costamere have been shown to localize in a similar pattern in *Drosophila* muscle and provide muscle integrity (Wagh et al., 2006; Clark et al., 2007; LaBeau-DiMenna et al., 2012; Clark and Kadrmas, 2013). α- and β- Integrin are known components of the costamere. As transmembrane proteins, they provide the link to the sarcolemma as well as the connective tissue. Additionally, integrins and their binding partners are known to regulate synaptic growth at the NMJ (Marrus, 2004; Tsai et al., 2008; 2012). In control animals βPS-Integrin localizes to the muscle sarcolemma and NMJ (Fig. 2.4*D*). Muscle expression is still present in third instar act^{E84K} larvae, however

NMJ staining is absent (Fig. 2.4*D*). Based on the muscle and locomotor phenotypes observed in older third instar larvae, we hypothesize that mutation of actin 57B destabilizes the connection of actin myofibrils with the costamere complex, causing slow muscle degeneration.

2.2.4 Defects in localization of postsynaptic spectrin cytoskeleton components in *act*^{E84K}

Spectrin was originally identified in erythrocytes after detergent treatment, however it is now known to be expressed in various tissues including the brain (Marchesi and Steers, 1968; Tillack et al., 1970; Fyrberg et al., 1980; Tobin et al., 1980; Bennett et al., 1982). In non-erythrocyte cells however, Spectrin is not uniformly distributed but is thought to establish specialized plasma membrane regions (Stewart et al., 1996; Zito et al., 1999; Dubreuil and Das, 2009). Mammals have 7 Spectrin genes, whereas invertebrate genomes contain three Spectrin genes. However, only α- and β-Spectrin have been detected at the *Drosophila* NMJ (Pielage et al., 2005; Wagh et al., 2006). Interaction of two spectrin repeats at the C-terminus of α-Spectrin with two spectrin repeats at the N-terminus of β-Spectrin leads to formation of anti-parallel heterodimers. Only β-Spectrin can bind to actin via its N-terminal CH domain. Interestingly, two spectrin heterodimers associate into heterotetramers with the CH domains at either end. This enables Spectrin to connect short actin filaments and form a lattice-like protein network at the plasma membrane [reviewed in (Marrus, 2004; Baines, 2010)].

At the *Drosophila* NMJ, α- and β-Spectrin localize both pre- and postsynaptically. Loss of presynaptic Spectrin leads to synapse retraction (Pielage et al., 2005; Graf et al., 2009; Viquez et al., 2009; Wairkar et al., 2009; Valakh et al., 2012; Enneking et al., 2013), whereas postsynaptic Spectrin has been shown to regulate active zone size and spacing (Meinertzhagen et al., 1998; Reiff et al., 2002; Sigrist et al., 2002; Pielage et al., 2006). Our data and the published expression pattern of Actin 57B suggest that mutation of glutamate 84 may alter a critical protein-binding site, leading to disruption of the postsynaptic actin-spectrin network. Immunostaining shows an enrichment of α-Spectrin at the postsynaptic subsynaptic reticulum (SSR) at wild-type NMJs (Fig 2.5*A*). In contrast, act^{E84K} homozygous larvae show a severe redistribution of α-Spectrin (Fig 2.5*A*). High resolution STORM microscopy confirms a loss of α-Spectrin molecules that normally form a postsynaptic halo around boutons (Fig 2.5*B, B'*). Recently it has been shown that Spectrin forms a periodic pattern in axons (Dickman et al., 2006; Pielage et al., 2006; Graf et al., 2009; Wairkar et al., 2009; Xu et al., 2013). Interestingly, presynaptic α-Spectrin appears grossly unaltered in act^{E84K} mutants, showing a similar pattern in axons compared to wild-type (Fig 2.5*C, C'*). This data is consistent with disruption of only the postsynaptic Actin 57B homolog to Spectrin localization, while presynaptic actin-spectrin interactions mediated through distinct Actin gene products are intact.

Spectrin is known to be recruited to actin filaments by the actin-capping protein adducin (Gardner and Bennett, 1987; Bennett et al., 1988; Kuhlman et al.,

1996; Li et al., 1998; reviewed in Clarke et al., 2012). *Drosophila* has a single adducin homolog, Hu-li Tai shao (Hts), which localizes both pre- and postsynaptically at the NMJ and regulates presynaptic synapse stabilization and growth (Fyrberg et al., 1980; Yue and Spradling, 1992; Pielage et al., 2011). Interestingly, adducin is also mislocalized in act^{E84K} mutants (Fig 2.5*D*). Adducin binds to the sides and barbed ends of actin and is a known capping protein (Kuhlman et al., 1996; Li et al., 1998). As discussed above, actin has been shown to form wisps or spikes in $spec^{em6}$ mutants (Ramachandran et al., 2009). However, actin structure at the NMJ of *hts* mutants has not been analyzed previously. Visualization of actin with phalloidin staining reveals a very different distribution in *hts* mutants compared to $spec^{em6}$ or act^{E84K} mutants (Fig. 2.5*E*). Actin is still present surrounding synaptic boutons in the postsynaptic compartment, albeit at reduced levels compared to wild-type NMJs. Strikingly, upon loss of hts, actin rings are present throughout the muscle, which are never observed in act^{E84K} mutants. In summary, the similarities in postsynaptic actin structure between $spec^{em6}$ and act^{E84K} mutants are consistent with loss of Spectrin-actin interactions based on the localization of the mutated E84 residue at the CH domain binding site.

2.2.5 The postsynaptic actin-protein network regulates DLG localization and SSR formation

Similar to vertebrate NMJs, muscle membrane folds enriched in neurotransmitter receptors, cell adhesion molecules and scaffolding proteins

surround type I synaptic boutons in *Drosophila*. Discs-large (DLG), the *Drosophila* PSD-95 homolog, localizes to the subsynaptic reticulum (SSR) and is a key organizer of muscle membrane fold expansion (Lahey et al., 1994; Budnik et al., 1996). Spectrin and adducin regulate targeting of DLG to the NMJ (Featherstone et al., 2001; Pielage et al., 2006; Wang et al., 2011). The disruption of the Spectrin network in act^{E84K} suggested potential DLG mislocalization in the mutants. To test this possibility, we analyzed DLG distribution in control and mutant animals. At wild-type NMJs, immunostaining reveals DLG enrichment at the SSR surrounding presynaptic boutons (Fig 2.6*A*). However, this tight DLG localization is lost in act^{E84K} mutants, with regions of more diffuse staining, as well as boutons with only a thin layer of DLG accumulation (Fig 2.6*B*). Consistent with a disruption in DLG localization, ultrastructural analysis of act^{E84K} mutant NMJs shows a severe disruption of the postsynaptic SSR membrane infoldings that normally surround presynaptic boutons. Electron microscopy sections of wild-type NMJs show numerous membrane folds surrounding each bouton (Fig 2.6*C*). Examination of act^{E84K} boutons reveals a less extensive SSR with fewer membrane layers and a reduction in SSR thickness (Fig 2.6*D*). Occasionally, membrane folds are missing entirely and regions of presynaptic membrane are seen directly abutting muscle myofibrils (Fig 2.6*D*). Preliminary analysis shows that synaptic vesicle (SV) number and vesicle clustering at the active zone is unchanged, consistent with a postsynaptic role for Actin 57B. In summary, our results indicate that interaction

of the main larval muscle Actin with the postsynaptic Spectrin skeleton is necessary for DLG targeting to the postsynaptic region and subsequent SSR formation.

2.2.6 Functional analysis of act^{E84K} mutants

Based on the structural phenotypes, we examined whether synaptic transmission is altered in act^{E84K} mutants. Sharp electrode recordings were carried out in 1 mM Ca^{2+} at muscle fibers 6/7 of 3rd instar larvae with an input resistance greater than 5 MΩ. Both spontaneous and evoked synaptic vesicle release was quantified. Evoked neurotransmitter release was decreased in the mutant (Fig. 2.7*A, B*) (average excitatory junctional potential (EJP) amplitude = control: 33.5 ± 1.8 mV, n=6; act^{E84K}: 18.9 ± 1.7 mV, n=7; $p \leq 0.0001$). A reduction in evoked amplitude could be secondary to presynaptic defects such as reduced SV release or SV size, or postsynaptic defects such as reduced glutamate receptor density or sensitivity. Measurement of spontaneous release amplitude revealed a reduction in the average miniature excitatory junctional potential (MEJP) amplitude compared to wild-type (Fig. 2.7*C, D*) (control: 1.3 ± 0.1 mV, n=10; act^{E84K}: 0.8 ± 0.1 mV, n=11; p=0.0009). Consistent with the reduction in active zone number, mini frequency is also decreased in mutant animals (Fig. 2.7*E*) (control: 2.0 ± 0.1 mV, n=10; act^{E84K}: 1.1 ± 0.2 mV, n=11; p=0.0001). Calculation of quantal content, the number of synaptic vesicles released upon an action potential, shows no significant difference (Fig. 2.7*F*) (control: 30.95 ± 2.2, n=6; act^{E84K}: 33.1 ± 1.8, n=7; p=0.4667), indicating

presynaptic release properties are unchanged in act^{E84K} mutants. Ultrastructural analysis did not reveal any differences in SV size compared to wild-type, arguing against a reduction in vesicular neurotransmitter content. In summary, our results indicate a postsynaptic defect is found in act^{E84K} mutants, manifested as a reduction in EJP and MEJP amplitude, but normal quantal content. The observed defects in active zone spacing, alignment and GluR clustering in act^{E84K} are consistent with the reduction in MEJP and EJP amplitude secondary to a decrease in postsynaptic transmission efficacy. Based on these results, we hypothesize that the impaired synaptic transmission is due to defects in GluR clustering and apposition upon loss of postsynaptic actin cytoskeleton integrity.

2.3 Discussion

Here we provide evidence that an important function of the postsynaptic actin cytoskeleton is to regulate postsynaptic protein organization, as well as presynaptic active zone density and alignment with postsynaptic glutamate receptor fields. In an unbiased EMS screen, we isolated a point mutant of actin 57B, act^{E84K}. In mutant animals the organization of the postsynaptic compartment is severely disrupted, showing prominent F-actin swirls, loss of Spectrin and DLG localization, and defects in SSR integrity. Notably, we demonstrate that actin 57B is required for proper active zone spacing and alignment. Our results indicate that the postsynaptic actin cytoskeleton is essential for establishing postsynaptic protein networks that control trans-synaptic communication and coordinated synapse formation.

2.3.1 Expression of Actin 57B is limited to the postsynaptic compartment

The act^{E84K} allele was isolated based on its striking presynaptic defects. The mapping results were unexpected as actin 57B mRNA is expressed solely in muscle cells in the embryo and larval stages (Fyrberg et al., 1983; Tobin et al., 1990). Additionally, gene expression of actin 57B is regulated by MEF2, a muscle-specific transcription factor (Kelly et al., 2002; Elgar et al., 2008). Although all data in the field indicate Act57B is only expressed in the postsynaptic compartment, we cannot definitely exclude a presynaptic role for the protein in some of the phenotypes. Rescue experiments using an overexpression

construct of wild-type actin 57B should provide this needed insight. Control and mutant constructs under the UAS promoter and carrying a N-terminal myc-tag, were generated and inserted into the *Drosophila* genome using phiC31 integrase mediated targeted insertion (Groth et al., 2004). As act^{E84K} heterozygotes show dominant phenotypes, with less severe, but observable, disruptions in the actin-spectrin cytoskeleton, we did not expect to fully rescue all observed phenotypes given the dominant phenotype. However, heterozygous animals are not larval lethal, but instead develop to adult stages. Unfortunately, overexpression of our constructs with tissue-specific drivers does not rescue larval lethality of the homozygous mutant. Additionally, although myc-tagged actin 57B protein is expressed as tested by Western Blot, it does not localize to the NMJ. From these results, we conclude that although both control and mutant constructs are expressed, they do not yield functional protein. Despite the lack of rescue experiments, the presented data is consistent with the published, exclusively postsynaptic expression of actin 57B. The location of the point mutation in the folded protein suggests impaired binding to members of the CH domain superfamily. In agreement with this hypothesis, postsynaptic Spectrin is severely mislocalized in act^{E84K}. Previous studies have shown very distinct phenotypes upon expression of α- and β- Spectrin RNAi either presynaptically in the neuron or postsynaptically in the muscle. Phenotypes resulting from postsynaptic RNAi expression are intriguingly similar to what we have observed in act^{E84K} mutant animals (Pielage et al., 2006). Postsynaptic knockdown leads to mislocalization

of DLG, impaired SSR formation and most notably to aberrant active zone spacing and increased glutamate receptor cluster size. In contrast, neuronal-specific knockdown of presynaptic Spectrin leads to very different phenotypes, as it is essential for synapse stabilization (Pielage et al., 2005). Evident by loss of presynaptic markers opposite preserved SSR markers, synaptic retraction occurs frequently in these animals. Thus, synapse retractions should be seen in act^{E84K} if the presynaptic actin-Spectrin network had been compromised. This phenotype, however, was not observed. In addition, functional analysis demonstrates a postsynaptic defect in act^{E84K} mutants, in contrast to changes seen upon presynaptic Spectrin RNAi expression or pharmacological disruption of presynaptic actin in cultured hippocampal neurons. Presynaptic Spectrin RNAi expression leads to impaired presynaptic release with a reduction in mini frequency and quantal content (Pielage et al., 2005). These defects are correlated with the severity of synapse disassembly. Additionally, pharmacological disruption of presynaptic actin allows for functional analysis in the absence of the added factor of synapse retraction (Morales et al., 2000). Using this approach, disruption of presynaptic actin has been shown to increase neurotransmitter release probability as manifested in a decreased paired pulse ratio. Conclusions from both studies are in contrast to what we observe in act^{E84K} mutants. The amplitude of evoked and spontaneous release events, as well as the mini frequency, are reduced, while quantal content is unchanged. These results demonstrate a postsynaptic defect in act^{E84K} mutants, resulting from

impaired pre- and postsynaptic alignment and clustering of glutamate receptors. In summary, our data support an exclusively postsynaptic role for actin 57B in organizing synaptic structure.

2.3.2 Mutation of Glutamate E84 disrupts an important protein binding site

Mapping of the isolated actin 57B allele revealed a point mutation in a highly conserved amino acid. Glutamate E84 has previously been shown to participate in binding to the CH domain superfamily (Honts et al., 1994; McGough et al., 1994; Hanein et al., 1997; Hodgkinson et al., 1997; Moores et al., 2000; Galkin, 2002; Sutherland-Smith et al., 2003). Based on our results, we hypothesize that interaction with postsynaptic β-Spectrin is impaired in act^{E84K}. The assembly of prominent F-actin swirls concentrating around the NMJ provided the first indication, as β-$spec^{em6}$ mutants are known to display a similar phenotype (Ramachandran et al., 2009). Loss of appropriate β-Spectrin localization to the postsynaptic SSR region, as well as the discussed similarities with published phenotypes upon expression of postsynaptic Spectrin RNAi, further supports this hypothesis. At this point we cannot rule out that interactions with Adducin, in addition to β -Spectrin, are also impaired in act^{E84K} mutants. Adducin (Hts) is a known actin binding protein, capping the fast growing end and associating with the sides of the actin filament (Mische et al., 1987; Li et al., 1998). Additionally, it is a member of the Spectrin cytoskeleton, facilitating actin-Spectrin binding (Gardner and Bennett, 1987; Matsuoka et al., 2000). The occurrence of actin swirls however is consistent with a disruption of β-Spectrin

binding, since it has to our knowledge only been associated with β-Spectrin mutants. Furthermore, analysis of *hts* mutants reveals a distinct rearrangement of the postsynaptic actin cytoskeleton, exhibiting reduced NMJ localization and aberrant F-actin rings throughout the muscle. Thus, loss of Adducin binding is unlikely to cause the phenotypes we observe.

In addition to β-Spectrin, the CH domain superfamily members dystrophin, utrophin and α-actinin localize postsynaptically and function in muscle structure and at the NMJ [reviewed in (Pilgram et al., 2009; Sparrow and Schöck, 2009)]. Mammalian dystrophin and utrophin are very similar to each other. While dystrophin is present mostly in the nervous system and muscle, utrophin is more widely expressed. *Drosophila* has only one homolog, dystrophin, encoding at least 6 isoforms (Neuman et al., 2005). Both dystrophin and utrophin associate with dystroglycan and other proteins to form the dystrophin-associated glycoprotein complex (DGC). In the muscle, the DGC localizes to the sarcolemma and links myofibrils to the extracellular matrix via the actin binding function of dystrophin. α-actinin also localizes to myofibrils as a component of the Z-disc. Here it provides an anchor site for actin filaments of adjacent sarcomeres and a link to the costamere complex in the sarcolemma via its interaction with integrins. All three members of the CH domain superfamily are essential for muscle integrity in flies and mammals (Moser, 1984; van der Plas, 2006; van der Plas et al., 2007; Clark and Kadrmas, 2013). Mutation of dystrophin in humans causes Duchenne muscular disorder (DMD), a disease characterized by

progressive muscle weakening and mental retardation in one third of patients (Hoffman et al., 1987; Koenig et al., 1987). Similarly, loss of all dystrophin isoforms in muscle using targeted RNAi expression leads to muscle degeneration in *Drosophila* (van der Plas et al., 2007). Therefore, the observed decline in muscle structure and decreased locomotion in late 3rd instar stages of act^{E84K} mutants is likely due to impaired interaction of actin with dystrophin and α-actinin, leading to a gradual loss of muscle integrity. Additionally, the importance of the DGC and α-actinin function has been described at the mammalian and fly NMJ. In mammals, they have been shown to be involved in ACh-receptor clustering via Rapsyn interaction (Wyszynski et al., 1997; Banks et al., 2003; Pilgram et al., 2009; Shi et al., 2012). Furthermore, α-actinin is known to bind to the cytoplasmic tail of NMDA receptors (Wyszynski et al., 1997). At the *Drosophila* NMJ, dystrophin has been implicated in modulating a retrograde signal that limits retrograde neurotransmitter release (van der Plas, 2006). In summary, other CH domain superfamily members besides β-Spectrin carry out important functions at the NMJ and in muscle. It is unlikely that disruption of the CH domain binding site in actin 57B specifically disrupts interaction with the β-Spectrin skeleton. Instead, multiple protein networks are likely to be perturbed in act^{E84K} mutants leading to defects in postsynaptic organization and muscle integrity.

2.3.3 Actin 57B regulates presynaptic active zone spacing and density via a trans-synaptic pathway

We provide evidence for involvement of actin 57B in both pre- and post-synaptic organization. Analysis of act^{E84K} 3rd instar larval NMJs revealed aberrant glutamate receptor clustering, active zone spacing and density. Notably, postsynaptic expression of β-Spectrin RNAi has been shown to disrupt glutamate receptor clustering and presynaptic active zone spacing in a similar fashion to what we observe (Pielage et al., 2006). Pielage et al. propose that the postsynaptic actin-spectrin skeleton forms a grid-like network, providing regular spacing for pre- and postsynaptic organization. In this model, the cell adhesion molecule Fasciclin II (FasII) is thought to integrate into this lattice via its interaction with DLG (Thomas et al., 1997). Thus, FasII is an obvious candidate to mediate trans-synaptic communication also in act^{E84K} mutants. Synaptic clustering of FasII is regulated by direct association with DLG at the NMJ (Thomas et al., 1997; Zito et al., 1997). This interaction is regulated by CaMKII-mediated phosphorylation, which in turn can be activated by increased postsynaptic activity and through a βPS-integrin dependent pathway (Koh et al., 1999; Beumer et al., 2002; Packard, 2003). Intriguingly, both DLG and βPS-integrin are mislocalized at the NMJ in act^{E84K}. Apposition defects have also been described after loss of other cell adhesion molecules, such as Neurexin-Neuroligin and Teneurins (Li et al., 2007; Banovic et al., 2010; Mosca et al., 2012). The *Drosophila* genome contains one Neurexin (DNrx) and four Neuroligin

(DNlg), of which only two have been studied to date (Li et al., 2007; Banovic et al., 2010; Chen et al., 2010; Sun et al., 2011). DNrx and DNlg2 localize primarily presynaptic, while DNlg1 expression is muscle-specific. Teneurins are transmembrane proteins required for synapse organization (Mosca et al., 2012). Ten-a localizes to the presynaptic membrane, whereas Ten-m is predominantly concentrated at the SSR. Upon loss of either the Neurexin-Neuroligin complex or Teneurins, alignment of BRP and DGluRIII is perturbed and ultrastructural analysis shows aberrant active zone structure. Although both cell adhesion complexes function at the NMJ, active zone apposition has been proposed to be mainly regulated by the Neurexin-Neuroligin complex, while Teneurins primarily organize the cytoskeleton (Mosca et al., 2012). Importantly, Ten-m has been shown to interact with the spectrin cytoskeleton, while Neuroligin binds PSD-95 in mammals and recruits DLG in *Drosophila* (Irie, 1997; Banovic et al., 2010; Mosca et al., 2012). Thus, previous studies suggest several cell adhesion pathways that likely mediate trans-synaptic signaling to regulate presynaptic active zone spacing and density. Due to the involvement of postsynaptic actin 57B in multiple protein networks, we hypothesize that the observed phenotypes are not solely due to impairment of a single signaling cascade, but may instead result from disruption of several channels of communication between the pre- and postsynaptic terminals. Future experiments will have to address this intriguing possibility.

Figure 2.1

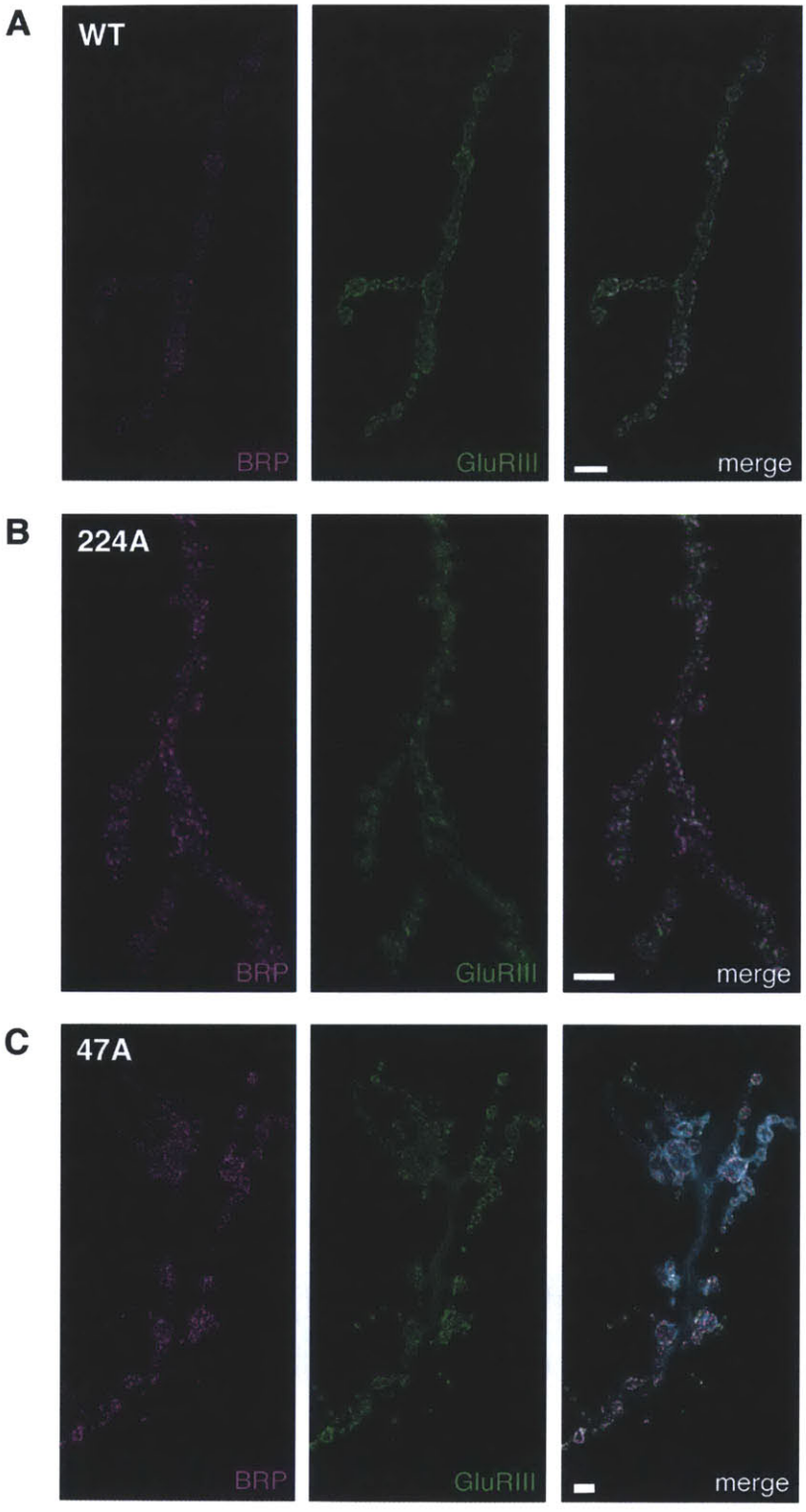
A
WT
BRP
GluRIII
merge
B
224A
BRP
GluRIII
merge
C
47A
BRP
GluRIII
merge

Figure 2.1: *Representative images of mutant alleles isolated in the EMS screen.*

Examples of muscle 4 NMJs stained with BRP and GluRIII in **(A)** wild-type, **(B)** 224A mutant larva. 224A mutant shows abnormal growth with small boutons sprouting from the main arbor. **(C)** Muscle 6/7 NMJ stained with BRP and GluRIII of 47A mutant larva. 47A mutant shows enlarged boutons.

Figure 2.2

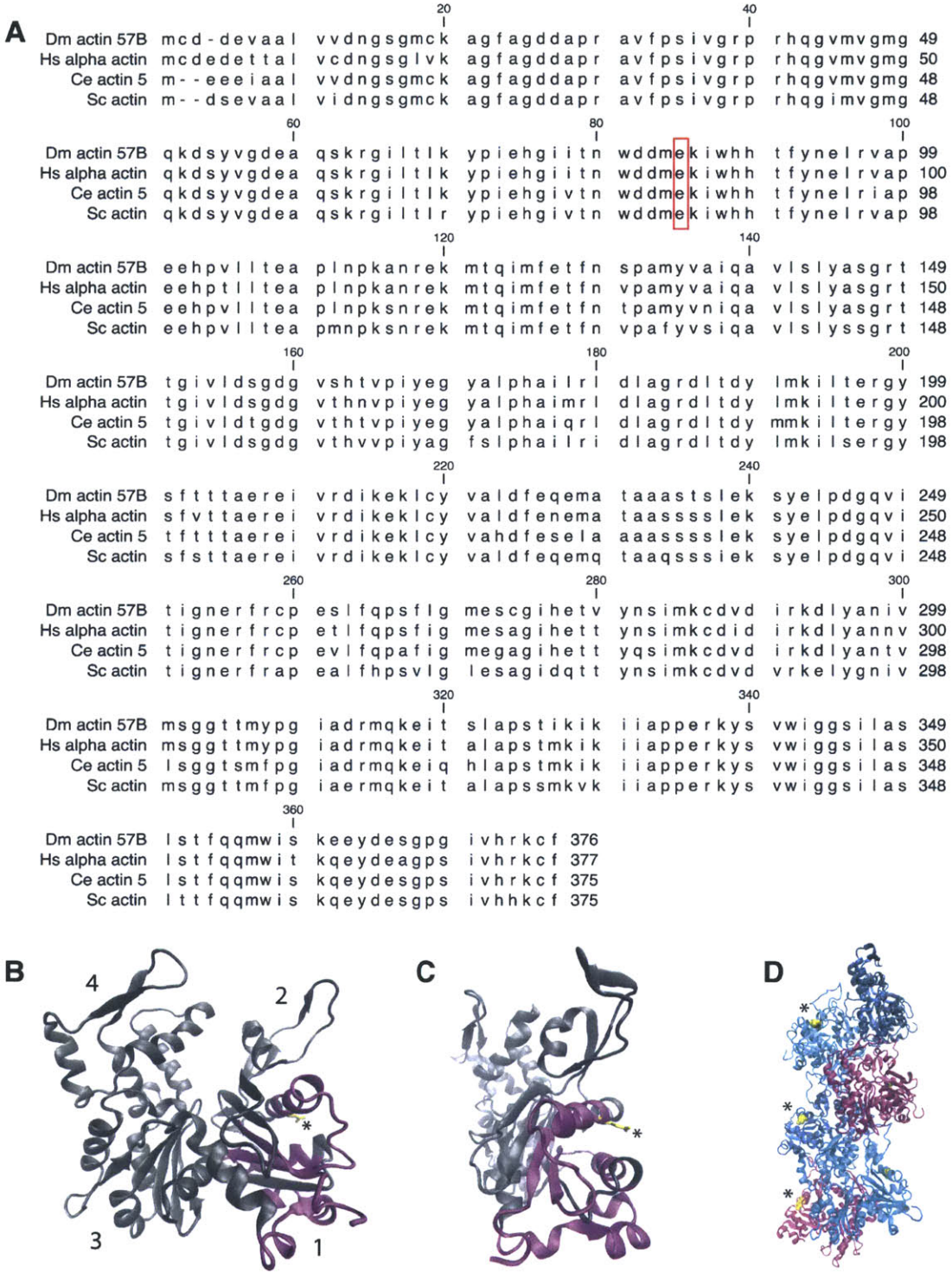
A
20
40
Dm actin 57B mcd-devaal vvdngsgmck agfagddapr avfpsivgrp rhqgvmvgmg 49
Hs alpha actin mcdedettal vcdngsglvk agfagddapr avfpsivgrp rhqgvmvgmg 50
Ce actin 5 m--eeeiaal vvdngsgmck agfagddapr avfpsivgrp rhqgvmvgmg 48
Sc actin m--dsevaal vidngsgmck agfagddapr avfpsivgrp rhqgimvgmg 48
60
80
100
Dm actin 57B qkdsyvgdea qskrgiltlk ypiehgiitn wddmekiwhh tfynelrvap 99
Hs alpha actin qkdsyvgdea qskrgiltlk ypiehgiitn wddmekiwhh tfynelrvap 100
Ce actin 5 qkdsyvgdea qskrgiltlk ypiehgivtn wddmekiwhh tfynelriap 98
Sc actin qkdsyvgdea qskrgiltlr ypiehgivtn wddmekiwhh tfynelrvap 98
120
140
Dm actin 57B eehpvlltea plnpkanrek mtqimfetfn spamyvaiqa vlslyasgrt 149
Hs alpha actin eehptlltea plnpkanrek mtqimfetfn vpamyvaiqa vlslyasgrt 150
Ce actin 5 eehpvlltea plnpksnrek mtqimfetfn tpamyvniqa vlslyasgrt 148
Sc actin eehpvlltea pmnpksnrek mtqimfetfn vpafyvsiqa vlslyssgrt 148
160
180
200
Dm actin 57B tgivldsgdg vshtvpiyeg yalphailrl dlagrdltdy lmkiltergy 199
Hs alpha actin tgivldsgdg vthnvpiyeg yalphaimrl dlagrdltdy lmkiltergy 200
Ce actin 5 tgivldtgdg vthtvpiyeg yalphaiqrl dlagrdltdy mmkiltergy 198
Sc actin tgivldsgdg vthvvpiyag fslphailri dlagrdltdy lmkilsergy 198
220
240
Dm actin 57B sftttaerei vrdikeklcy valdfeqema taaastslek syelpdgqvi 249
Hs alpha actin sfvttaerei vrdikeklcy valdfenema taasssslek syelpdgqvi 250
Ce actin 5 tfttttaerei vrdikeklcy vahdfesela aaasssslek syelpdgqvi 248
Sc actin sfsttaerei vrdikeklcy valdfeqemq taaqsssiek syelpdgqvi 248
260
280
300
Dm actin 57B tignerfrcp eslfqpsflg mescgihetv ynsimkcdvd irkdlyaniv 299
Hs alpha actin tignerfrcp etlfqpsfig mesagihett ynsimkcdid irkdlyannv 300
Ce actin 5 tignerfrcp evlfqpafig megagihett yqsimkcdvd irkdlyantv 298
Sc actin tignerfrap ealfhpsvlg lesagidqtt ynsimkcdvd vrkelygniv 298
320
340
Dm actin 57B msggttmypg iadrmqkeit slapstikik iiapperkys vwiggsilas 349
Hs alpha actin msggttmypg iadrmqkeit alapstmkik iiapperkys vwiggsilas 350
Ce actin 5 lsggtsmfpg iadrmqkeiq hlapstmkik iiapperkys vwiggsilas 348
Sc actin msggttmfpg iaermqkeit alapssmkvk iiapperkys vwiggsilas 348
360
Dm actin 57B lstfqqmwis keeydesgpg ivhrkcf 376
Hs alpha actin lstfqqmwit kqeydeagps ivhrkcf 377
Ce actin 5 lstfqqmwis kqeydesgps ivhrkcf 375
Sc actin lttfqqmwis kqeydesgps ivhhkcf 375
B
4
2
3
1
C
D

Figure 2.2: *Glutamate E84 is a highly conserved residue and part of the binding site of the CH domain superfamily.*

(A) Alignment of *Drosophila* (Dm) actin 57B. Glutamate E84 is highly conserved from yeast to humans. (Hs *Homo sapiens*, Ce *Caenorhabditis elegans*, Sc *Saccharomyces cerevisiae*). **(B-C)** Structure of actin monomer. 1-4 denotes actin subdomains. Glutamate E84 is highlighted in yellow and marked by asterisk. Residues implicated in binding to members of the CH domain superfamily are highlighted in magenta. **(D)** Structure of F-actin. 6 actin monomers are shown. Glutamate E84 localizes to the outside surface of the filament, it is highlighted in yellow and marked by asterisk.

Figure 2.3

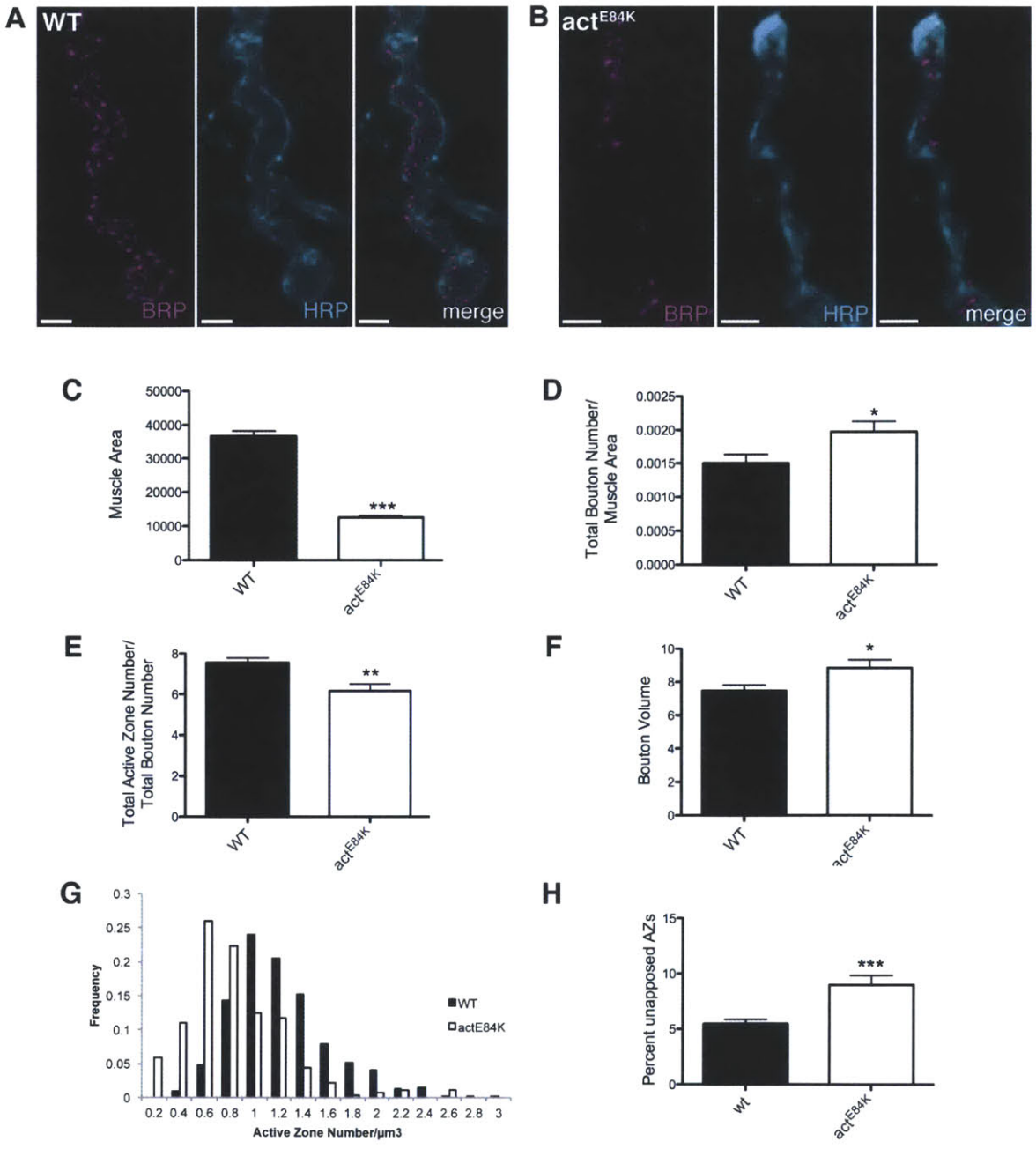
A
WT
BRP
HRP
merge
B
act^E84K
BRP
HRP
merge
C
Muscle Area
50000
40000
30000
20000
10000
0
***
WT
actE84K
D
Total Bouton Number/ Muscle Area
0.0025
0.0020
0.0015
0.0010
0.0005
0.0000
*
WT
actE84K
E
Total Active Zone Number/ Total Bouton Number
8
6
4
2
0
**
WT
actE84K
F
Bouton Volume
10
8
6
4
2
0
*
WT
actE84K
G
Frequency
0.3
0.25
0.2
0.15
0.1
0.05
0
WT
actE84K
0.2 0.4 0.6 0.8 1 1.2 1.4 1.6 1.8 2 2.2 2.4 2.6 2.8 3
Active Zone Number/µm3
H
Percent unapposed AZs
15
10
5
0
***
wt
actE84K

Figure 2.3: *Actin 57B regulates active zone spacing and alignment as well as NMJ morphology.*

(A) BRP puncta are regularly distributed in wild-type boutons. **(B)** Active zone spacing is disrupted in act^{E84K}. **(C)** act^{E84K} larvae are smaller compared to age-matched wild-type larvae. **(D)** Total bouton number is slightly increased in act^{E84K}. **(E)** Active zone density is decreased in act^{E84K}. **(F)** Quantification of bouton volume in wild-type and act^{E84K}. **(G)** The frequency plot shows a shift towards fewer active zones per volume in act^{E84K}. **(H)** Proper alignment of BRP and GluRIII clusters is disrupted and the number of unapposed active zones is increased in act^{E84K}. Scale bar in (A,B) 2μm.

Figure 2.4

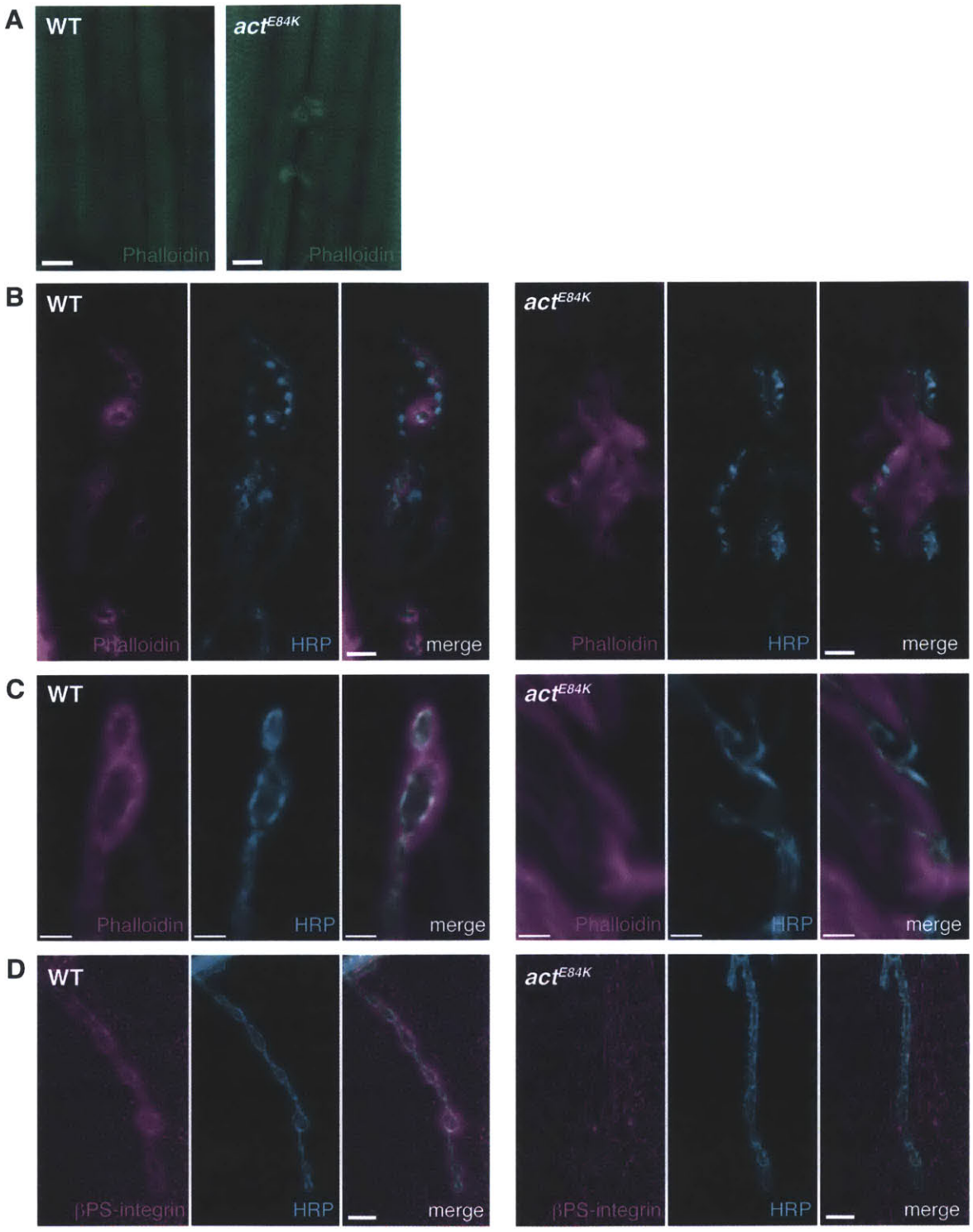
A
WT
act^E84K
Phalloidin
Phalloidin
B
WT
act^E84K
Phalloidin
HRP
merge
Phalloidin
HRP
merge
C
WT
act^E84K
Phalloidin
HRP
merge
Phalloidin
HRP
merge
D
WT
act^E84K
βPS-integrin
HRP
merge
βPS-integrin
HRP
merge

Figure 2.4: *Assembly of the postsynaptic actin cytoskeleton is impaired in* act^{E84K}.

(A) Sarcomere structure is preserved in act^{E84K}. However, actin swirls concentrate around the NMJ. Scale bar 20μm. **(B)** The actin halo seen at wild-type NMJs is disrupted in act^{E84K}. Here, actin swirls surround boutons. Scale bar 10μm. **(C)** Higher magnification of the actin cytoskeleton organization in wild-type and mutant. Scale bar 2μm. **(D)** Localization of βPS-Integrin is disrupted in act^{E84K}. Scale bar 5μm.

Figure 2.5

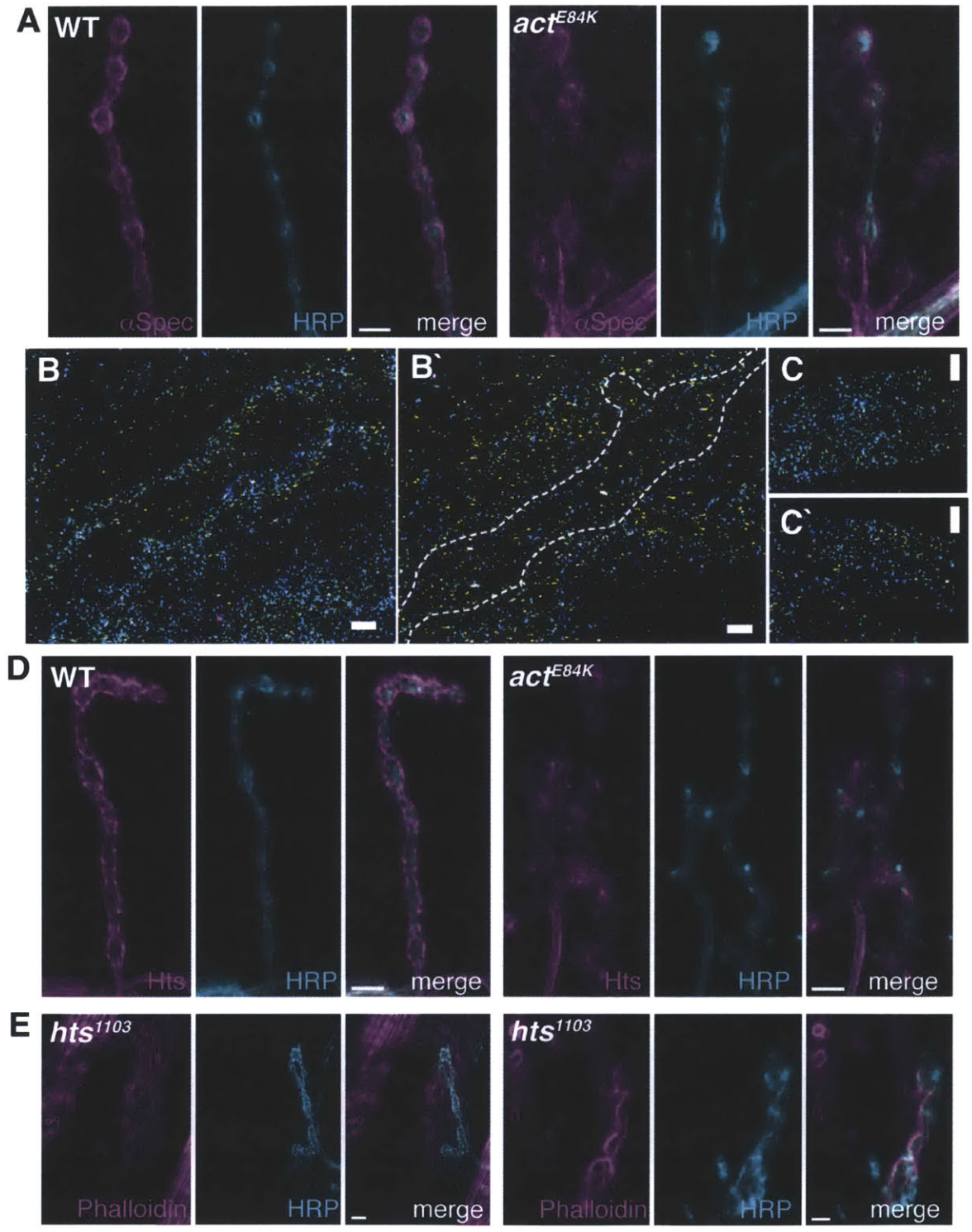
A
WT
αSpec
HRP
merge
act^E84K
αSpec
HRP
merge
B
B`
C
C`
D
WT
Hts
HRP
merge
act^E84K
Hts
HRP
merge
E
hts^1103
Phalloidin
HRP
merge
hts^1103
Phalloidin
HRP
merge

Figure 2.5: *The postsynaptic spectrin skeleton is disrupted in* act^{E84K}.

(A) Localization of the spectrin skeleton component α-Spectrin is disrupted in act^{E84K}. Scale bar 5μm. High resolution **(B, B`)** STORM imaging confirms the mislocalization of α-Spectrin at the NMJ of $act^{E84K}$ animals. **(C, C`)** STORM images of axons in wild-type and act^{E84K} animals. An outline of the NMJ and axon is given in act^{E84K} for clarification. Scale bar 1μm. **(D)** Adducin is mislocalized in act^{E84K}. Scale bar 5μm. **(E)** The postsynaptic actin cytoskeleton organization is disrupted in hts^{1103} mutants. Scale bar 5μm and 2μm.

Figure 2.6

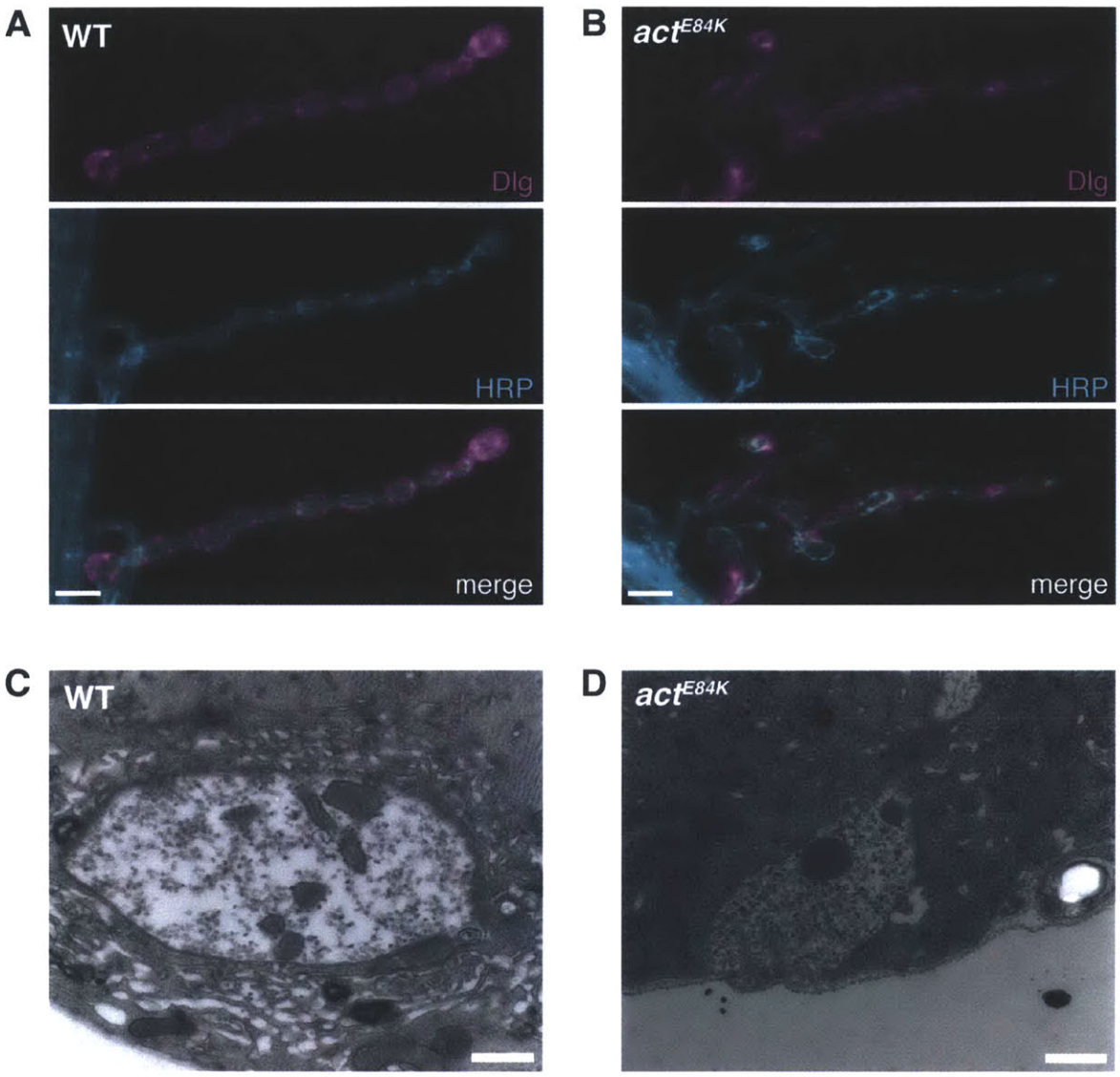

Figure 2.6: *Localization of DLG and SSR formation is disrupted in act^{E84K}.*

(A,B) DLG localizes to the SSR in wild-type animals and is severely mislocalized in *act^{E84K}* mutants. Scale bar 5μm. **(C,D)** Ultrastructural analysis shows severe disruption of the subsynaptic reticulum (SSR). Muscle myofibrils directly abut presynaptic membrane upon loss of SSR membrane folds in *act^{E84K}*. Scale bar 500nm.

Figure 2.7

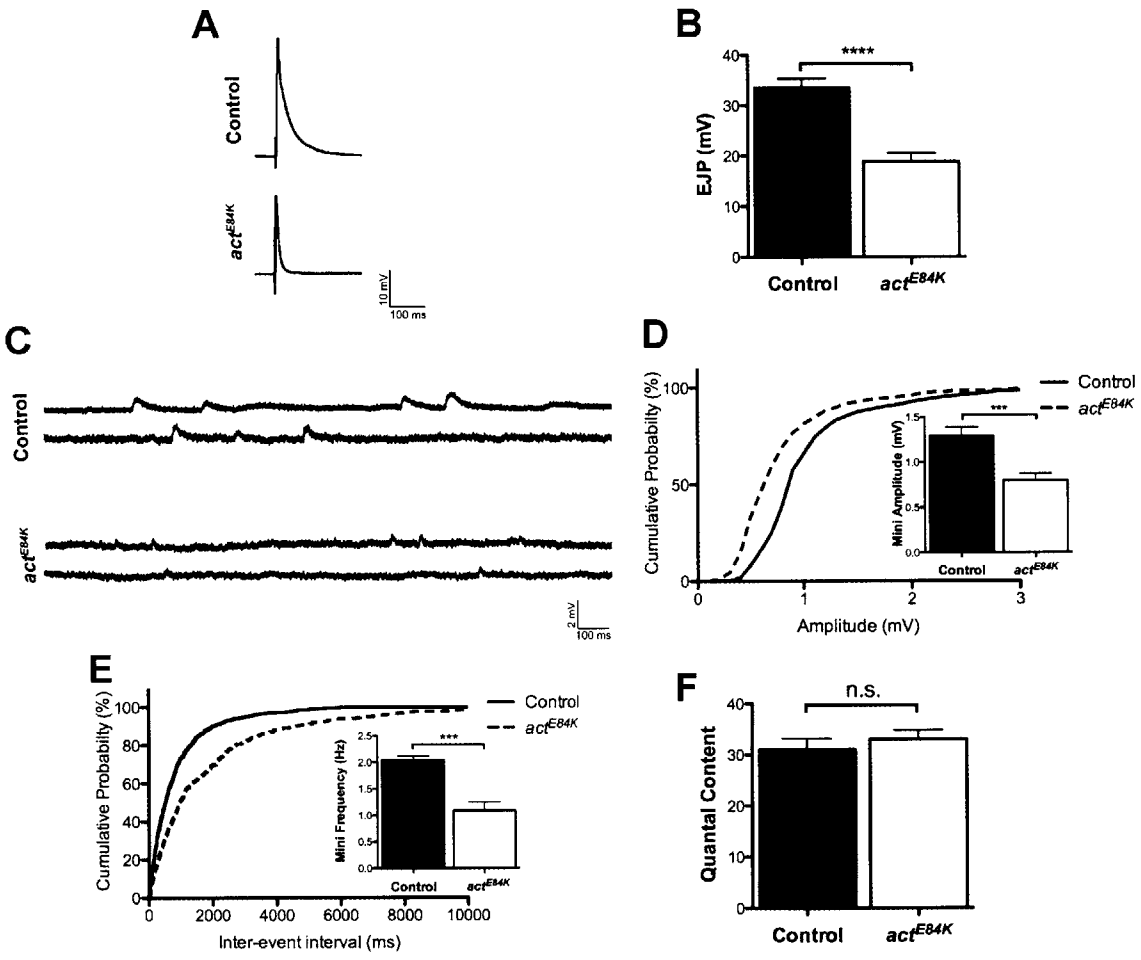
A
Control
act^E84K
10 mV
100 ms
B
EJP (mV)
****
Control
act^E84K
C
Control
act^E84K
2 mV
100 ms
D
Cumulative Probability (%)
Control
act^E84K
***
Mini Amplitude (mV)
Amplitude (mV)
E
Cumulative Probability (%)
Control
act^E84K
***
Mini Frequency (Hz)
Inter-event interval (ms)
F
n.s.
Quantal Content
Control
act^E84K

Figure 2.7: *Functional analysis of act^{E84K} mutants.*

(A, B) Representative traces and quantification of evoked transmitter release. EJP amplitude is significantly decreased in *act^{E84K}*. **(C, D)** Representative traces and quantification of spontaneous transmitter release. MEJP amplitude is reduced in mutant animals. **(E)** Mini frequency is reduced in *act^{E84K}*. **(F)** Quantal content, number of synaptic vesicles release per action potential, is unchanged.

Materials and Methods

EMS screen and fly stocks

The EMS mutagenesis screen was performed according to standard protocols. A Canton-S line was isogenized prior to mutagenesis (wild-type). Each round, 500 isogenized wild-type males were fed 25mM EMS and a total of 5 rounds was performed. Mutagenized males were crossed to virgins of the second chromosome balancer line In(2LR)Gla, wg^{Gla-1}/CyOGFP. Single male progeny was crossed to In(2LR)Gla, wg^{Gla-1}/CyOGFP, and stocks of the mutagenized chromosome/CyOGFP were established. Each line was screened for non-GFP wandering third instar larvae, which were dissected and stained using anti-Bruchpilot and anti- GluRIII antibodies (details see below). Bloomington stock BL1401 wg^{Sp-1} Bl^{1} L^{rm} Bc^{1} Pu^{2} Pin^{B}/SM5 was used for recombination mapping, followed by deficiency mapping and PCR screening.

Homozygous act^{E84K} mutants and age-matched isogenized Canton-S control larvae were reared on molasses plates with yeast paste. Adult flies were allowed to lay eggs for 16hrs. GFP-negative 1^{st} instar larvae were transferred onto fresh plates after 24hrs. 3^{rd} instar larvae were dissected 5 days after the first transfer.

Immunohistochemistry

Age-matched control and act^{E84K} 3^{rd} instar larvae were dissected in cold calcium-free HL3.1 saline (Feng et al., 2004) and fixed for 30 min in HL3.1

containing 4% formaldehyde before antibody staining. Larvae were mounted in Vectashield mounting medium (Vector Laboratories) or Prolong Gold antifade reagent (Invitrogen). The following antibodies were used: mouse anti-Bruchpilot, 1:250 (Wagh et al., 2006) [obtained from Developmental Studies Hybridoma Bank (DSHB)]; rabbit anti-GluRIII, 1:1000 (Marrus, 2004); mouse anti-α-Spectrin, 1:50 (DSHB); rabbit anti-β-Spectrin, 1:500 (gift from R. Dubreuil); mouse anti-DLG, 1:1000 (DSHB); mouse anti-βPS-integrin, 1:50 (DSHB); mouse anti-adducin, 1:50 (DSHB); DyLight 649 conjugated anti-horseradish peroxidase, 1:4000 (Jackson Immunoresearch). Secondary antibodies were conjugated to Alexa-488 or Rhodamine Red-X (Jackson Immunoresearch). Alexa 488 or Rhodamine conjugated phalloidin was used to stain F-actin (Invitrogen).

Imaging and quantification

Larvae were imaged at room temperature either on a Zeiss Axioplan microscope equipped with a LSM510 laser scanning head or a PerkinElmer Ultraview Vox spinning disk confocal microscope using oil-immersion 40x n.a. 1.3, 63x n.a. 1.3 or 100x n.a. 1.3 objectives. Images were acquired with either Pascal or Volocity software depending on the microscope. The postsynaptic actin cytoskeleton was imaged in muscle 12/13, segment A2-A4. Quantification of active zone phenotypes were done on NMJs of muscle 4, segment A3-A4. For quantification of active zone number and alignment, images were deconvolved prior to quantification using the Volocity analysis software. Active zone number per bouton, bouton volume and number of boutons was quantified. For alignment

quantification, the number of unapposed BRP and GluRIII puncta were counted separately. Total active zone number was calculated from total number of BRP puncta plus total number of unapposed GluRIII clusters. Number of total unapposed active zones is the number of unapposed BRP plus the number of unapposed GluRIII, divided by the total active zone number. Statistical analysis was done using Prism software (GraphPad, La Jolla, CA) and error bars represent mean +/- standard error of the mean.

Electron Microscopy

Age-matched control and mutant 3rd instar larvae were dissected, fixed, and processed for electron microscopy as previously described (Akbergenova and Bykhovskaia, 2009). Briefly, dissected larvae were fixed in 1% glutaraldehyde, 4% formaldehyde, 0.1 M sodium cacodylate for 3 h at 4°C. Afterwards samples were washed in HL3.1 for 1 h, wash buffer was changed every 20 min during this time. Then, samples were post-fixed for 30 min in 1% osmium tetroxide, followed by a 20 min wash in distilled water. After dehydration through a graded series of ethanol and acetone, the sample was embedded in Embed 812 epoxy resin (Electron Microscopy Sciences). Thin sections (70–90 nm) were collected on Formvar/carbon coated copper slot grids, and contrasted with 2% uranyl acetate and lead citrate.

Electrophysiology

Analysis of age-matched 3rd instar larvae was performed in modified HL3 solution (70 mM NaCl, 5mM KCl, 4 mM $MgCl_2$, 1 mM $CaCl_2$, 10 mM $NaHCO_3$, 115 mM sucrose, 5 mM HEPES, pH 7.2) at muscle fiber 6, segment A3. To record evoked EJPs, cut nerves were sucked into a pipette filled with working solution and stimulated using a programmable pulse stimulator. Data acquisition and analysis were performed using Clampfit 9.0 software (Axon Instruments, Foster City, CA). Statistical analysis was done using Prism software (GraphPad, La Jolla, CA) and error bars represent mean +/- standard error of the mean.

References

Akbergenova Y, Bykhovskaia M (2009) Molecular and Cellular Neuroscience. Molecular and Cellular Neuroscience 40:199–206.

Atwood HL, Govind CK, Wu CF (1993) Differential ultrastructure of synaptic terminals on ventral longitudinal abdominal muscles in Drosophila larvae. J Neurobiol 24:1008–1024.

Baines AJ (2010) The spectrin–ankyrin–4.1–adducin membrane skeleton: adapting eukaryotic cells to the demands of animal life. Protoplasma 244:99–131.

Banks GB, Fuhrer C, Adams ME, Froehner SC (2003) The postsynaptic submembrane machinery at the neuromuscular junction: requirement for rapsyn and the utrophin/dystrophin-associated complex. J Neurocytol 32:709–726.

Banovic D, Khorramshahi O, Owald D, Wichmann C, Riedt T, Fouquet W, Tian R, Sigrist SJ, Aberle H (2010) Drosophila neuroligin 1 promotes growth and postsynaptic differentiation at glutamatergic neuromuscular junctions. Neuron 66:724–738.

Bennett V, Baines AJ (2001) Spectrin and ankyrin-based pathways: metazoan inventions for integrating cells into tissues. Physiol Rev 81:1353–1392.

Bennett V, Davis J, Fowler WE (1982) Brain spectrin, a membrane-associated protein related in structure and function to erythrocyte spectrin. Nature 299:126.

Bennett V, Gardner K, Steiner JP (1988) Brain adducin: a protein kinase C substrate that may mediate site-directed assembly at the spectrin-actin junction. J Biol Chem 263:5860–5869.

Beumer K, Matthies HJG, Bradshaw A, Broadie K (2002) Integrins regulate DLG/FAS2 via a CaM kinase II-dependent pathway to mediate synapse elaboration and stabilization during postembryonic development. Development 129:3381–3391.

Budnik V, Koh Y, Guan B, Hartmann B, Hough C (1996) Regulation of synapse structure and function by the Drosophila tumor suppressor gene dlg. Neuron.

Chen J, Mizushige T, Nishimune H (2011) Active zone density is conserved during synaptic growth but impaired in aged mice. J Comp Neurol 520:434–452.

Chen K, Gracheva EO, Yu S-C, Sheng Q, Richmond J, Featherstone DE (2010) Neurexin in Embryonic Drosophila Neuromuscular Junctions Mei L, ed. PLoS ONE 5:e11115.

Chen K, Merino C, Sigrist SJ, Featherstone DE (2005) The 4.1 protein coracle

mediates subunit-selective anchoring of Drosophila glutamate receptors to the postsynaptic actin cytoskeleton. J Neurosci 25:6667–6675.

Clark KA, Bland JM, Beckerle MC (2007) The Drosophila muscle LIM protein, Mlp84B, cooperates with D-titin to maintain muscle structural integrity. J Cell Sci 120:2066–2077.

Clark KA, Kadrmas JL (2013) Drosophila melanogastermuscle LIM protein and alpha-actinin function together to stabilize muscle cytoarchitecture: A potential role for Mlp84B in actin-crosslinking. Cytoskeleton:n/a–n/a.

Clarke GL, Chen J, Nishimune H (2012) Presynaptic Active Zone Density during Development and Synaptic Plasticity. Front Mol Neurosci 5:12.

Coyle IP, Koh Y-H, Lee W-CM, Slind J, Fergestad T, Littleton JT, Ganetzky B (2004) Nervous wreck, an SH3 adaptor protein that interacts with Wsp, regulates synaptic growth in Drosophila. Neuron 41:521–534.

Dalva MB, McClelland AC, Kayser MS (2007) Cell adhesion molecules: signalling functions at the synapse. Nat Rev Neurosci 8:206–220.

Dickman DK, Lu Z, Meinertzhagen IA, Schwarz TL (2006) Altered Synaptic Development and Active Zone Spacing in Endocytosis Mutants. Current Biology 16:591–598.

Dubreuil RR, Das A (2009) Spectrin: Organization and Function in Neurons. Encyclopedia of Neuroscience:213–218 Available at: http://dx.doi.org/10.1016/B978-008045046-9.00731-2.

Elgar SJ, Han J, Taylor MV (2008) mef2 activity levels differentially affect gene expression during Drosophila muscle development. Proc Natl Acad Sci USA 105:918–923.

Enneking E-M, Kudumala SR, Moreno E, Stephan R, Boerner J, Godenschwege TA, Pielage J (2013) Transsynaptic Coordination of Synaptic Growth, Function, and Stability by the L1-Type CAM Neuroglian Bellen HJ, ed. PLoS Biol 11:e1001537.

Featherstone DE, Davis WS, Dubreuil RR, Broadie K (2001) Drosophila alpha- and beta-spectrin mutations disrupt presynaptic neurotransmitter release. J Neurosci 21:4215–4224.

Feng Y, Ueda A, Wu C-F (2004) A modified minimal hemolymph-like solution, HL3. 1, for physiological recordings at the neuromuscular junctions of normal and mutant Drosophila larvae. J Neurogenet 18:377–402.

Fyrberg EA, Fyrberg CC, Biggs JR, Saville D, Beall CJ, Ketchum A (1998) Functional nonequivalence of Drosophila actin isoforms. Biochem Genet 36:271–287.

Fyrberg EA, Kindle KL, Davidson N, Kindle KL (1980) The actin genes of Drosophila: a dispersed multigene family. Cell 19:365–378.

Fyrberg EA, Mahaffey JW, Bond BJ, Davidson N (1983) Transcripts of the six

Drosophila actin genes accumulate in a stage- and tissue-specific manner. Cell 33:115–123.

Galkin VE (2002) The utrophin actin-binding domain binds F-actin in two different modes: implications for the spectrin superfamily of proteins. J Cell Biol 157:243–251.

Gardner K, Bennett V (1987) Modulation of spectrin-actin assembly by erythrocyte adducin. Nature 328:359–362.

Giagtzoglou N, Ly C, Bellen H (2009) Cell adhesion, the backbone of the synapse:"vertebrate" and 'invertebrate' perspectives. Cold Spring Harbor Perspectives in Biology 1.

Graf ER, Daniels RW, Burgess RW, Schwarz TL, DiAntonio A (2009) Rab3 Dynamically Controls Protein Composition at Active Zones. Neuron 64:663–677.

Greener MJ, Roberts RG (2000) Conservation of components of the dystrophin complex in Drosophila. FEBS Letters 482:13–18.

Groth AC, Fish M, Nusse R, Calos MP (2004) Construction of transgenic Drosophila by using the site-specific integrase from phage phiC31. Genetics 166:1775–1782.

Hanein D, Matsudaira P, DeRosier DJ (1997) Evidence for a conformational change in actin induced by fimbrin (N375) binding. J Cell Biol 139:387–396.

Hodgkinson JL, EL-Mezgueldi M, Craig R, Vibert P, Marston SB, Lehman W (1997) 3-D image reconstruction of reconstituted smooth muscle thin filaments containing calponin: visualization of interactions between F-actin and calponin. J Mol Biol 273:150–159.

Hoffman EP, Brown RH Jr, Kunkel LM (1987) Dystrophin: the protein product of the Duchenne muscular dystrophy locus. Cell 51:919–928.

Honts JE, Sandrock TS, Brower SM, O'Dell JL, Adams AE (1994) Actin mutations that show suppression with fimbrin mutations identify a likely fimbrin-binding site on actin. J Cell Biol 126:413–422.

Irie M (1997) Binding of Neuroligins to PSD-95. Science 277:1511–1515.

Kelly KK, Meadows SM, Cripps RM (2002) Drosophila MEF2 is a direct regulator of Actin57B transcription in cardiac, skeletal, and visceral muscle lineages. Mech Dev 110:39–50.

Koenig M, Hoffman EP, Bertelson CJ, Monaco AP, Feener C, Kunkel LM (1987) Complete cloning of the Duchenne muscular dystrophy (DMD) cDNA and preliminary genomic organization of the DMD gene in normal and affected individuals. Cell 50:509–517.

Koh YH, Popova E, Thomas U, Griffith LC, Budnik V (1999) Regulation of DLG localization at synapses by CaMKII-dependent phosphorylation. Cell 98:353–363.

Kuhlman PA, Hughes CA, Bennett V, Fowler VM (1996) A new function for adducin. Calcium/calmodulin-regulated capping of the barbed ends of actin filaments. J Biol Chem 271:7986–7991.

LaBeau-DiMenna EM, Clark KA, Bauman KD, Parker DS, Cripps RM, Geisbrecht ER (2012) Thin, a Trim32 ortholog, is essential for myofibril stability and is required for the integrity of the costamere in Drosophila. Proc Natl Acad Sci USA 109:17983–17988.

Lahey T, Gorczyca M, Jia XX, Budnik V (1994) The Drosophila tumor suppressor gene dlg is required for normal synaptic bouton structure. Neuron 13:823–835.

Li J, Ashley J, Budnik V, Bhat MA (2007) Crucial Role of Drosophila Neurexin in Proper Active Zone Apposition to Postsynaptic Densities, Synaptic Growth, and Synaptic Transmission. Neuron 55:741–755.

Li X, Matsuoka Y, Bennett V (1998) Adducin preferentially recruits spectrin to the fast growing ends of actin filaments in a complex requiring the MARCKS-related domain and a newly defined oligomerization domain. J Biol Chem 273:19329–19338.

Marchesi VT, Steers E (1968) Selective solubilization of a protein component of the red cell membrane. Science 159:203–204.

Marrus SB (2004) Differential Localization of Glutamate Receptor Subunits at the Drosophila Neuromuscular Junction. Journal of Neuroscience 24:1406–1415.

Matsuoka Y, Li X, Bennett V (2000) Adducin: structure, function and regulation. Cell Mol Life Sci 57:884–895.

McGough A, Way M, DeRosier D (1994) Determination of the alpha-actinin-binding site on actin filaments by cryoelectron microscopy and image analysis. J Cell Biol 126:433–443 Available at: http://jcb.rupress.org/content/126/2/433.full.pdf#page=1&view=FitH.

Meinertzhagen IA, Govind CK, Stewart BA, Carter JM, Atwood HL (1998) Regulated spacing of synapses and presynaptic active zones at larval neuromuscular junctions in different genotypes of the flies Drosophila and Sarcophaga. J Comp Neurol 393:482–492.

Mische SM, Mooseker MS, Morrow JS (1987) Erythrocyte adducin: a calmodulin-regulated actin-bundling protein that stimulates spectrin-actin binding. J Cell Biol 105:2837–2845.

Moores CA, Keep NH, Kendrick-Jones J (2000) Structure of the utrophin actin-binding domain bound to F-actin reveals binding by an induced fit mechanism. J Mol Biol 297:465–480.

Morales M, Colicos MA, Goda Y (2000) Actin-dependent regulation of neurotransmitter release at central synapses. Neuron 27:539–550.

Mosca TJ, Hong W, Dani VS, Favaloro V, Luo L (2012) Trans-synaptic Teneurin

signalling in neuromuscular synapse organization and target choice. Nature:1–7.

Moser H (1984) Duchenne muscular dystrophy: pathogenetic aspects and genetic prevention. Human genetics 66:17–40.

Neuman S, Kovalio M, Yaffe D, Nudel U (2005) The Drosophila homologue of the dystrophin gene – Introns containing promoters are the major contributors to the large size of the gene. FEBS Letters 579:5365–5371.

Nishimune H (2012) Active zones of mammalian neuromuscular junctions: formation, density, and aging. Annals of the New York Academy of Sciences 1274:24–32.

Nunes P, Haines N, Kuppuswamy V, Fleet DJ, Stewart BA (2006) Synaptic vesicle mobility and presynaptic F-actin are disrupted in a N-ethylmaleimide-sensitive factor allele of Drosophila. Mol Biol Cell 17:4709–4719.

Packard M (2003) FASt remodeling of synapses in Drosophila. Current Opinion in Neurobiology 13:527–534.

Petersen SA, Fetter RD, Noordermeer JN, Goodman CS, DiAntonio A (1997) Genetic analysis of glutamate receptors in Drosophila reveals a retrograde signal regulating presynaptic transmitter release. Neuron 19:1237–1248.

Pielage J, Bulat V, Zuchero JB, Fetter RD, Davis GW (2011) Hts/Adducin Controls Synaptic Elaboration and Elimination. Neuron 69:1114–1131.

Pielage J, Fetter RD, Davis GW (2005) Presynaptic spectrin is essential for synapse stabilization. Curr Biol 15:918–928.

Pielage J, Fetter RD, Davis GW (2006) A postsynaptic spectrin scaffold defines active zone size, spacing, and efficacy at the Drosophila neuromuscular junction. J Cell Biol 175:491–503.

Pilgram GSK, Potikanond S, Baines RA, Fradkin LG, Noordermeer JN (2009) The Roles of the Dystrophin-Associated Glycoprotein Complex at the Synapse. Mol Neurobiol 41:1–21.

Ramachandran P, Barria R, Ashley J, Budnik V (2009) A critical step for postsynaptic F-actin organization: Regulation of Baz/Par-3 localization by aPKC and PTEN. Devel Neurobio 69:583–602.

Reiff DF, Thiel PR, Schuster CM (2002) Differential regulation of active zone density during long-term strengthening of Drosophila neuromuscular junctions. Journal of Neuroscience 22:9399–9409.

Shi L, Fu AKY, Ip NY (2012) Molecular mechanisms underlying maturation and maintenance of the vertebrate neuromuscular junction. Trends in Neurosciences 35:441–453.

Sigrist SJ, Schmitz D (2011) Structural and functional plasticity of the cytoplasmic active zone. Current Opinion in Neurobiology 21:144–150.

Sigrist SJ, Thiel PR, Reiff DF, Schuster CM (2002) The postsynaptic glutamate receptor subunit DGluR-IIA mediates long-term plasticity in Drosophila. Journal of Neuroscience 22:7362–7372.

Sparrow JC, Schöck F (2009) The initial steps of myofibril assembly: integrins pave the way. Nat Rev Mol Cell Biol 10:293–298.

Stewart BA, Schuster CM, Goodman CS, Atwood HL (1996) Homeostasis of synaptic transmission in Drosophila with genetically altered nerve terminal morphology. J Neurosci 16:3877–3886.

Sun M, Xie W (2012) Cell adhesion molecules in Drosophila synapse development and function. Sci China Life Sci 55:20–26.

Sun M, Xing G, Yuan L, Gan G, Knight D, With SI, He C, Han J, Zeng X, Fang M, Boulianne GL, Xie W (2011) Neuroligin 2 Is Required for Synapse Development and Function at the Drosophila Neuromuscular Junction. J Neurosci 31:687–699.

Sutherland-Smith AJ, Moores CA, Norwood FLM, Hatch V, Craig R, Kendrick-Jones J, Lehman W (2003) An Atomic Model for Actin Binding by the CH Domains and Spectrin-repeat Modules of Utrophin and Dystrophin. J Mol Biol 329:15–33.

Thomas U, Kim E, Kuhlendahl S, Koh YH, Gundelfinger ED, Sheng M, Garner CC, Budnik V (1997) Synaptic clustering of the cell adhesion molecule fasciclin II by discs-large and its role in the regulation of presynaptic structure. Neuron 19:787–799.

Tillack TW, Marchesi SL, Marchesi VT, Steers E (1970) A comparative study of spectrin: a protein isolated from red blood cell membranes. Biochim Biophys Acta 200:125–131.

Tobin S, Zulauf E, Sanchez F, Craig E (1980) Multiple actin-related sequences in the Drosophila melanogaster genome. Cell.

Tobin SL, Cook PJ, Burn TC (1990) Transcripts of individual Drosophila actin genes are differentially distributed during embryogenesis. Dev Genet 11:15–26.

Tsai P-I, Kao H-H, Grabbe C, Lee Y-T, Ghose A, Lai T-T, Peng K-P, Van Vactor D, Palmer RH, Chen R-H, Yeh S-R, Chien C-T (2008) Fak56 functions downstream of integrin alphaPS3betanu and suppresses MAPK activation in neuromuscular junction growth. Neural Dev 3:26.

Tsai P-I, Wang M, Kao H-H, Cheng Y-J, Lin Y-J, Chen R-H, Chien C-T (2012) Activity-dependent retrograde laminin A signaling regulates synapse growth at Drosophila neuromuscular junctions. Proceedings of the National Academy of Sciences 109:17699–17704.

Valakh V, Naylor SA, Berns DS, DiAntonio A (2012) A large-scale RNAi screen identifies functional classes of genes shaping synaptic development and

maintenance. Dev Biol:1–9.

van der Plas MC (2006) Dystrophin Is Required for Appropriate Retrograde Control of Neurotransmitter Release at the Drosophila Neuromuscular Junction. Journal of Neuroscience 26:333–344.

van der Plas MC, Pilgram GSK, de Jong AWM, Bansraj MRKS, Fradkin LG, Noordermeer JN (2007) Drosophila Dystrophin is required for integrity of the musculature. Mech Dev 124:617–630.

Viquez NM, Fuger P, Valakh V, Daniels RW, Rasse TM, Diantonio A (2009) PP2A and GSK-3 Act Antagonistically to Regulate Active Zone Development. Journal of Neuroscience 29:11484–11494.

Wagh D, Rasse T, Asan E, Hofbauer A, Schwenkert I, Durrbeck H, Buchner S, Dabauvalle M, Schmidt M, Qin G (2006) Bruchpilot, a Protein with Homology to ELKS/CAST, Is Required for Structural Integrity and Function of Synaptic Active Zones in Drosophila. Neuron 49:833–844.

Wairkar YP, Toda H, Mochizuki H, Furukubo-Tokunaga K, Tomoda T, Diantonio A (2009) Unc-51 Controls Active Zone Density and Protein Composition by Downregulating ERK Signaling. J Neurosci 29:517–528.

Wang S, Yang J, Tsai A, Kuca T, Sanny J, Lee J, Dong K, Harden N, Krieger C (2011) Drosophila adducin regulates Dlg phosphorylation and targeting of Dlg to the synapse and epithelial membrane. Dev Biol:1–12.

Wyszynski M, Lin J, Rao A, Nigh E, Beggs AH, Craig AM, Sheng M (1997) Competitive binding of alpha-actinin and calmodulin to the NMDA receptor. Nature 385:439–442.

Xu K, Zhong G, Zhuang X (2013) Actin, Spectrin, and Associated Proteins Form a Periodic Cytoskeletal Structure in Axons. Science 339:452–456.

Yue L, Spradling AC (1992) hu-li tai shao, a gene required for ring canal formation during Drosophila oogenesis, encodes a homolog of adducin. Genes & Development 6:2443–2454.

Zito K, Fetter RD, Goodman CS, Isacoff EY (1997) Synaptic clustering of Fasciclin II and Shaker: essential targeting sequences and role of Dlg. Neuron 19:1007–1016.

Zito K, Parnas D, Fetter RD, Isacoff EY, Goodman CS (1999) Watching a synapse grow: noninvasive confocal imaging of synaptic growth in Drosophila. Neuron 22:719–729.

CHAPTER 3

A presynaptic endosomal trafficking pathway controls synaptic growth signaling

Aline Dorret Blunk[1], Avital Rodal[1,2], Yulia Akbergenova[1], Ramon A. Jorquera[1], Lauren K. Buhl[1] and J. Troy Littleton[1]

[1]The Picower Institute of Learning and Memory, Department of Brain and Cognitive Sciences, Massachusetts Institute for Technology, Cambridge, MA 02139

[2]The Department of Biology, Brandeis University, Waltham, MA 02453

Aline Blunk performed Y2H experiments characterizing the Nwk-SNX16 interaction, generated transgenic lines that disrupt this interaction to analyze *in vivo*, characterized SNX16 localization *in vivo* and analyzed synaptic growth in *snx16* LOF and double mutants. Avital Rodal characterized Nwk-SNX16 interaction using GST pull-down and performed all live imaging experiments. She also analyzed synaptic growth in the mutant lines and demonstrated SNX16 function at the branch point to the MVB. Ramon Jorquera performed electrophysiology and Yulia Akbergenova performed electron microscopy.

This chapter has been published (Rodal et al., 2011)

3.1 Introduction

Growth factor signaling in neurons controls the expansion of synaptic arbors in response to activity and external stimuli, leading to long-lasting changes in synapse strength and connectivity that underlie learning and memory. Receptor complexes regulating growth factor signal transduction are internalized via endocytosis and directed to specific subcellular membrane compartments from which they exhibit distinct signaling properties, due to compartment-specific post-translational modifications and degradative events, or interactions with local binding partners (Sadowski et al., 2008). Therefore, defining the mechanisms by which the rate and direction of flow of endosomal protein traffic are controlled is critical to determining how neuronal signal transduction pathways are tuned up and down after activation. A host of protein factors control membrane traffic through the interconnected tubules and vesicles of the endosomal system, and sorting occurs by isolation of cargo in membrane domains of defined geometry and lipid composition (Bonifacino and Rojas, 2006). Proteins modulating membrane dynamics and organization are thus well positioned to control the sorting and activities of signaling complexes during endosomal processing.

The *Drosophila* larval neuromuscular junction (NMJ) serves as a useful model for regulation of synaptic growth signaling as the muscle surface area expands 100-fold over four days of larval development, requiring increased input from its innervating motor neuron to drive contraction. NMJ synaptic arbors expand by adding matched pre- and post-synaptic specializations (termed

synaptic boutons) in response to motor neuron synaptic activity, retrograde signals from the muscle to the neuron, and anterograde signals from the neuron to the muscle (McCabe et al., 2003; Packard et al., 2002; Yoshihara et al., 2005). Mutants in proteins regulating endocytosis fail to properly attenuate growth factor signaling at the NMJ, resulting in abnormal overgrowth of the synaptic arbor, with the hallmark phenotype of increased arbor branching and the formation of "satellite" boutons off the main axis of the axon terminal (Dickman et al., 2006). One such gene, *nervous wreck* (*nwk*), encodes a neuron-specific member of the F-BAR (Fes/CIP4 homology Bin-Amphiphysin-Rvs)/SH3 (Src Homology 3) family of lipid-binding proteins that control the force-generating assembly of actin filaments at endosomal compartments by activating WASp (Wiskott-Aldrich Syndrome protein)/Arp2/3 (Actin-related protein 2/3)-mediated actin polymerization (Coyle et al., 2004). Nwk attenuates the retrograde BMP (Bone Morphogenic Protein) signal mediated by Glass Bottom Boat (Gbb) through its presynaptic receptor Thickveins (Tkv) (O'Connor-Giles et al., 2008), co-localizes with the recycling endosome marker Rab11 and functions together with the endosomal GTPase Cdc42 to control WASp/Arp2/3-mediated actin assembly (Rodal et al., 2008). However, the mechanisms by which Nwk attenuates synaptic growth factor signaling at this compartment are unknown.

Here we describe the identification of a novel Nwk binding partner, Sorting Nexin 16 (SNX16). SNX16 is a member of the Sorting Nexin family of proteins that regulate endosomal traffic and are defined by a phosphoinositide-binding PX

(Phox Homology) domain (Hanson and Hong, 2003; Choi et al., 2004; Cullen, 2008). We demonstrate that SNX16- and Nwk-containing compartments transiently interact in nerve terminals and that signaling at early endosomes is attenuated either through Nwk-SNX16 interactions or through ESCRT (Endosomal Sorting Complex Required for Transport)-mediated internalization into the endosomal lumen. SNX16/Nwk-mediated traffic regulates synaptic growth signaling cascades, including the BMP and Wingless (Wg) pathways, and is specifically required to down-regulate activated receptors. Our results provide a mechanism by which protein traffic between endosomal intermediates at synapses controls the output of signal transduction pathways leading to synaptic growth.

3.2 Results

3.2.1 Nwk physically interacts with SNX16

Nwk is a predicted lipid-binding protein that activates actin polymerization *in vitro* through WASp/Arp2/3 (Rodal et al., 2008), and thus may define an actin-dependent step of endocytosis critical for the down-regulation of growth factor signaling at the *Drosophila* NMJ. However, the specific mechanism by which it acts is unclear. To elucidate the function of Nwk in membrane traffic, we conducted a yeast two-hybrid screen using full-length Nwk as bait, and identified a carboxy terminal fragment (aa 236-407) of the *Drosophila CG6410* gene product as a Nwk-interacting protein. We named this gene *Snx16*, as it encodes the single *Drosophila* homolog of the mammalian protein Sorting Nexin 16 (SNX16), which is involved in membrane traffic at endosomal compartments (Choi et al., 2004; Hanson and Hong, 2003). SNX16 homologs are found in animals ranging from insects to mammals (Suppl. Fig. S1), but neither *Snx16* nor *nwk* is recognizable in *C. elegans*. *Drosophila* SNX16 consists of a poorly conserved amino terminal region, a highly conserved PX domain (which is predicted to bind to phosphoinositides), and a conserved carboxy terminal coiled-coil domain.

To define the domains of Nwk and SNX16 required for their interaction, we generated a series of deletion constructs and assayed their ability to interact in the yeast two-hybrid assay (Fig. 3.1A). SNX16-Nwk interactions required a region

of the SNX16 coiled-coil domain near the PX domain (aa 346-363). Three glutamate residues in this region are highly conserved in all examined Snx16 homologs (Fig. 3.1B), and mutation of these three glutamates to alanine (E347A, E350A, E351A, hereafter referred to as $SNX16^{3A}$) abolished yeast two-hybrid interactions between full-length Nwk and SNX16 (246-407). The SNX16-binding site on Nwk mapped to aa 637-700, encompassing the second SH3 domain. However, the mutation W677A, which disrupts the ability of this SH3 domain to bind to proline-rich targets (Rodal et al., 2008), did not abolish the Nwk-SNX16 interaction, suggesting that binding is not mediated by canonical interactions of the SH3 domain.

To validate the Nwk-SNX16 interaction observed in the yeast two-hybrid assay, we conducted GST pull-down assays from *Drosophila* head extracts. GST-SNX16 (335-407; coiled coil domain) precipitated endogenous Nwk from *Drosophila* head extracts (Fig. 3.1C). Endogenous SNX16 is expressed at low levels and was difficult to detect with our antibodies; therefore we overexpressed SNX16 or SNX16-GFP using the GAL4/UAS system (Brand and Perrimon, 1993) and the pan-neuronal GAL4 driver $elav^{C155}$, and evaluated the ability of this overexpressed protein to associate with Nwk in *Drosophila* head extracts. SNX16 and SNX16-GFP each associated specifically with GST-Nwk (1-731), but not GST alone (Fig. 3.1D). In addition, GST-Nwk (1-731) co-precipitated with recombinant SNX16 (220-407; PX and coiled coil domain) from *E. coli* extracts, but only poorly with $SNX16^{3A}$ (220-407) (Fig. 3.1E). As we were unable to detect

association of endogenous SNX16 with Nwk by co-immunoprecipitation (unpublished data) and only a small proportion of SNX16 or Nwk in extracts precipitated with its reciprocal GST-tagged binding partner, we hypothesize that the interaction between Nwk and SNX16 is transient and likely regulated by additional protein or lipid binding partners.

3.2.2 SNX16 localizes to early endosomes

Mammalian SNX16 promotes the traffic of growth factor receptors from early to late endosomes (Choi et al., 2004; Hanson and Hong, 2003). To determine the cellular compartment in which *Drosophila* SNX16 acts, we first localized SNX16 in cultured *Drosophila* cells. SNX16-GFP and SNX16-mCherry localized to the perimeter of intracellular structures that were distributed throughout the cell interior, but excluded from the nucleus (Fig. 3.2A and 3.2B). Localization of SNX16-GFP to these structures was severely reduced upon treatment with wortmannin, a phosphatidylinositol-3-kinase inhibitor, consistent with the predicted affinity of the SNX16 PX domain for phosphatidylinositol-3-phosphate (PI(3)P) and suggesting that the PX domain is critical for SNX16 association with endomembranes (Fig 3.2A). We co-transfected cells with SNX16-mCherry or SNX16^{3A}-mCherry and tagged markers of early endosomes (GFP-Rab5) and recycling endosomes (GFP-Rab11) and spread them on Concanavalin A for better resolution of internal structures (Rogers et al., 2003).

SNX16 co-localized with a subset of Rab5-positive structures (Pearson's correlation coefficient (PCC) of 0.41 +/- 0.11, n=4), but only poorly with Rab11 (PCC of 0.11 +/- 0.01, n=5) (Fig. 3.2B). SNX16^{3A}-mCherry localization was similar to SNX16-mCherry (Fig. 3.2B). We then transfected *Drosophila* cells with the human transferrin receptor and assessed endocytic uptake of its labeled ligand, transferrin. Transferrin was not recycled back to the cell surface in these cells, as has previously been shown in similar cell types (Van Hoof et al., 2005), but instead accumulated in an intracellular compartment labeled by Rab5 and SNX16, but not Rab11 (Fig 3.2C, PCC of 0.64 vs 0.45). We conclude that SNX16 resides in an early endosomal compartment that is a functional site of receptor-mediated endocytosis. Finally, we expressed Nwk-GFP in cultured cells. While other F-BAR proteins induce massive lipid tubulation when expressed in cultured cells (Frost et al., 2009), Nwk localization was primarily cytoplasmic, with occasional faint intracellular puncta. When SNX16-mRFP was co-expressed in these cells, we observed that Nwk-GFP structures overlapped with a small subset of SNX16 puncta (Fig. 3.2D, PCC of 0.83 +/- 0.01, n=5). Thus, Nwk and SNX16 partially co-localize in heterologous cells.

We next localized SNX16 at the *Drosophila* NMJ using the pan-neuronal GAL4 driver *elav*^{C155}, as we were unable to detect endogenous Snx16 in embryos or larvae using our antisera (Suppl. Fig. S2). Both SNX16 and SNX16-GFP localized to several bright puncta in each synaptic bouton, which overlapped well with the early endosomal markers Rab5 and Rab4 (Fig. 3.3A-B) but not the

recycling endosome marker Rab11 (Fig. 3.3C). 80.9% +/- 8.6% of SNX16 puncta per NMJ overlapped with Rab5 puncta (n=5 NMJs) and 77.2 +/- 15.1% of SNX16 puncta per NMJ overlapped with Rab4 puncta (n=4 NMJs). It has previously been reported that the BMP receptor, Tkv, which is misregulated in *nwk* mutants (O'Connor-Giles et al. 2008), resides in Rab5-positive endosomal structures at the NMJ (Wang et al., 2007), and we found that SNX16 puncta co-localized with Tkv-GFP (Fig. 3.3D, 35.3 +/- 10.2% of SNX16 puncta overlapped with Tkv-GFP puncta; n=5 NMJs). SNX16-GFP also co-localized with the presynaptic portion of Hrs (Lloyd et al., 2002), a component of the ESCRT complex that drives internalization of cargo into the endosomal lumen (Fig. 3.3E). 49.4 +/- 3.7% of SNX16-GFP puncta overlapped with Hrs puncta (n=5 NMJs, note that Hrs is predominantly postsynaptic with a more minor presynaptic component (Lloyd et al., 2002), and that only this fraction of presynaptic Hrs puncta contain neuronally expressed SNX16). Finally, immuno-electron microscopy with anti-GFP antibodies detected both SNX16-GFP and $SNX16^{3A}$-GFP on the outside surface of ~200 nm diameter compartments at the NMJ (Fig. 3.3F), in which internal vesicles could sometimes be seen. Thus, we conclude that SNX16 localizes primarily to early endosomes and multi-vesicular bodies (MVBs) that are sites of receptor traffic at the *Drosophila* larval NMJ.

3.2.3 Nwk localizes to a novel compartment that transiently interacts with SNX16 endosomes at the NMJ

In fixed tissue, Nwk localizes to a synaptic subdomain termed the "periactive zone" (Roos and Kelly, 1999; Sone et al., 2000) that closely surrounds sites of synaptic vesicle release. SNX16-GFP puncta localized within or adjacent to Nwk-positive periactive zones in fixed NMJs, but it was difficult to infer the nature of their functional relationship from this localization. We reasoned that analysis of the dynamic localization of SNX16 and Nwk relative to each other would provide more information about their relationship. Pan-neuronally expressed Nwk-mRFP (Fig. 3.4A, previously described in (O'Connor-Giles et al., 2008)) rescues the temperature sensitive seizure phenotype of *nwk* mutant adult *Drosophila* (unpublished data), suggesting that it encodes a functional protein. In contrast to the periactive zone localization of either endogenous or overexpressed a-Nwk immunoreactivity in fixed tissue (Coyle et al., 2004; Rodal et al., 2008), Nwk-mRFP localized diffusely in live nerve terminals, with several bright puncta per NMJ (Fig. 3.4B; 2.6 +/- 0.5 particles/ NMJ on muscle 6/7 in segments A2 and A3, n=5 NMJs). However, when these samples were fixed and extracted with detergents for antibody staining, mRFP fluorescence collapsed towards more defined structures in each bouton, similar to endogenous or overexpressed, untagged Nwk, and bright puncta were difficult to distinguish in or near these structures (Fig. 3.4C). Since we had not previously identified these Nwk puncta in fixed tissue, we stained fixed, extracted Nwk-mRFP larvae with

anti-Nwk and anti-mRFP antibodies (Fig. 3.4C and unpublished data). Neither antibody recognized Nwk-mRFP puncta in fixed, extracted tissue, suggesting that the Nwk puncta are in a structure that is poorly accessible to antibodies and disrupted upon detergent extraction. These results suggest that the previously described periactive zone localization of Nwk is likely triggered by fixation and extraction, and that the diffuse and occasionally punctate localization of Nwk-mRFP observed in live tissue reflects a physiologically relevant pattern.

To further understand the nature of the Nwk compartment, we co-localized Nwk-mRFP with GFP-Rab11. Nwk and Rab11 co-localize in fixed cells (Rodal et al., 2008) and Rab11 is a marker of the recycling endosome. GFP-Rab11 exhibited a very similar pattern in live NMJs to Nwk-mRFP (largely diffuse with occasional puncta), and many GFP-Rab11 puncta co-localized (Fig. 3.4D) and moved together (unpublished data) with Nwk-mRFP puncta. Thus, the Nwk compartment has features of a recycling endosome, which in diverse cell types acts to recycle endocytosed cargo from early endosomes to the plasma membrane.

We imaged the dynamics of Nwk and SNX16 compartments using spinning disk confocal microscopy to rapidly record their positions. Nwk-mRFP and SNX16-GFP particles moved within synaptic boutons with no apparent directionality. Nwk puncta made frequent contact with SNX16 puncta and sometimes Nwk and SNX16 puncta translocated together within the bouton for several seconds, and then separated (Fig. 3.4 E). In each NMJ, Nwk particles

contacted SNX16 particles an average of 1.2 +/- 0.40 times/min, or 0.78 +/- 0.45 times/min/Nwk particle (n=14 particles in 5 NMJs). These results suggest that Nwk and SNX16 exist in independent compartments that transiently interact, perhaps leading to exchange of cargo.

Transfer of cargo-containing membranes is likely to require a scission event, and Nwk interacts with dynamin (O'Connor-Giles et al., 2008; Rodal et al., 2008), a GTPase that drives membrane scission (Mettlen et al., 2009). We therefore reasoned that acute inhibition of dynamin with the small molecule inhibitor dynasore (Macia et al., 2006) might block the transfer of membranes between SNX16 and Nwk compartments. To validate the use of dynasore in *Drosophila*, we tested if dynasore treatment mimics the synaptic vesicle endocytosis defects in the dynamin mutant *Shibire*^{ts1}, which exhibits progressive rundown of the evoked excitatory post-synaptic currents (EPSCs) during high-frequency stimulation of the nerve (Delgado et al., 2000), while wild-type NMJs decline to a semi-steady state that is sustained by vesicle recycling. Indeed, dynasore (but not vehicle treatment) causes a progressive run-down of EPSCs (Suppl. Fig. S3). To test the role of dynamin in Nwk-SNX16 particle interactions, we treated dissected larvae with dynasore under conditions that cycle through the entire NMJ pool of dynamin (Ramaswami et al., 1994) and then fixed them without extraction for imaging of puncta. We found that 53.9 +/- 8.4 % Nwk-mRFP particles colocalized or collapsed adjacent to a SNX16-GFP particle upon treatment with dynasore (Fig. 3.4F; n=59 particles in 15 NMJs). In contrast, only

17% +/- 7.6% of Nwk-mRFP particles were found colocalizing or near to a SNX16-GFP particle in control DMSO treatments (Fig. 3.4F; n=35 particles in 16 NMJs). Thus, dynamic interactions between Nwk and SNX16 particles in NMJs depend on dynamin, suggesting that their associations may lead to exchange of membrane and/or cargo between compartments.

3.2.4 Nwk attenuates the growth-promoting activity of SNX16

To explore the function of SNX16 at the NMJ using genetics, we overexpressed *Snx16*-GFP and the Nwk-binding mutant $Snx16^{3A}$-GFP in the nervous system using the GAL4 driver $elav^{C155}$. Wild-type *Snx16*-GFP overexpressing larval NMJs exhibit a small but significant increase in bouton number compared to wild-type controls (Fig. 3.5A-D). However, when we overexpressed $Snx16^{3A}$-GFP, we observed a much more dramatic NMJ overgrowth phenotype with excessive branching of axon terminal arbors, similar to the *nwk* mutant phenotype, with an increase in both overall bouton number and satellite bouton number (Fig. 3.5A-D). We recapitulated this result with two independent transgenic insertions of $Snx16^{3A}$-GFP (Fig. 3.5B-D), and verified that expression levels were similar between wild-type and mutant transgenes (unpublished data).

To evaluate if the overexpression phenotype of *Snx16*-GFP was related to its function with Nwk, we tested if co-overexpression of Nwk could alter the

synaptic overgrowth phenotype of SNX16 overexpression. Nwk overexpression on its own does not cause a synaptic growth phenotype (Fig. 3.5E; Rodal et al, 2008; O'Connor-Giles et al. 2008). We found that co-overexpression of Nwk-mRFP (but not a control RFP transgene) suppresses the synaptic overgrowth phenotype resulting from overexpression of wild-type *Snx16*-GFP, but notably not *Snx16*^{3A}-GFP (Fig. 3.5E), suggesting that the *Snx16* phenotype results from an imbalance in specific Nwk-SNX16 physical interactions and substantiating these interactions *in vivo*. Finally, we tested if BMP signaling, which is upregulated in Nwk mutants (O'Connor-Giles et al. 2008) was also increased upon overexpression of *Snx16*, by measuring the levels of Trio protein, a Rac GTPase exchange factor whose expression is directly increased by BMP signals (Ball et al., 2010). Trio protein levels were increased at the NMJ in *Snx16*-GFP and *Snx16*^{3A}-GFP-expressing larvae (Fig. 3.5E). These results suggest that interactions of Snx16 with Nwk are critical for attenuation of synaptic growth signals downstream of BMP signaling.

Two models are consistent with the synaptic overgrowth phenotype resulting from *Snx16*^{3A}-GFP overexpression. One interpretation is that Snx16 positively regulates and acts upstream of Nwk together with some additional factor, and upon overexpression of *Snx16*^{3A}-GFP, this factor is titrated away from endogenous Nwk, resulting in a *nwk* loss-of-function phenotype. The second interpretation is that *nwk* negatively regulates *Snx16*, and SNX16^{3A}-GFP is thus an overactive form of the protein that drives unregulated synaptic growth. To

distinguish the order in which *nwk* and *Snx16* act, we generated loss-of-function alleles of *Snx16*. In the first model described above, *nwk; Snx16* double mutants would be expected to phenocopy *nwk* mutants. In the second model, *nwk; Snx16* mutants would be expected to phenocopy *Snx16* mutants.

We used two complementary sources for loss-of-function alleles of *SNX16*. First, we obtained a PiggyBac transposable element insertion (PBac[RB]CG6410^{e01600}) that disrupts the coding region of *Snx16* (*Snx16*^{PB}), 366 bp downstream of the Snx16 start codon (Fig. 3.6A). This allele reduces *Snx16* transcript to 1% of the wild-type level in quantitative RT-PCR, but does not affect the adjacent gene *CG10934* (Fig. 3.6B). Second, we imprecisely excised a P element (P[EPgy2]EY10175) inserted 51 bp 5' of the predicted transcriptional start site of *Snx16*, resulting in deletion of the entire *SNX16* coding region (Fig. 3.6A). Animals containing heterozygous combinations of *Snx16* mutant alleles with each other and with the 20-gene deficiency Df(2R)Exel7150 were viable and fertile. We examined NMJ morphology in these animals and found no statistically significant phenotype compared to genetically matched controls (Fig. 3.6C-D), although there was a trend towards reduced synaptic growth.

To examine the genetic relationship between *nwk* and *Snx16*, we generated double mutants of the null allele *nwk*^{2} (Coyle et al., 2004) with *Snx16* mutants, and found that allelic combinations of *Snx16*^{PB}, *Snx16*^{D1}, and *Snx16*^{D2} significantly suppressed synaptic overgrowth in *nwk*^{2} mutant larvae compared to genetically matched controls (Fig. 3.6 C-D). The *nwk* mutant synaptic overgrowth

phenotype was restored in *Snx16*; *nwk* double mutants by re-expression of wild-type *Snx16* in neurons (Fig. 3.6 C), though we note that this rescue construct also produces mild synaptic overgrowth phenotypes in a wild-type background (Fig. 3.5 A). Taken together, our results show that multiple different loss-of-function alleles of *Snx16* suppress the *nwk* mutant phenotype. We also tested if upregulated BMP signaling in nwk^2 (O'Connor Giles et al. 2008) was suppressed by *Snx16* and found that both phosphorylated Mad (Mothers against decapentaplegic, the downstream target of BMP receptors) and Trio protein levels at the NMJ were increased in *nwk* and suppressed in $Snx16^{PB}$; nwk^2 (Fig. 3.6E). These results rule out the model that Snx16 acts as an upstream activator of Nwk, as in that case *Snx16* mutants would be expected to phenocopy the *nwk* mutant, and instead indicate that synaptic overgrowth in *nwk* mutants results from a failure to downregulate the growth-promoting activity of *Snx16*.

3.2.5 Snx16 is required for synaptic growth mediated by the BMP and Wg signaling cascades

Synaptic growth at the *Drosophila* larval NMJ requires the coordinated activities of several signal transduction cascades (Marques and Zhang, 2006). One such pathway has been demonstrated to function downstream of Nwk (O'Connor-Giles et al., 2008) and acts downstream of a retrograde signal mediated by the BMP family member Gbb and its receptors Tkv, Wit (Wishful

Thinking), and Sax (saxophone) (Marques and Zhang, 2006). Another prominent pathway is the presynaptic component of a cascade mediated by Wg (Wingless) and its receptors dFz2 (Frizzled 2) and Arr (arrow) (Franco et al., 2004; Miech et al., 2008). We tested if Snx16 functions to promote signaling in these two pathways by generating double mutants between *Snx16* and BMP and Wg pathway mutants.

Dad (daughters against decapentaplegic) is a negative regulator of BMP signaling, and loss-of-function mutations in *dad* cause excessive BMP signaling and synaptic overgrowth (O'Connor-Giles et al., 2008; Sweeney and Davis, 2002). Loss of *Snx16* strongly suppressed synaptic overgrowth in *dad* mutants (Fig 3.7A). In addition, the synaptic overgrowth phenotypes caused by overexpression of Snx16-GFP and $Snx16^{3A}$-GFP were both suppressed by loss-of-function mutations in *wit*, the BMP receptor. These results suggest that like *nwk*, synaptic growth mediated by *Snx16* requires BMP signaling. To test the involvement of the Wg pathway, we employed *sgg* (*shaggy*) /Glycogen Synthase Kinase-3b, which is negatively regulated by Wg. A dominant negative *Sgg* mutant (sgg^{DN}) expressed in neurons mimics the presynaptic component of activated Wg signaling and causes synaptic overgrowth (Franco et al., 2004). Mutation of *Snx16* suppressed synaptic overgrowth caused by sgg^{DN} (Fig. 3.7B). Nwk has not previously been implicated in Wg signaling, so we tested if the synaptic overgrowth phenotype in *nwk* requires the activity of the Wg pathway, Loss-of-function mutations in *arrow*, the Wg co-receptor, cause only subtle synaptic

growth defects (Fig. 3.7B and Miech et al., 2009), but strongly suppress synaptic overgrowth in *nwk*, similar to results with *nwk* and BMP pathway mutants that have previously implicated Nwk in BMP signaling (O'Connor-Giles et al., 2008; Rodal et al. 2008). These results suggest that BMP and Wg-mediated synaptic growth requires *Snx16* and that Nwk/SNX16-mediated membrane traffic is broadly used to constrain a variety of synaptic growth signals.

Overexpression of an activated version of the BMP receptor, Tkv^{Q199D}, which signals in the absence of ligand and co-receptor (Hoodless et al., 1996; Wieser et al., 1995), enhances the synaptic overgrowth phenotype of *nwk* mutants (O'Connor-Giles et al., 2008). We tested whether this mutant receptor might elucidate the fate of signaling receptors in the absence of Nwk-SNX16 interactions by co-overexpressing it in the *Snx16*-GFP and $Snx16^{3A}$-GFP overexpressing backgrounds. Strikingly, we found that tkv^{Q199D} dramatically enhanced the synaptic overgrowth phenotype of $Snx16^{3A}$-GFP but had no effect on *Snx16*-GFP (Fig. 3.7C), suggesting that activated receptors were acutely sensitive to Nwk-SNX16-mediated traffic. Previously, we and others have not been able to detect rerouting of endogenous or overexpressed wild-type signaling receptors at steady state in *nwk* mutant NMJs (O'Connor-Giles et al., 2008; Rodal et al., 2008). We reasoned that the activated receptor, which is sensitive to this genetic background, might reveal a subpopulation of redistributed receptor. Indeed, we found that Tkv^{Q199D} (but not endogenous Tkv) was primarily found at the plasma membrane at steady-state in *Snx16*-GFP-

expressing NMJs, but accumulated in intracellular structures including Snx16-positive endosomes in *Snx16*^{3A}-GFP expressing NMJs (Fig. 3.7D), suggesting that Tkv^{Q199D} is specifically rerouted in this mutant, resulting in increased signaling.

3.2.6 Hrs downregulates receptor signaling in the absence of SNX16

While a dominant active Nwk-binding mutant of SNX16 promotes synaptic growth, loss-of-function *Snx16* mutants suppress synaptic growth, suggesting that SNX16 has a growth-promoting activity at the early endosome separate from its negative regulatory Nwk-binding activity. We hypothesized that since SNX16 is a peripheral membrane protein on endosomes, it may act by limiting the internalization of activated receptors into multivesicular bodies (MVB) via the ESCRT pathway (Raiborg et al., 2009). In this model (Fig. 3.8A), attenuation of receptor signaling is balanced between SNX16/Nwk-mediated sorting to the recycling endosome and ESCRT-mediated internalization of receptor into the endosomal lumen, with SNX16 representing a branch point between these two pathways. We predicted that if MVB formation were inhibited, *Snx16* loss-of-function mutants would produce synaptic overgrowth, the opposite phenotype from that of *Snx16*; *nwk*, *Snx16*; *dad*, or *Snx16*; *sgg*^{DN} double mutants. To test this hypothesis, we made double mutants between *Snx16* and *hrs*^{D28}, a mutant in a component of the ESCRT machinery (Lloyd et al., 2002). Hrs is broadly used in many cell types for endosomal cargo traffic, and both *hrs* single and *hrs*; *Snx16* double mutants are sick and die between early larval and early pupal stages. We

examined NMJ growth in single and double mutants. *hrs* mutants have been shown to have no defect in synaptic growth (Lloyd et al., 2002); however, *hrs; Snx16* double mutants exhibited significant over-proliferation of overall bouton number and satellite bouton number compared to *hrs* single mutants (Fig. 3.8B), in sharp contrast to the reduction in synaptic growth in the *Snx16* mutant backgrounds (Figs. 3.6 and 3.7). These results suggest that receptor signaling in *Snx16* animals is attenuated by internalization into the endosomal lumen, whereas animals containing wild-type *Snx16* do not depend on MVB function to attenuate signaling, presumably due to SNX16/Nwk-mediated sorting to the recycling endosome.

To further explore the relationship between MVB formation and Snx16 function, we used electron microscopy to examine the ultrastructure of synaptic boutons in *Snx16*-GFP and *Snx16*^{3A}-GFP overexpressing larvae, where synaptic overgrowth is apparent (Fig. 3.5). Morphologically distinct MVBs are rarely observed in thin sections of wild type synaptic boutons by electron microscopy but were frequently observed in *Snx16*^{3A}-GFP overexpressing boutons (Fig. 3.8 C). We hypothesize that this increase in MVB formation results from stalled membrane traffic at the early endosome when SNX16/Nwk-mediated traffic is disrupted. Taken together, these results support a model in which SNX16 functions at the intersection of a branch point in endosomal traffic of synaptic growth receptors from the early endosome to either the recycling endosome or to a degradative MVB pathway.

3.3 Discussion

Endocytic membrane traffic regulates signaling by synaptic growth factor receptors and may be used as a point of control in tuning receptor traffic in response to neuronal activity. The neuronal F-BAR/SH3 protein Nwk is involved in endocytic membrane traffic that attenuates synaptic growth signaling, but the mechanism by which it acts has been unknown. Here we identified a physical interaction between Nwk and the early endosomal protein SNX16 that is critical for downregulating the synaptic growth-promoting activity of SNX16. This interaction may bring together the actin polymerizing activity of the first SH3 domain of Nwk (Rodal et al. 2008) with the potential lipid-binding/tubulating activities of the F-BAR domain of Nwk and the PX domain of SNX16, driving tubule-based membrane flux from early to recycling endosomes.

3.3.1 Function of the interaction between Nwk and SNX16

Sorting nexins form a large family of proteins that share a common phosphoinositide-binding PX domain and are involved in diverse aspects of membrane traffic (Cullen, 2008). The best-characterized members of this family are the Snx-BAR family, including Snx1 (tied to endosome-to-golgi traffic) and Snx9 (tied to the internalization step of endocytosis), which each contains both a lipid-tubulating BAR domain and a PX domain. Crystal structures and functional studies of Snx9 have shown that its BAR and PX domains form a single lipid

binding and deforming module with combined specificities that neither domain exhibits alone (Pylypenko et al., 2007; Wang et al., 2008a; Yarar et al., 2008). As such, SNX16/Nwk interactions may form an analogous F-BAR/PX module via an intermolecular rather than intramolecular interaction. We have not been able to purify sufficient amounts of SNX16 to directly test its effects on lipid binding by Nwk; therefore further analysis of their interaction will require an approach to isolate SNX16 *in vitro*. Interestingly, the SNX16-Nwk interaction depends on a region of Nwk surrounding its second SH3 domain, raising the possibility that this region of Nwk may exert intramolecular effects on the N-terminal F-BAR domain, as has previously been shown for other F-BAR proteins (Rao et al., 2010). Further, Nwk binds to the coiled-coil region of SNX16 (Fig. 3.1), which is involved in SNX16 dimerization (Choi et al., 2004; Hanson and Hong, 2003), suggesting that Nwk may act on SNX16 by affecting its dimerization state.

Mammalian SNX16 has been implicated in trafficking of the EGF receptor from early to late endosomes, which may mediate downregulation of receptor signaling (Choi et al., 2004; Hanson and Hong, 2003). However, the mechanism by which SNX16 promotes this trafficking step is not understood and no loss-of-function studies on SNX16 have been reported. A mutant of mammalian SNX16 that lacks 60 amino acids corresponding to the *Drosophila* SNX16 Nwk-binding site (Fig. 3.1B), blocks trafficking of SNX16 and EGF to late endosomes, leading to increased EGF signaling (Hanson and Hong, 2003). Interestingly, the F-BAR protein FBP17 has been reported to interact with SNX2 (Fuchs et al., 2001).

These results raise the possibility that BAR family-sorting nexin interactions may be broadly used to control membrane traffic in cells.

3.3.2 Synaptic growth signaling is attenuated by transient interactions between SNX16 and Nwk compartments

We found that *Drosophila* SNX16 localizes to an early endosomal compartment at the NMJ defined by the small GTPases Rab4 and Rab5 (Figs. 3.2 and 3.3). This compartment accumulates signaling receptors such as the BMP receptors Tkv and Wit (Fig. 3.3 and (Wang et al., 2007)), and signaling is amplified when receptors are stalled in this compartment (Wang et al., 2007), suggesting that the SNX16 compartment is an active site of signaling. By identifying specific *Snx16* mutants that disrupt interactions with Nwk, we were able to separate the requirements for receptor downregulation at early endosomes and show that activated receptors specifically require SNX16/Nwk mediated traffic to recycle to the plasma membrane (Fig. 3.7).

We previously observed that Nwk co-localizes with the recycling endosome marker Rab11 in fixed tissue and cooperates with Cdc42, which is thought to function at the recycling endosome, to activate WASp/Arp2/3-mediated actin polymerization (Rodal et al., 2008). Together with the result that *rab11* mutants exhibit synaptic overgrowth similar to *nwk* mutants (Khodosh et al., 2006), we concluded that Nwk functions at recycling endosomes, which are

downstream of early endosomes. Here we show that Nwk tagged with fluorescent proteins localizes to novel punctate structures in heterologous cells (Fig. 3.2) and nerve terminals (Fig. 3.4). These puncta had not been observed using anti-Nwk antibodies against either endogenous or overexpressed Nwk in fixed tissue (Rodal et al. 2008), as they are poorly preserved upon fixation (Fig. 3.4). In living synapses, Rab11 co-localizes with Nwk to mobile puncta, SNX16-containing early endosomes interact transiently with Nwk puncta, and inhibition of the GTPase dynamin blocks separation of these compartments (Fig. 3.4). Dynamin inhibition has previously been shown to disrupt endosomal function in the fly NMJ (Wucherpfennig et al., 2003), so we cannot be certain that the collapse of SNX16-Nwk compartments under these conditions is due to the specific interactions of these proteins with dynamin. However, since SNX16-Nwk interactions lead to downregulation of synaptic growth signals, our data is consistent with a model in which exchange of receptors from the SNX16 endosome to the Nwk/Rab11 endosome leads to attenuation of receptor signaling. Binding of Nwk to the cytoplasmic tail of the BMP receptor Tkv may mediate this event (O'Connor-Giles et al., 2008), but further experiments will be required to directly examine cargo transfer in the future. Since there are significant cytoplasmic pools of both Nwk and SNX16, we also cannot exclude the contribution of these soluble proteins to membrane traffic in the nerve terminal, or the possibility that overexpression of Nwk and Snx16 in order to visualize live trafficking events does not faithfully recapitulate the behaviors of

endogenous proteins. However, the transient interaction of Nwk and SNX16 puncta correlates well with our genetic results showing that *nwk* attenuates a synaptic growth-promoting activity of *Snx16* at early endosomes.

Since Nwk and SNX16-labeled compartments transiently interact in nerve terminals, temporal control of the interaction between their lipid-binding domains may provide a mechanism to acutely drive membrane tubulation in a regulated fashion. Further, the association of SNX16 with endosomes depends on phosphoinositides, as the PI(3)-kinase inhibitor wortmannin disrupts localization of SNX16 in cultured cells (Fig. 3.2), indicating that regulation of phospholipid composition may also contribute to the membrane deforming activities of SNX16 and Nwk.

3.3.3 SNX16 acts at a branch point between endosomal sorting pathways

We found that *Snx16* loss of function mutants suppress synaptic overgrowth resulting from loss of Nwk-mediated traffic as well as from activation of Wg and BMP signaling pathways (Figs. 3.6 and 3.7). These data suggest that SNX16 plays an active role in promoting synaptic growth at the endosome, aside from its function in signal attenuation through Nwk. We found that Snx16 is required to restrict synaptic growth when MVB formation is hampered in *hrs* mutants (Fig. 3.8), suggesting that receptor entry into the endosomal lumen is an alternative signal attenuation pathway. Further, we found that overexpression of

a mutant *Snx16* that cannot bind Nwk promotes the accumulation of endosomal structures at the NMJ (Figs. 3.7D and 3.8C) and drives excess synaptic growth, suggesting that Snx16 may play an role in MVB maturation and acts at the branch point between endosomal sorting pathways. Defining the mechanism by which SNX16 promotes synaptic growth will require further structure-function analysis of the active domains of the protein aside from its Nwk-binding coiled-coil.

3.3.4 Activity-dependence of synaptic receptor endocytosis

Traffic through endocytic compartments has proven to be a critical point of regulation in the nervous system. Synaptic vesicle endocytosis is controlled by synaptic activity through calcium-dependent dephosphorylation of endocytic proteins (Cousin, 2009), and postsynaptic trafficking of AMPA receptors through the recycling endosome is increased in response to activity via the calcium-dependent motor myosin V (Wang et al., 2008b). Rab5-positive compartments at the *Drosophila* NMJ have been previously characterized for their role in the synaptic vesicle cycle (Wucherpfennig et al., 2003), and it will be interesting to determine how receptor-mediated endocytosis and synaptic vesicle endocytosis are coordinately or separately regulated in response to activity. Synaptic growth at the *Drosophila* NMJ is positively regulated by calcium influx through voltage-gated calcium channels (Rieckhof et al., 2003), and endosome number increases

in response to activity (Akbergenova and Bykhovskaia, 2009). It is tempting to speculate that calcium influx acts through conserved mechanisms for modulating membrane dynamics to delay the attenuation of receptor signaling by SNX16/Nwk-mediated traffic, leading to increased synapse growth in response to activity. A key future goal will be to determine specific points of activity-dependent regulation of membrane traffic in presynaptic endosomes.

Figure 3.1

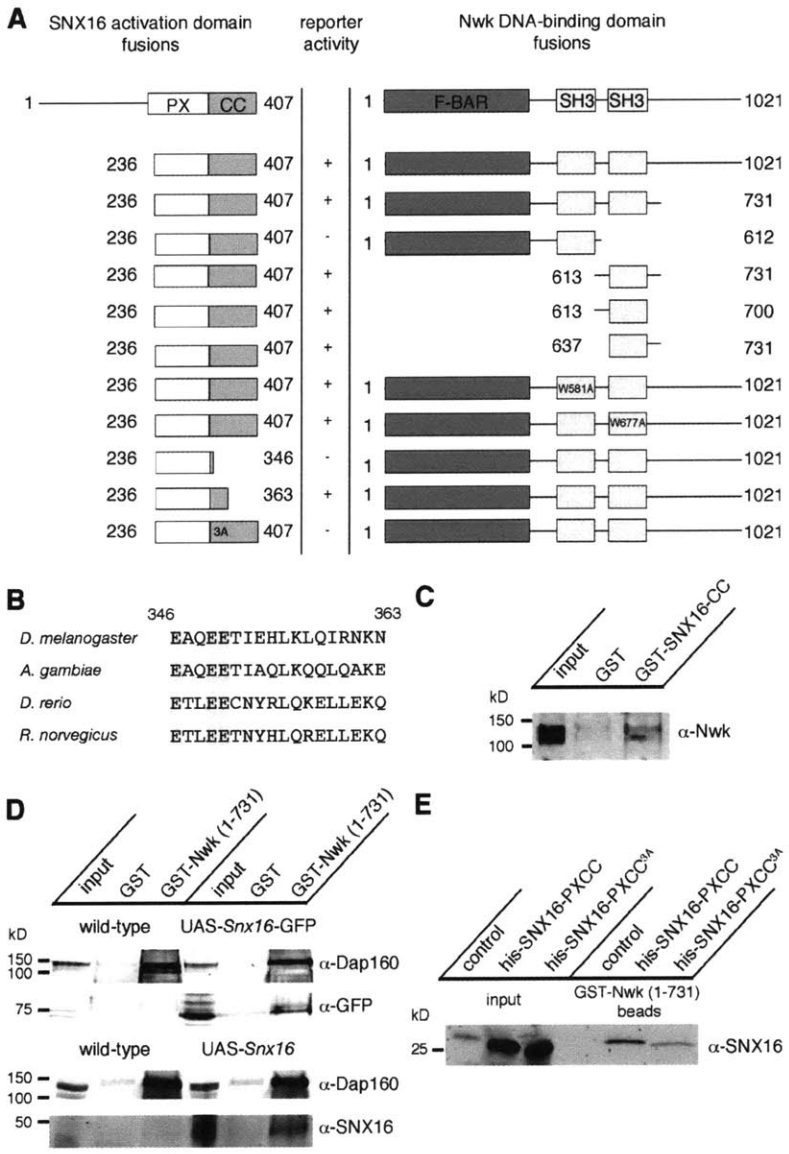
A
SNX16 activation domain fusions
reporter activity
Nwk DNA-binding domain fusions
PX
CC
F-BAR
SH3
SH3
W581A
W677A
3A
B
346
363
D. melanogaster EAQEETIEHLKLQIRNKN
A. gambiae EAQEETIAQLKQQLQAKE
D. rerio ETLEECNYRLQKELLEKQ
R. norvegicus ETLEETNYHLQRELLEKQ
C
input
GST
GST-SNX16-CC
kD
150
100
α-Nwk
D
input
GST
GST-Nwk (1-731)
wild-type
UAS-Snx16-GFP
α-Dap160
α-GFP
UAS-Snx16
α-SNX16
E
control
his-SNX16-PXCC
his-SNX16-PXCC3A
input
GST-Nwk (1-731) beads
α-SNX16

Figure 3.1: *SNX16 physically interacts with Nwk.*

(A) Schematic of Nwk and SNX16 domain organization and summary of yeast two-hybrid interactions. **(B)** Alignment of SNX16 homologs between amino acids 346 and 363 of *Drosophila* SNX16. Accession numbers and a full SNX16 alignment are shown in Suppl. Fig. S1. Shaded glutamate residues are required for Nwk-Snx16 interactions. **(C)** GST and GST-SNX16 (335-407; coiled-coil) were used to precipitate binding partners from wild-type *Drosophila* head extracts. Equal amounts of precipitates were immunoblotted with a-Nwk antibodies. Lane 1 represents 2.5% of the input compared to experimental samples. **(D)** GST and GST-Nwk (1-731) were used to precipitate binding partners from wild-type, UAS-*Snx16*, and UAS-*Snx16*-GFP-expressing *Drosophila* head extracts. Equal amounts of precipitates were immunoblotted with a-GFP, a-SNX16, or a-Dap160 antibodies. Dap160 has previously been shown to interact with Nwk (Rodal et al. 2008, O'Connor-Giles et al., 2008). Lanes 1 and 4 represent 2% of the input compared to experimental samples. **(E)** GST-Nwk (1-731) was co-expressed in *E. coli* with empty vector, SNX16 (220-407; PX and coiled coil domains) or $SNX16^{3A}$ (220-407), precipitated on glutathione agarose, and immunoblotted with a-SNX16 antibodies.

Figure 3.2

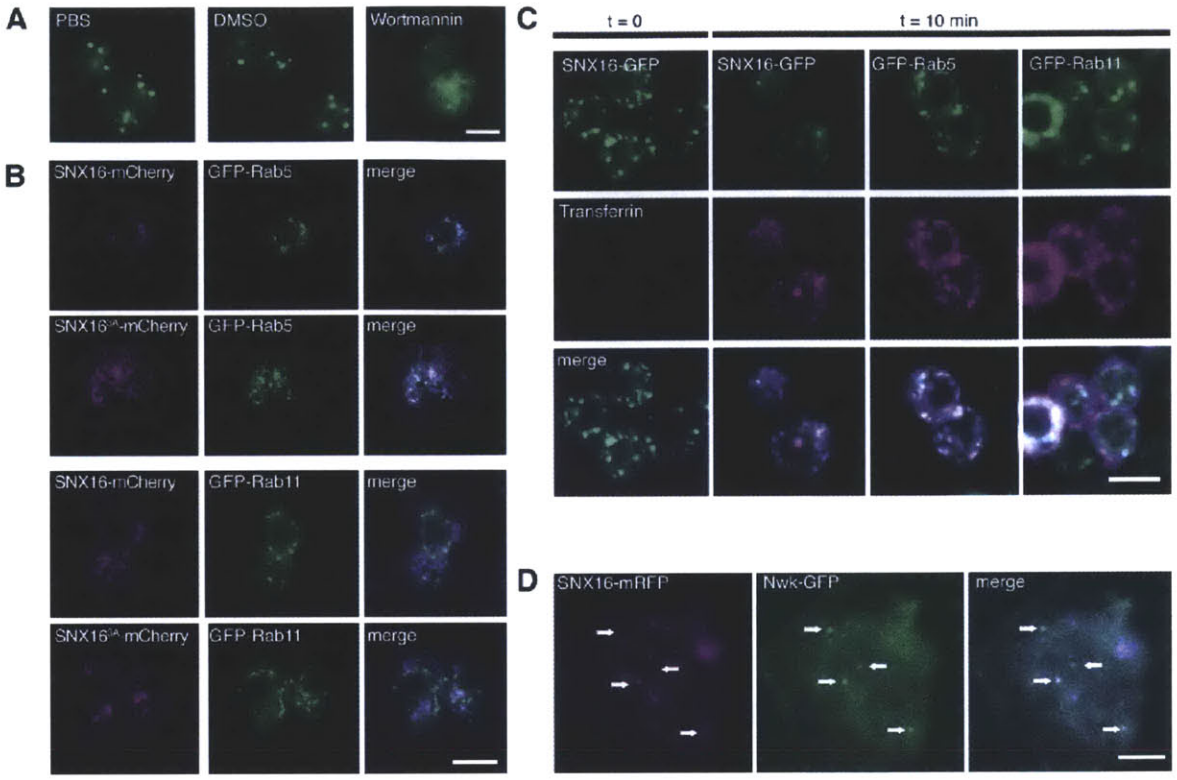
A
PBS
DMSO
Wortmannin
B
SNX16-mCherry
GFP-Rab5
merge
SNX16$^{\Delta}$-mCherry
GFP-Rab5
merge
SNX16-mCherry
GFP-Rab11
merge
SNX16$^{\Delta}$-mCherry
GFP-Rab11
merge
C
t = 0
t = 10 min
SNX16-GFP
SNX16-GFP
GFP-Rab5
GFP-Rab11
Transferrin
merge
D
SNX16-mRFP
Nwk-GFP
merge

Figure 3.2: *SNX16 localizes to Rab5-positive early endosomes.*

Scale bars are 10 mm. **(A)** Kc167 cells transfected with *Snx16*-GFP were treated with wortmannin, then fixed and imaged by confocal microscopy. Single confocal sections are shown. **(B)** S2 cells transfected with the indicated constructs were spread on Concanavalin A, fixed, and imaged. 2D projections of confocal stacks are shown. **(C)** Kc167 cells transfected with human transferrin receptor and the indicated constructs were incubated with Alexa 546-labeled transferrin for the indicated times, then fixed and imaged. Single confocal sections are shown. **(D)** Nwk localizes to a subset of SNX16 puncta. S2 cells were transfected with *Snx16*-mRFP and *nwk*-GFP and spread on Concanavalin A before fixation and imaging. A 2D projection of a confocal stack is shown.

Figure 3.3

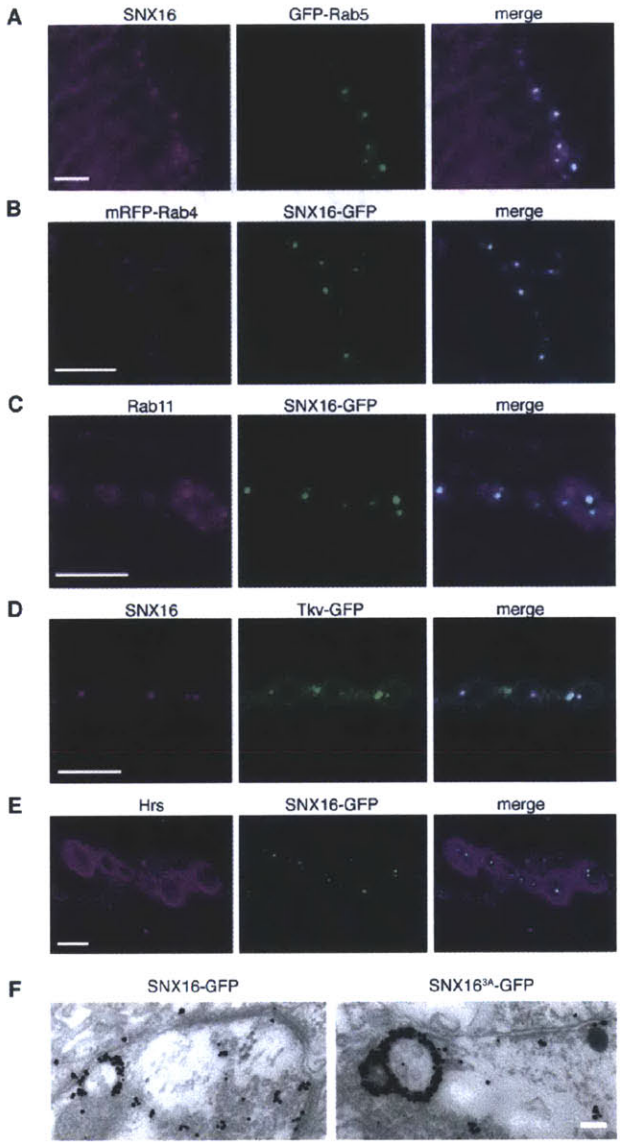
A
SNX16
GFP-Rab5
merge
B
mRFP-Rab4
SNX16-GFP
merge
C
Rab11
SNX16-GFP
merge
D
SNX16
Tkv-GFP
merge
E
Hrs
SNX16-GFP
merge
F
SNX16-GFP
SNX16^{3A}-GFP

Figure 3.3: *Localization of SNX16 to endosomes at the Drosophila NMJ.*

(A) *elav*^{C155}; UAS-*Snx16*; UAS-GFP-*Rab5* larvae stained with a-SNX16 antibodies. **(B)** *elav*^{C155}; UAS-*Snx16*-GFP; UAS-mRFP-*Rab4* larvae. **(C)** *elav*^{C155}; UAS-*Snx16*-GFP larvae stained with a-Rab11 antibodies. **(D)** *elav*^{C155}; UAS-*Snx16*; UAS-*tkv*-GFP larvae stained with a-SNX16 antibodies. **(E)** *elav*^{C155}; UAS-*Snx16*-GFP larvae stained with a-Hrs antibodies (also available in JCB dataviewer). **(F)** *elav*^{C155}; UAS-*Snx16*-GFP and UAS-*Snx16*^{3A}-GFP larvae stained with a-GFP antibodies and processed for immuno-electron microscopy. Scale bars 5 mm (A-E) and 100 nm (F).

Figure 3.4

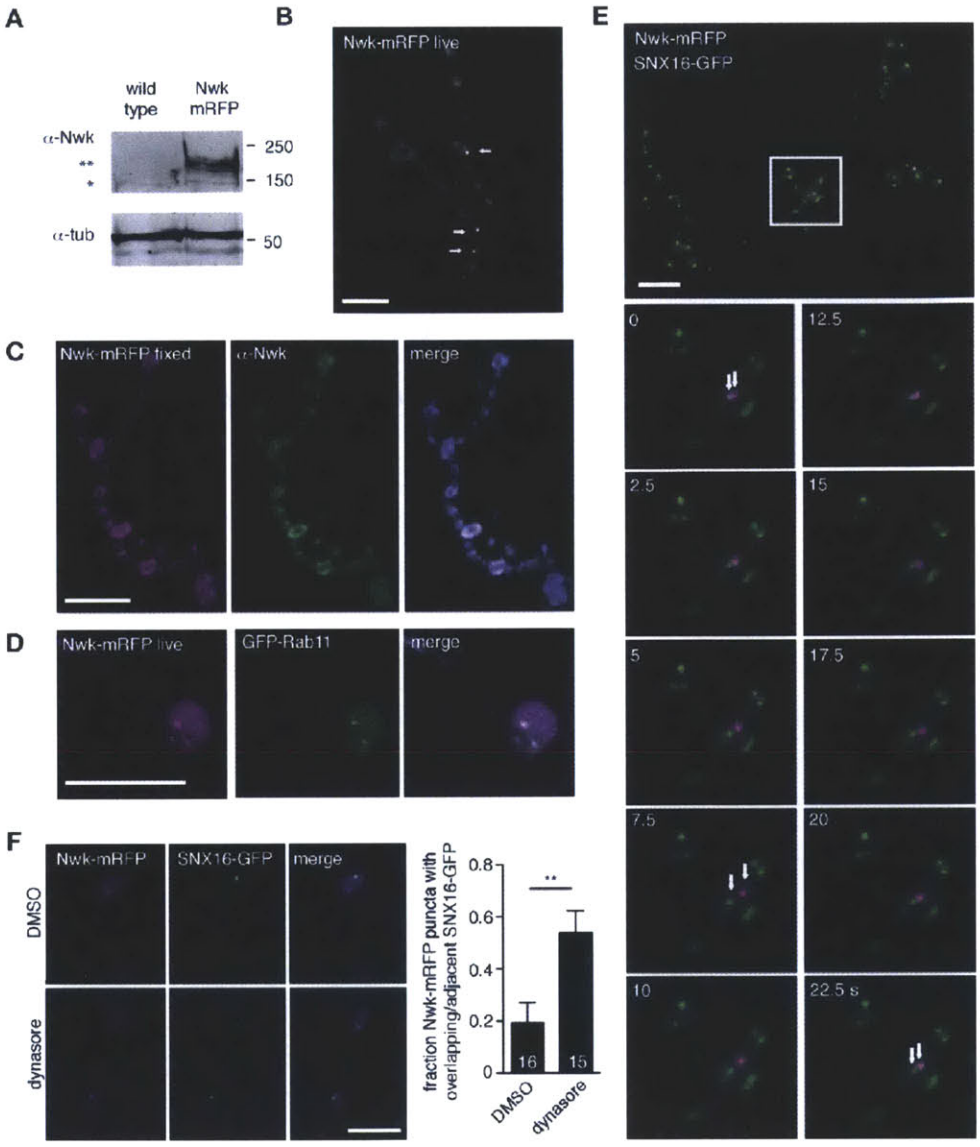
A
wild type
Nwk mRFP
α-Nwk
**
*
250
150
α-tub
50
B
Nwk-mRFP live
C
Nwk-mRFP fixed
α-Nwk
merge
D
Nwk-mRFP live
GFP-Rab11
merge
E
Nwk-mRFP
SNX16-GFP
0
12.5
2.5
15
5
17.5
7.5
20
10
22.5 s
F
Nwk-mRFP
SNX16-GFP
merge
DMSO
dynasore
fraction Nwk-mRFP puncta with overlapping/adjacent SNX16-GFP
0.8
0.6
0.4
0.2
0
**
16
15
DMSO
dynasore

Figure 3.4: *Nwk in live NMJs localizes to puncta that transiently interact with SNX16 endosomes.*

Scale bars are 10 mm. **(A)** *elav*^{C155}; Nwk-mRFP expression in a-Nwk immunoblots of *Drosophila* larval fillet extracts. Single asterisk indicates endogenous Nwk; double asterisk indicates Nwk-mRFP. **(B)** Localization of Nwk-mRFP in live 3rd instar NMJs. **(C)** Localization of Nwk-mRFP in fixed 3rd instar NMJs. Nwk collapses to discrete structures upon fixation, and Nwk puncta are not strongly detected by a-Nwk antibodies. **(D)** Nwk-mRFP puncta colocalize with GFP-Rab11 at NMJs. **(E)** Localization of Nwk-mRFP and SNX16-GFP in live 3rd instar larval NMJs. **(F)** The dynamin inhibitor dynasore drives association of Nwk and SNX16 particles. Quantification shows mean fraction of Nwk particles with a SNX16 particle within 1 mm of their center.

Figure 3.5

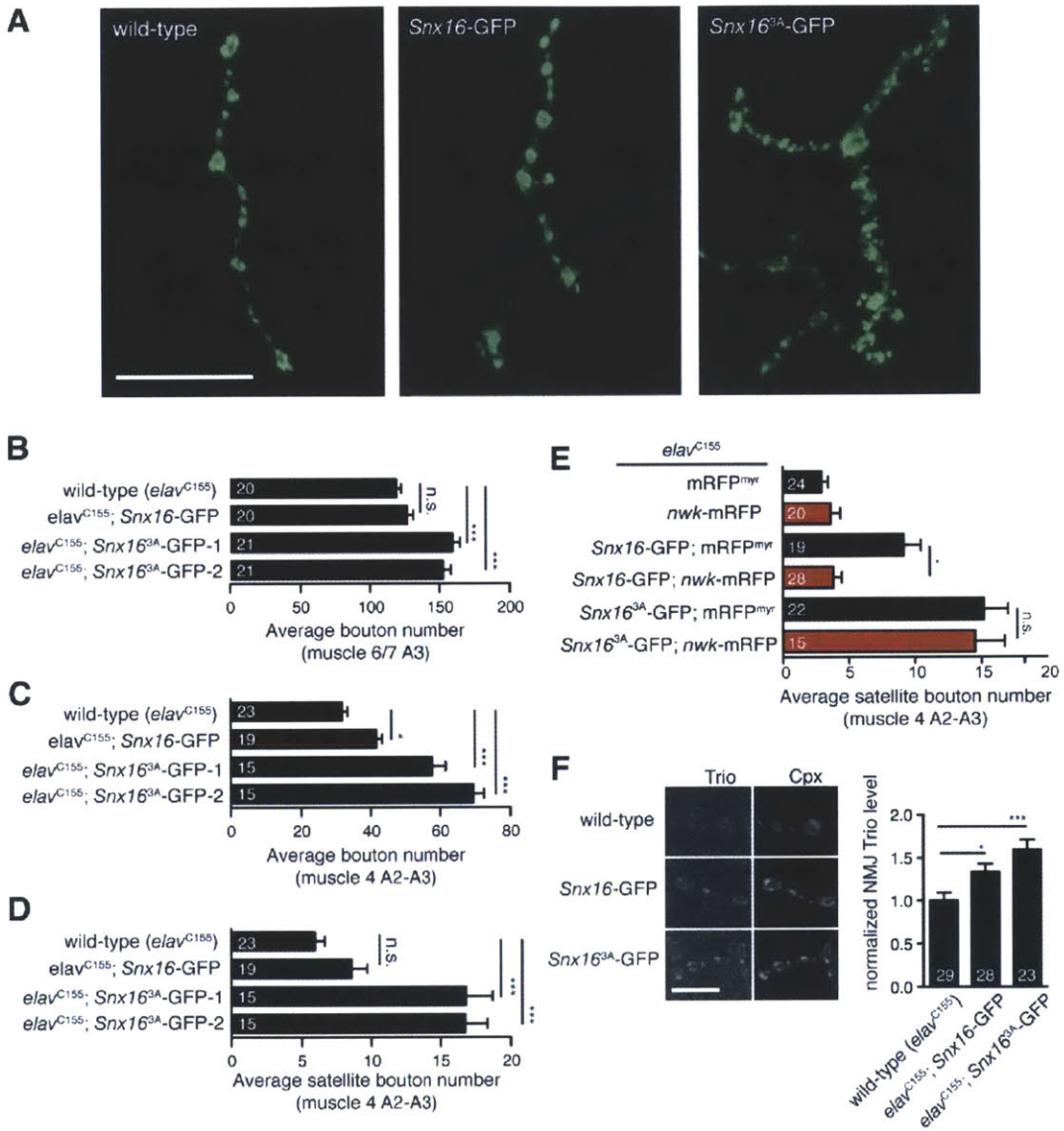
A
wild-type
Snx16-GFP
Snx16^3A-GFP
B
wild-type (elav^C155)
elav^C155; Snx16-GFP
elav^C155; Snx16^3A-GFP-1
elav^C155; Snx16^3A-GFP-2
20
20
21
21
n.s.
***
***
0
50
100
150
200
Average bouton number
(muscle 6/7 A3)
C
wild-type (elav^C155)
elav^C155; Snx16-GFP
elav^C155; Snx16^3A-GFP-1
elav^C155; Snx16^3A-GFP-2
23
19
15
15
*
***
***
0
20
40
60
80
Average bouton number
(muscle 4 A2-A3)
D
wild-type (elav^C155)
elav^C155; Snx16-GFP
elav^C155; Snx16^3A-GFP-1
elav^C155; Snx16^3A-GFP-2
23
19
15
15
n.s.
***
***
0
5
10
15
20
Average satellite bouton number
(muscle 4 A2-A3)
E
elav^C155
mRFP^myr
nwk-mRFP
Snx16-GFP; mRFP^myr
Snx16-GFP; nwk-mRFP
Snx16^3A-GFP; mRFP^myr
Snx16^3A-GFP; nwk-mRFP
24
20
19
28
22
15
*
n.s.
0
5
10
15
20
Average satellite bouton number
(muscle 4 A2-A3)
F
Trio
Cpx
wild-type
Snx16-GFP
Snx16^3A-GFP
normalized NMJ Trio level
2.0
1.5
1.0
0.5
0.0
*
***
29
28
23
wild-type (elav^C155)
elav^C155; Snx16-GFP
elav^C155; Snx16^3A-GFP

Figure 3.5: *A Nwk-binding mutant of Snx16 recapitulates the nwk phenotype.*

(A) Representative confocal projections of anti-Complexin (Cpx) staining from NMJs of the indicated genotype under the control of the *elav*^{C155} GAL4 driver. Scale bar is 20 mm. **(B)** Quantification of average bouton number for muscle 6/7. **(C)** Quantification of average bouton number for muscle 4. **(D)** Quantification of average satellite bouton number for muscle 4. **(E)** Co-overexpression of Nwk-mRFP suppresses the *Snx16* but not the *Snx16*^{3A} overexpression phenotype. **(F)** *Snx16*^{3A} overexpression increases BMP signaling. Trio protein levels are increased in muscle 6/7 NMJs. Scale bar is 5 mm.

Figure 3.6

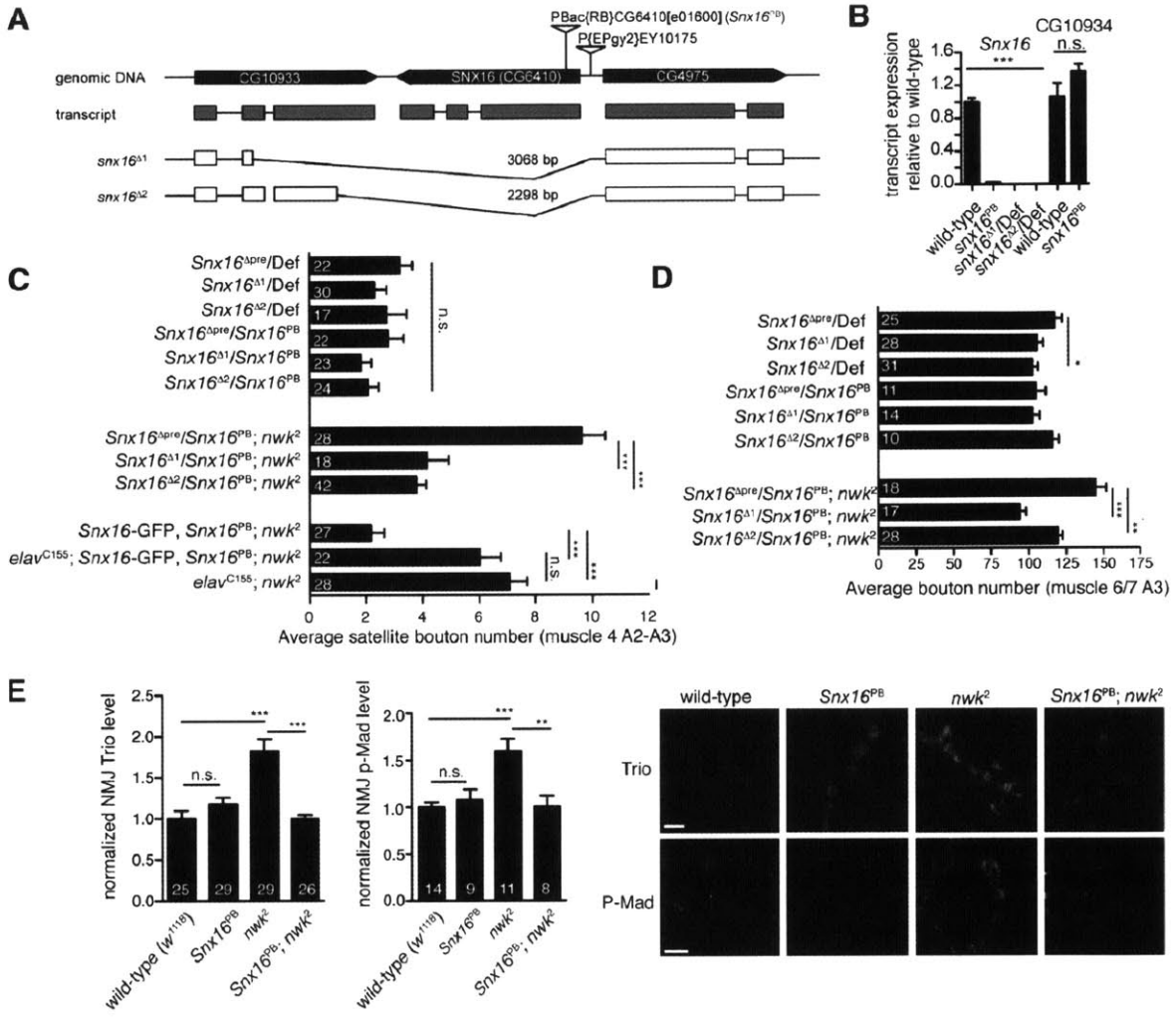
A
PBac{RB}CG6410[e01600] (Snx16^PB)
P{EPgy2}EY10175
genomic DNA
CG10933
SNX16 (CG6410)
CG4975
transcript
snx16^Δ1
3068 bp
snx16^Δ2
2298 bp
B
CG10934
Snx16
n.s.
***
transcript expression relative to wild-type
1.6
1.2
0.8
0.4
0.0
wild-type
snx16^PB
snx16^Δ1/Def
snx16^Δ2/Def
wild-type
Snx16^PB
C
Snx16^Δpre/Def 22
Snx16^Δ1/Def 30
Snx16^Δ2/Def 17
Snx16^Δpre/Snx16^PB 22
Snx16^Δ1/Snx16^PB 23
Snx16^Δ2/Snx16^PB 24
n.s.
Snx16^Δpre/Snx16^PB; nwk^2 28
Snx16^Δ1/Snx16^PB; nwk^2 18
Snx16^Δ2/Snx16^PB; nwk^2 42
***
***
Snx16-GFP, Snx16^PB; nwk^2 27
elav^C155; Snx16-GFP, Snx16^PB; nwk^2 22
elav^C155; nwk^2 28
n.s.
***
***
0 2 4 6 8 10 12
Average satellite bouton number (muscle 4 A2-A3)
D
Snx16^Δpre/Def 25
Snx16^Δ1/Def 28
Snx16^Δ2/Def 31
Snx16^Δpre/Snx16^PB 11
Snx16^Δ1/Snx16^PB 14
Snx16^Δ2/Snx16^PB 10
*
Snx16^Δpre/Snx16^PB; nwk^2 18
Snx16^Δ1/Snx16^PB; nwk^2 17
Snx16^Δ2/Snx16^PB; nwk^2 28
***
**
0 25 50 75 100 125 150 175
Average bouton number (muscle 6/7 A3)
E
normalized NMJ Trio level
2.5
2.0
1.5
1.0
0.5
0.0
***
***
n.s.
25 29 29 26
wild-type (w^1118)
Snx16^PB
nwk^2
Snx16^PB; nwk^2
normalized NMJ p-Mad level
2.0
1.5
1.0
0.5
0.0
***
**
n.s.
14 9 11 8
wild-type (w^1118)
Snx16^PB
nwk^2
Snx16^PB; nwk^2
wild-type
Snx16^PB
nwk^2
Snx16^PB; nwk^2
Trio
P-Mad

Figure 3.6: *Loss of SNX16 suppresses the nwk mutant phenotype.*

(A) Schematic of *snx16* loss-of-function mutants. **(B)** Quantitative RT-PCR of *Snx16* and *CG10934* transcript levels. **(C)** Quantification of average satellite bouton number for muscle 4 NMJs. **(D)** Quantification of average bouton number for muscle 6/7 NMJs. **(E)** Elevated BMP signaling in *nwk* NMJs is suppressed in *Snx16*; *nwk* NMJs. Scale bar is 5 mm.

Figure 3.7

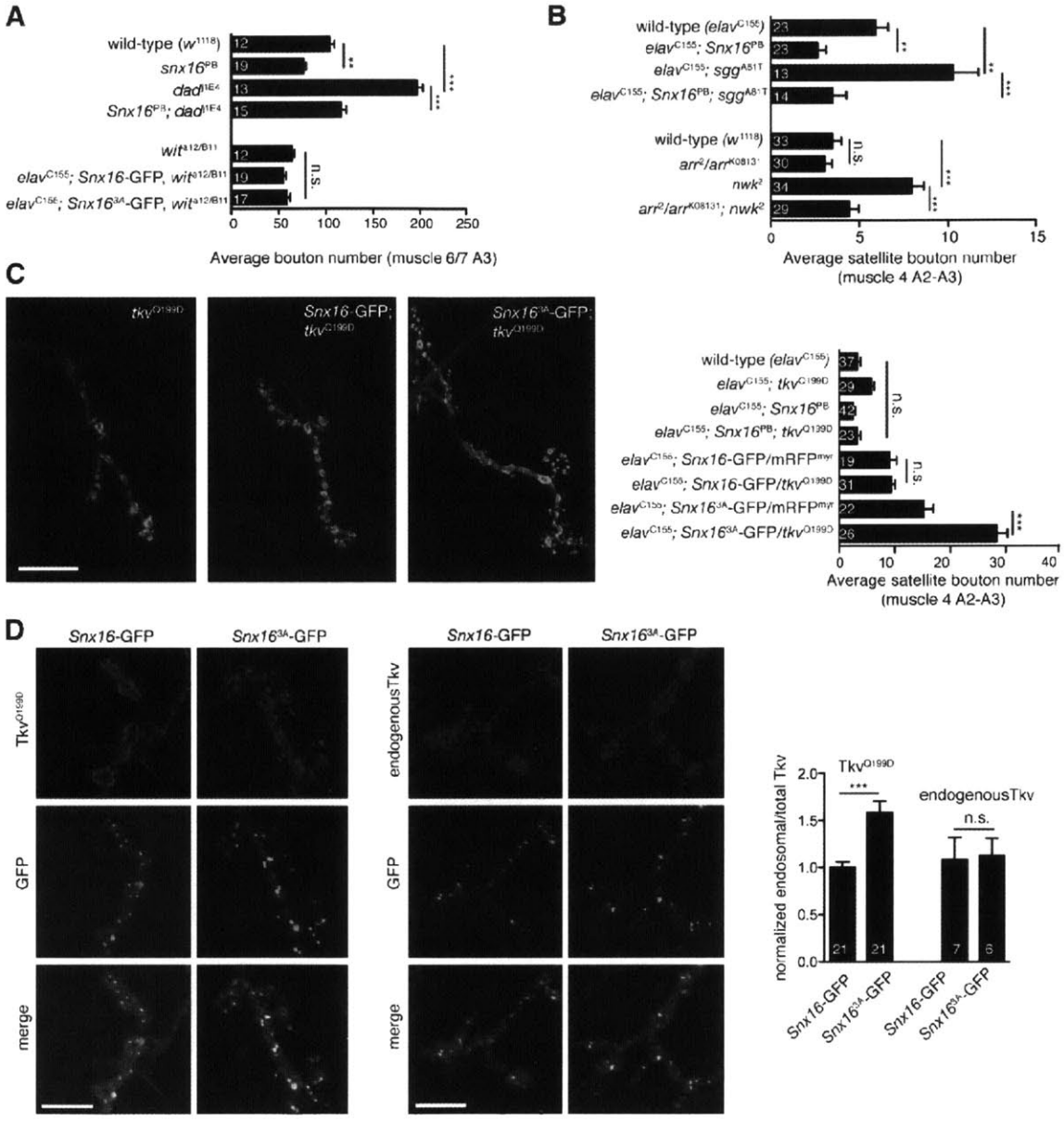
A
wild-type (w1118)
snx16PB
dad1E4
Snx16PB; dad1E4
wit12/B11
elavC155; Snx16-GFP, wit12/B11
elavC155; Snx16 3A-GFP, wit12/B11
12
19
13
15
12
19
17
n.s.
0 50 100 150 200 250
Average bouton number (muscle 6/7 A3)
B
wild-type (elavC155)
elavC155; Snx16PB
elavC155; sggA51T
elavC155; Snx16PB; sggA51T
wild-type (w1118)
arr2/arrK0813
nwk2
arr2/arrK08131; nwk2
23
23
13
14
33
30
34
29
n.s.
0 5 10 15
Average satellite bouton number
(muscle 4 A2-A3)
C
tkvQ199D
Snx16-GFP; tkvQ199D
Snx16 3A-GFP; tkvQ199D
wild-type (elavC155)
elavC155; tkvQ199D
elavC155; Snx16PB
elavC155; Snx16PB; tkvQ199D
elavC155; Snx16-GFP/mRFPmyr
elavC155; Snx16-GFP/tkvQ199D
elavC155; Snx16 3A-GFP/mRFPmyr
elavC155; Snx16 3A-GFP/tkvQ199D
37
29
42
23
19
31
22
26
n.s.
n.s.
0 10 20 30 40
Average satellite bouton number
(muscle 4 A2-A3)
D
Snx16-GFP
Snx16 3A-GFP
TkvQ199D
endogenousTkv
GFP
merge
normalized endosomal/total Tkv
0.0 0.5 1.0 1.5 2.0
TkvQ199D
endogenousTkv
***
n.s.
21
21
7
6
Snx16-GFP
Snx16 3A-GFP
Snx16-GFP
Snx16 3A-GFP

Figure 3.7: *Snx16 is required for synaptic growth mediated by BMP and Wg cascades.*

(A) Quantification of average bouton number for muscle 6/7 NMJs from larvae defective in BMP signaling. **(B)** Quantification of average satellite bouton number for muscle 4 NMJs defective in Wg signaling. **(C)** Representative confocal images of muscle 4 NMJs from *Snx16-GFP; tkv*^{Q199D} larvae and quantification of average satellite bouton number. Control UAS data are identical to Fig. 3.5E. Scale bar is 20 mm. **(D)** Localization of Tkv^{Q199D} and endogenous Tkv to Snx16-positive endosomes. Quantification shows muscle 4, segments A2-A4 a-Tkv integrated density in GFP-positive pixels relative to total NMJ a-Tkv integrated density, in single confocal sections. Scale bars are 10 mm.

Figure 3.8

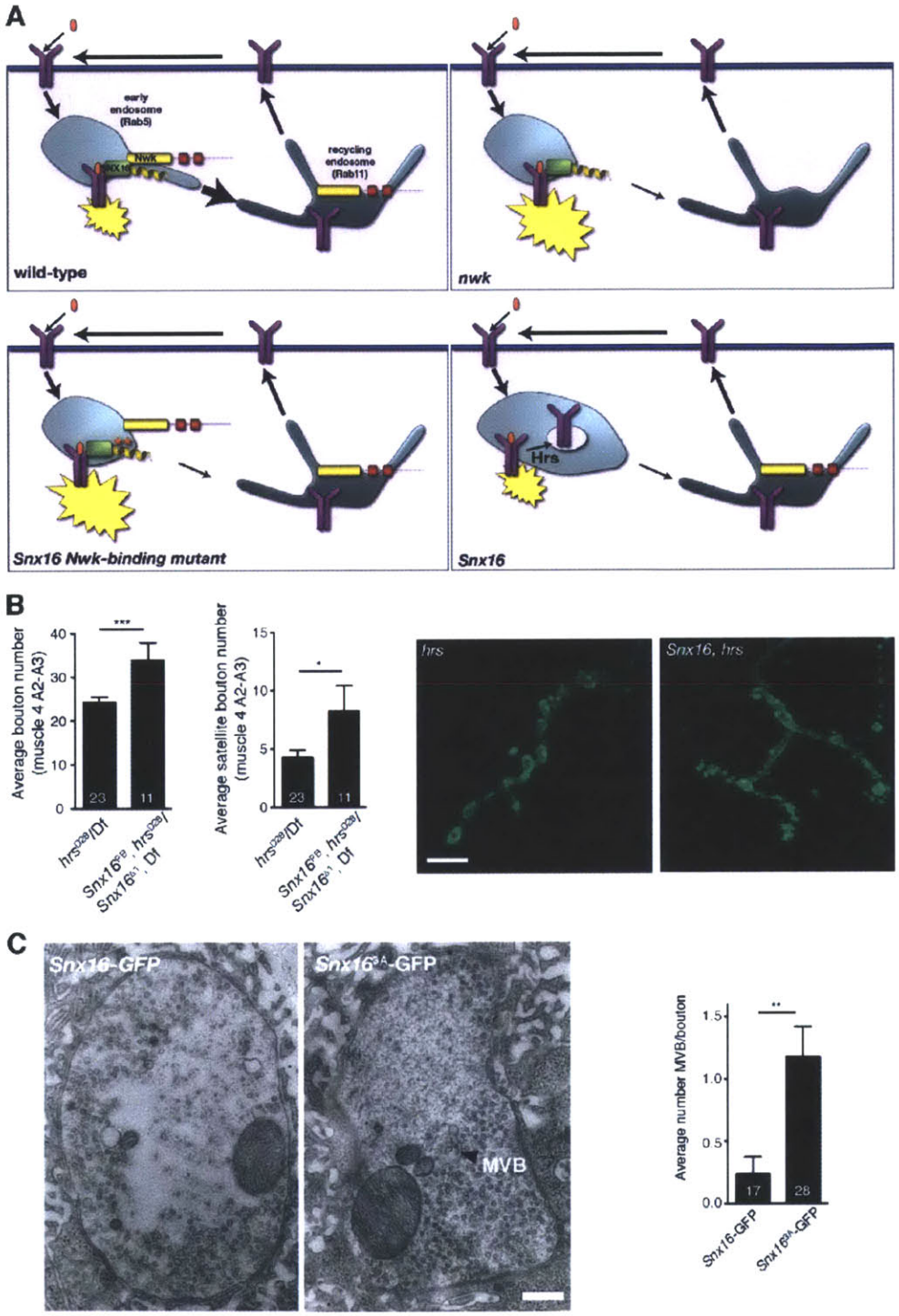
A
early endosome (Rab5)
recycling endosome (Rab11)
wild-type
nwk
Hrs
Snx16 Nwk-binding mutant
Snx16
B
Average bouton number (muscle 4 A2-A3)
Average satellite bouton number (muscle 4 A2-A3)
hrs
Snx16, hrs
C
Snx16-GFP
MVB
Average number MVB/bouton
Snx16-GFP
Snx16^3A-GFP

Figure 3.8: *A branched pathway model for attenuation of synaptic growth signals by endosomal traffic.*

(A) Model depicting how Nwk and SNX16 may drive tubulation-based sorting of synaptic growth receptors from the signal-permissive early endosome to the recycling endosome, where signaling (indicated by yellow starburst) is attenuated. In the absence of Nwk or Nwk-SNX16 interactions, receptors are retained in the early endosome. In the absence of SNX16, receptors are downregulated by internalization into the endosomal lumen. **(B)** Representative confocal images of Cpx-stained NMJs from $hrs^{D28}/Df(exel6277)$ and $Snx16^{PB}$, $hrs^{D28}/Snx16^{D1}$, $Df(exel6277)$ larvae and quantification of average bouton number. Scale bar is 10 mm. **(C)** Overexpression of $SNX16^{3A}$ increases MVB number. Electron micrographs of type 1b boutons from SNX16-GFP and $SNX16^{3A}$-GFP-expressing larvae and quantification of MVB structures. Scale bar is 200 nm.

Figure S1

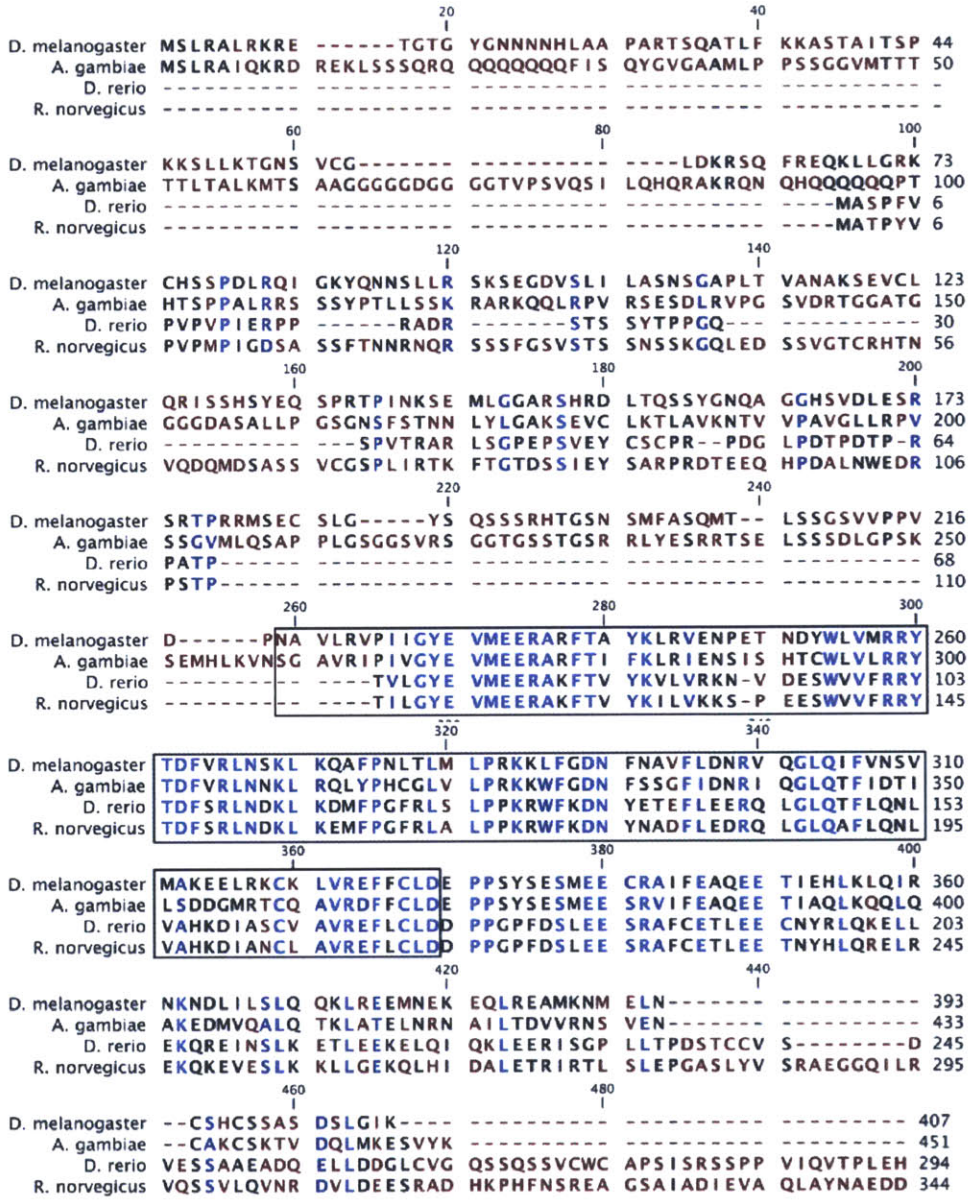

Figure S1 associated with Fig. 3.1: *Alignment of SNX16 Homologs.*

SNX16 homologs were aligned using Clustalw2 (Larkin et al., 2007). Accession numbers are XP_001688026 (*A. gambiae*), NP_991228 (*D. rerio*), and AAG25677 (*R. norvegicus*) and boxed area indicates PX domain.

Figure S2

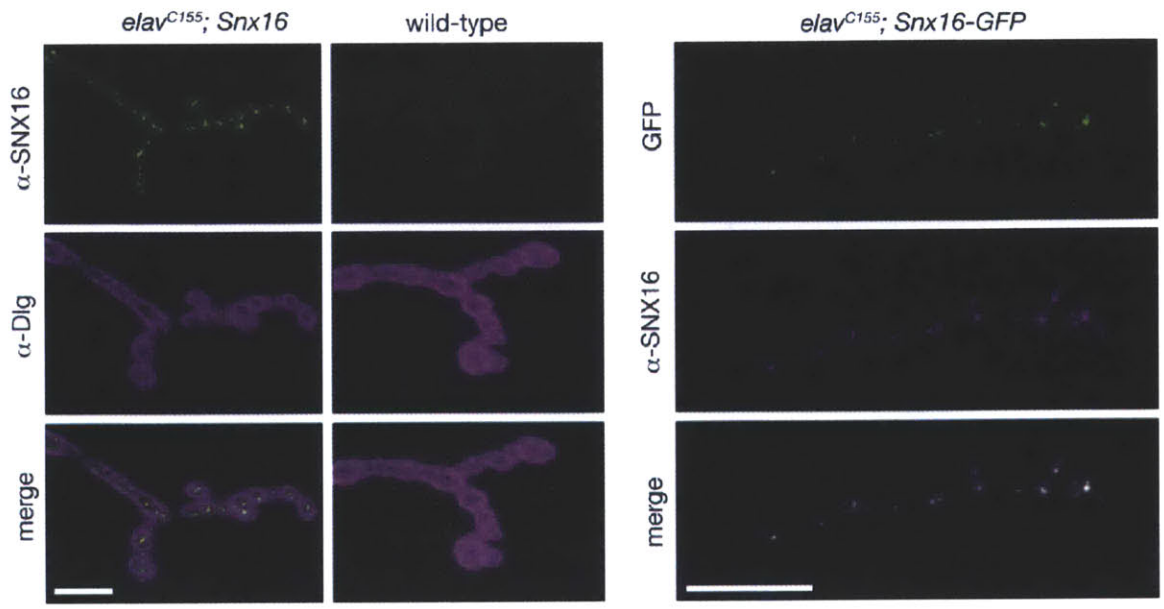

Figure S2 associated with Fig. 3.2: *Specificity of a-SNX16 antibodies.*

Third instar larvae of the indicated genotypes were stained with the indicated antibodies and imaged at muscle 4, segment A2 or A3. Left and middle panels were imaged under the identical settings. Scale bar is 10 mm.

Figure S3

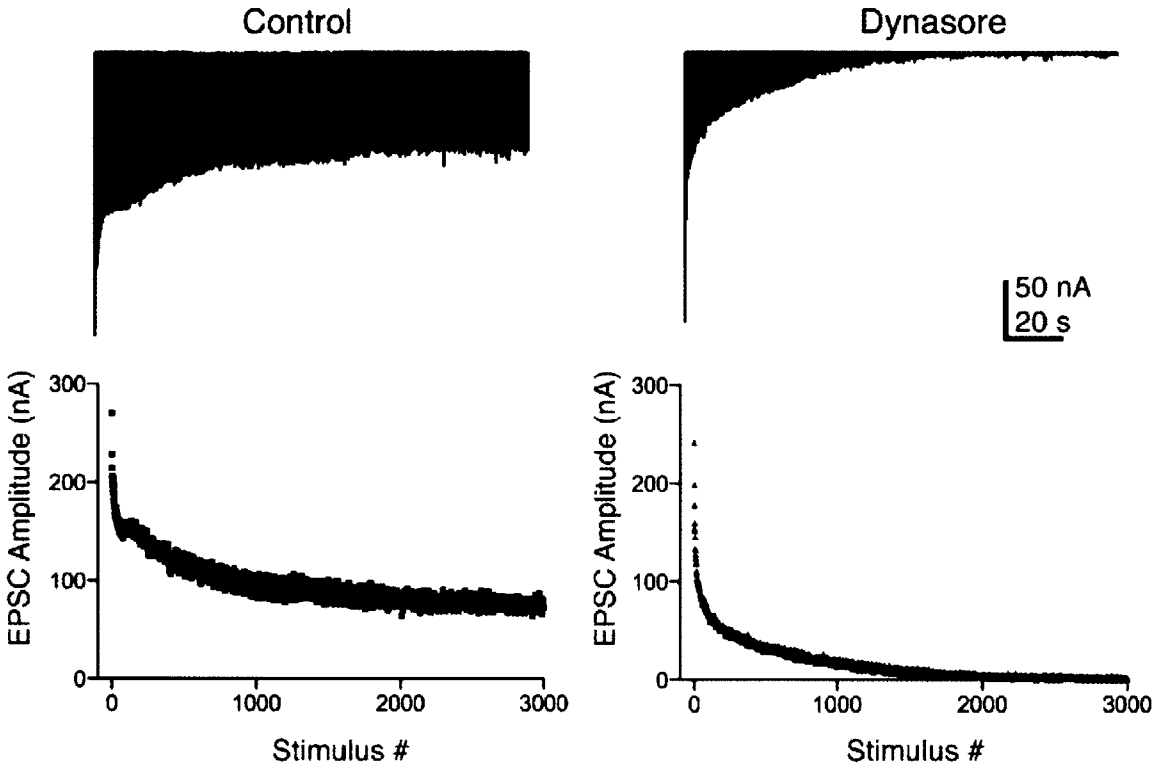

Figure S3 associated with Fig. 3.4: *Voltage-clamp recordings at the NMJ of 3rd instar larvae.*

Excitatory postsynaptic currents were elicited by stimulating the nerve at 20 Hz in DMSO (upper left panel) or dynasore-treated synapses (upper right panel). The postsynaptic current traces represent continuous tetanizing stimulus trains. Lower panels show quantification of average EPSCs in control and treated synapses (n=4 animals).

Materials and Methods

Fly stocks and generation of *Snx16* mutants

Flies were cultured using standard media and techniques. UAS-*Snx16* and UAS-*Snx16*-GFP lines were constructed in pUAST (Brand and Perrimon, 1993) carrying the *Snx16* cDNA (Berkeley *Drosophila* Genome Project clone SD19533), and point mutations were generated by site-directed mutagenesis. Sequence-verified constructs were injected into w^{1118} flies at the Duke Model Systems Transgenic Facility or at Genetic Services Inc. (Cambridge, MA). P element line p(EPgy2)EY10175, carrying an insertion 39 bp 5' to the Snx16 start codon, was isogenized and crossed to *w; P/CyOD2-3* to mobilize the insertion. Approximately 500 candidate white-eyed lines were tested by PCR across the P element insertion site and *snx16D* lines and a precise excision ($Snx16^{Dpre}$) were verified by sequencing across the deletion. Nwk-mRFP and Tkv^{Q199D} lines were obtained from K. O'Connor-Giles, and Tkv-GFP flies from M. Gonzalez-Gaitan.

RT-PCR

Quantitative RT-PCR was carried out using an Applied Biosystems 7300 Real-Time PCR System. Total RNA was extracted from 10-15 adult flies per sample, single stranded cDNA was synthesized, and PCR was carried out in triplicate for each of two independent total RNA samples per genotype using QuantiTect SYBR Green PCR Master Mix (Qiagen). A final dissociation step was carried out to evaluate product integrity, and reaction samples were run on a

1.2% agarose gel and stained with ethidium bromide. The primer sequences were as follows: *Act88F* 5'-ACTTCTGCTGGAAGGTGGAC-3' and 5'-ATCCGCAAGGATCTGTATGC-3', *Snx16* 5'-ACTGCGCGAGGAGATGAACGA-3' and 5'-CTCCGATTGGCGAAGGTCTACT-3', and *CG10934* 5'-TGAAAGAGCAGAGCCAACACG-3' and 5'-CGACACAACGCTCTTCTTCTTCTC-3'.

Antibodies

A fragment of *Snx16* encoding amino acids 230-408 was cloned into pGEX-4T (Promega), expressed in BL21(DE3) *E. coli,* and purified from sarkosyl-solubilized extracts using glutathione agarose, followed by re-solubilization in Triton X-100 (Frangioni and Neel, 1993). The purified fusion protein was dialyzed into phosphate-buffered saline (PBS) and injected into guinea pigs (Invitrogen, Inc). Guinea pig sera were then affinity purified against a His-tagged fragment of SNX16 encoding amino acids 335-407, purified as previously described for His-tagged WASp WH1 domain using the antigen immobilized on nitrocellulose (Rodal et al., 2008), and used at 1:250 for immunohistochemistry (IHC) and at 1:1000 for immunoblots (IB). a-Tkv antibodies (1:200 IHC) were provided by M.B. O'Connor. a-Nwk antibody #970 (1:1000 IHC, 1:2000 IB; Coyle et al., 2004), a-Dap160 (1:20,000 IB; Roos and Kelly, 1998), polyclonal a-mRFP (1:250 IHC; Clontech), a-GFP (1:1000 IB; Abcam), a-Hrs (1:1000 IHC; Lloyd et al., 2002), a-phospho-Mad PS1 (1:1000 IHC; Persson et al., 1998)) a–Trio (1:10 mAb supernatant IHC; Awasaki et al., 2000)) and a-Rab11 (1:100 IHC; Khodosh et al.,

2006) antibodies have been described previously. Secondary antibodies for imaging were conjugated to Cy2 or Rhodamine Red-X (Jackson Immunoresearch).

Yeast two-hybrid and GST pull-down assays

Yeast two-hybrid assays were conducted using the Matchmaker system (Clontech, Mountain View, CA). Full-length Nwk was cloned into pAS2-1, transformed into yeast strain AH109, and used to screen $1.5x10^6$ transformants of a pACT2 Matchmaker library generated from whole *Drosophila* adult cDNA (Clontech) for growth on minimal media lacking leucine, tryptophan, histidine, and adenine. Candidate colonies were further selected for growth on the above media containing 10 mM 3-aminotriazole. DNA from colonies passing this secondary screen was purified and retransformed into AH109 yeast cells carrying plasmid pGBKT7-NWK. Directed two-hybrid tests were conducted with NWK constructs in pGBKT7 (Rodal et al., 2008) and *Snx16* constructs in pAct2 (Clontech). The Nwk SH3a point mutant W581A and the SH3b point mutant W677A were previously described (Rodal et al., 2008). Yeast cells containing both prey and bait constructs were selected on minimal media lacking leucine and tryptophan, then restruck on plates lacking histidine and containing 3-aminotriazole. Yeast colonies were scored for growth after 3 d at 30°C.

GST pull-down assays were conducted as previously described (Rodal et al., 2008). Briefly, GST fusions were purified from bacterial lysates in PBS with

0.5 mM dithiothreitol, and used to precipitate binding partners from wild-type and elav-Gal4^{C155}; UAS-*Snx16*-GFP or UAS-*Snx16* fly head extracts made in 25mM Tris pH 7.5, 75 mM NaCl, and 0.2% Nonidet P-40 (Fig. 3.1 C, D) or from BL21 DE3 Rosetta cells (Invitrogen) co-expressing GST-Nwk and pET28a, pET28a-*Snx16* (220-407) or pET28a-*Snx16*^{3A} (220-407) and bound to glutathione agarose in 25 mM Tris pH 7.5, and 75 mM KCl (Fig. 3.1E).

Cell Culture

rab5, *rab11*, *Snx16* and *nwk* cDNAs were tagged with mRFP, mCherry, and GFP under the control of the actin promoter or UAS sequences using Gateway technology (Invitrogen). Kc167 or S2 cells (Cherbas and Cherbas, 1998) were cultured according to standard protocols and transfected using Effectene reagent (Qiagen). Transfected cells were incubated for 2-3 d at 20°C, and then fixed for 15 min in phosphate-buffered saline containing 4% formaldehyde. Cells were washed twice with phosphate-buffered saline and imaged for mCherry or mRFP and GFP localization on a Zeiss Axioplan microscope (see below). For Figures 3.2B, 3.2C, and 3.2E, cells were spread for 1 h on coverslips coated with Concanavalin A before fixation (Rogers et al., 2003). For wortmannin experiments, cells were transfected as above, washed with phosphate-buffered saline (PBS), and treated with 100 mM wortmannin or DMSO alone as a control for 45 min before fixation and imaging. For transferrin uptake assays, Kc167 cells transfected as above with pUASt-human transferrin receptor (hTfR) (Strigini and Cohen, 2000), actin promoter-Gal4, and the

indicated constructs were incubated at room temperature with culture media containing 5 mg/ml Alexa 546-labeled transferrin (Invitrogen). Cells were washed twice with PBS, then fixed and processed as above.

Immunohistochemistry and analysis of NMJ morphology

For analysis of NMJ morphology and protein localization at the NMJ, flies were cultured at low density at 25°C. Wild-type controls for each experiment were selected to be closely genetically matched to experimental genotypes. For *hrs* and *hrs; Snx16* mutants, which survived poorly, 1st and 2nd instar larvae were transferred to grape juice plates and grown to 3rd instar. Wild-type and *Snx16* animals grew large and pupated much more quickly than *hrs* mutants under these conditions and thus were not included as controls. Wandering 3rd instar larvae were dissected in calcium-free HL3.1 saline (Feng et al., 2004) and fixed for 30 min in HL3.1 containing 4% formaldehyde before antibody staining.

Larvae were mounted in 70% glycerol in PBS and imaged at room temperature on a Zeiss Axioplan microscope equipped with a LSM510 laser scanning head and oil-immersion 40x n.a. 1.3 or 100x n.a. 1.3 objectives. Images were acquired with Pascal software. For analysis of NMJ morphology, NMJs on muscle 6/7, segment A3 and muscle 4, segments A2-A3 were selected for analysis. NMJs were stained with a-Cpx and Cy2-conjugated secondary antibodies (Huntwork and Littleton, 2007) and a-Dlg and Rhodamine Red-X-conjugated secondary antibodies (Parnas et al., 2001). Both type 1b and type 1s

boutons were quantified on muscle 6/7. Only type Ib innervation, delineated by extensive postsynaptic anti-Dlg staining, was quantified on muscle 4. Satellite boutons were defined as strings of five or fewer boutons extending from the main axis of the NMJ.

For dynasore experiments, dissected larvae were incubated for 10 minutes in HL3.1 with 90 mM KCl and 2 mM $CaCl_2$ (Verstreken et al., 2008) and 100 mm dynasore (Sigma) in 0.2% DMSO, or 0.2% DMSO alone. High potassium solution was used to ensure that all synaptic dynamin was cycled through a blockable state by stimulating complete synaptic vesicle release and re-uptake (Ramaswami et al., 1994). Animals were briefly washed in HL3.1, then fixed for 30 minutes in HL3.1 with 4% formaldehyde before imaging by laser scanning confocal microscopy (note that fixation without detergent extraction preserves Nwk puncta).

Live imaging

Wandering 3rd instar larvae expressing *Snx16*-GFP and *nwk*-mRFP under the control of the pan-neuronal GAL4 driver $elav^{C155}$ were dissected as above, mounted in HL3.1 under a coverslip, and imaged at room temperature with a 63x n.a. 1.4 objective on a Zeiss Observer Z1 microscope equipped with a Yokagawa CSU-X1 spinning disk confocal head and a QuantEM 512SC EMCCD camera (3I, Inc.). Confocal stacks of NMJs were collected at a frame rate of approximately 1 stack/2.5 sec. Movies were created from maximum intensity projections of these

stacks using SlideBook software (3I, Inc.) and displayed at 10x live speed.

Electron Microscopy

Wandering 3rd instar larvae expressing *Snx16*-GFP or *Snx16*^{3A}-GFP were dissected, fixed, and processed for electron microscopy as previously described (Akbergenova and Bykhovskaia, 2009). Briefly, filleted larvae were fixed in 1% glutaraldehyde, 4% formaldehyde, 0.1 M sodium cacodylate for 2 h at room temperature and then 4°C overnight. After washing in 0.1 M sodium cacodylate, 0.1 M sucrose, samples were post-fixed for 1 h in 1% osmium tetroxide, dehydrated through a graded series of ethanol and acetone, and embedded in Embed 812 epoxy resin (Electron Microscopy Sciences). Thin sections (70–90 nm) were collected on Formvar/carbon coated copper slot grids, and contrasted with lead citrate. For immuno-EM, samples were fixed for 20 min in 4% paraformaldehyde in PBS, blocked for 1 h in 1% BSA in PBS, followed by incubation for 3 h in a-GFP ab6556 (Abcam) and then 2 h in a doubly-conjugated Alexa Fluor 594 and 1.4 nm nanogold secondary antibody (Nanoprobes). The gold signal was enhanced for 7 min using Gold Enhance (Nanoprobes), followed by a second 1 h fixation in 1% glutaraldehyde and 4% paraformaldehyde, and then embedded and sectioned as above. Thin sections (70-90 nm) were imaged at 80 kV on an FEI Tecnai G2 Spirit electron microscope equipped with an AMT CCD camera. Type 1b boutons with small clear vesicles (Atwood et al., 1993; Jia et al., 1993) were scored for the presence of MVBs.

Electrophysiology

Evoked postsynaptic currents were recorded from segment A3, muscle 6 in 3rd instar larvae using two-electrode voltage-clamp (OC-725, Warner Instruments, Hamden, CT) at -80 mV holding potential (Acharya et al., 2006; Barber et al., 2009). All experiments were performed in modified HL3 solution (70 mM NaCl, 5mM KCl, 4 mM $MgCl_2$, 2 mM $CaCl_2$, 10 mM NaHCO3, 115 mM sucrose, 5 mM HEPES, pH 7.2). Animals were pre-treated with 100 mm dynasore or DMSO control for 3-5 minutes prior to beginning stimulation and recording, and dynasore or DMSO were present throughout the recording. Data acquisition and analysis were performed using pClamp software (Axon Instruments, Foster City). For stimulation, nerves were cut close to the ventral ganglion and sucked into a pipette filled with working solution. The nerve was stimulated at 20Hz using a programmable pulse stimulator (Master-8, A. M. P. I., Jerusalem, Israel).

Image and Statistical Analyses

All image analysis was performed in Image J, and quantitative co-localization was performed using the JaCOP plugin (Bolte and Cordelieres, 2006). For quantification of Trio protein levels from 2D projections of confocal stacks, mean Trio and Cpx levels were measured within Cpx-positive NMJs on muscle 6/7, segments A2-A4. Muscle background mean intensity for both signals was also measured and subtracted from the NMJ measurement. Mean background-

subtracted Trio intensity was then normalized to background-subtracted mean Cpx intensity. Mean Cpx intensity did not vary between genotypes. Phospho-Mad intensities were measured within a-Csp (Cysteine-string protein (Zinsmaier et al., 1994))-positive NMJs. For quantification of Tkv localization, SNX16-GFP pixels were selected from single confocal sections of muscle 6/7, segments A2-A4, and the integrated density of Tkv in these structures was measured relative to entire NMJ Tkv signal in the section. *Snx16*^{3A} data were separately normalized to the *Snx16* mean for either Tkv^{Q199D} or endogenous Tkv due to their different expression levels above background.

All errors shown are mean +/- s.e.m, and the number of samples averaged in each measurement in bar graphs is indicated at the base of each bar. Statistical significance was calculated using GraphPad Prism software using ANOVA followed by pairwise Tukey's tests or using student's T-tests where only two groups were compared, with * denoting $p < 0.05$, ** $p < 0.01$, and *** $p < 0.005$.

References

Acharya, U., M.B. Edwards, R.A. Jorquera, H. Silva, K. Nagashima, P. Labarca, and J.K. Acharya. 2006. *Drosophila melanogaster* Scramblases modulate synaptic transmission. *J Cell Biol.* 173:69-82.

Akbergenova, Y., and M. Bykhovskaia. 2009. Enhancement of the endosomal endocytic pathway increases quantal size. *Mol Cell Neurosci.* 40:199-206.

Atwood, H.L., C.K. Govind, and C.F. Wu. 1993. Differential ultrastructure of synaptic terminals on ventral longitudinal abdominal muscles in *Drosophila* larvae. *J Neurobiol.* 24:1008-24.

Awasaki, T., M. Saito, M. Sone, E. Suzuki, R. Sakai, K. Ito, and C. Hama. 2000. The *Drosophila* trio plays an essential role in patterning of axons by regulating their directional extension. *Neuron.* 26:119-31.

Ball, R.W., M. Warren-Paquin, K. Tsurudome, E.H. Liao, F. Elazzouzi, C. Cavanagh, B.S. An, T.T. Wang, J.H. White, and A.P. Haghighi. 2010. Retrograde BMP signaling controls synaptic growth at the NMJ by regulating trio expression in motor neurons. *Neuron.* 66:536-49.

Barber, C.F., R.A. Jorquera, J.E. Melom, and J.T. Littleton. 2009. Postsynaptic regulation of synaptic plasticity by synaptotagmin 4 requires both C2 domains. *J Cell Biol.* 187:295-310.

Bolte, S., and F.P. Cordelieres. 2006. A guided tour into subcellular colocalization analysis in light microscopy. *J Microsc.* 224:213-32.

Bonifacino, J.S., and R. Rojas. 2006. Retrograde transport from endosomes to the *trans*-golgi network. *Nat Rev Mol Cell Biol.* 7:568-79.

Brand, A.H., and N. Perrimon. 1993. Targeted gene expression as a means of altering cell fates and generating dominant phenotypes. *Development.* 118:401-15.

Cherbas, L., and P. Cherbas. 1998. Cell culture. *In Drosophila*: A practical approach D.B. Roberts, editor. IRL Press, Oxford,.

Choi, J.H., W.P. Hong, M.J. Kim, J.H. Kim, S.H. Ryu, and P.G. Suh. 2004. Sorting nexin 16 regulates EGF receptor trafficking by phosphatidylinositol-3-phosphate interaction with the Phox domain. *J Cell Sci.* 117:4209-18.

Cousin, M.A. 2009. Activity-dependent bulk synaptic vesicle endocytosis-a fast, high capacity membrane retrieval mechanism. *Mol Neurobiol.* 39:185-9.

Coyle, I.P., Y.H. Koh, W.C. Lee, J. Slind, T. Fergestad, J.T. Littleton, and B. Ganetzky. 2004. Nervous wreck, an SH3 adaptor protein that interacts with Wsp, regulates synaptic growth in *Drosophila*. *Neuron.* 41:521-34.

Cullen, P.J. 2008. Endosomal sorting and signalling: an emerging role for sorting nexins. *Nat Rev Mol Cell Biol.* 9:574-82.

Delgado, R., C. Maureira, C. Oliva, Y. Kidokoro, and P. Labarca. 2000. Size of vesicle pools, rates of mobilization, and recycling at neuromuscular synapses of a *Drosophila* mutant, *shibire*. *Neuron.* 28:941-53.

Dickman, D.K., Z. Lu, I.A. Meinertzhagen, and T.L. Schwarz. 2006. Altered synaptic development and active zone spacing in endocytosis mutants. *Curr Biol.* 16:591-8.

Feng, Y., A. Ueda, and C.F. Wu. 2004. A modified minimal hemolymph-like solution, HL3.1, for physiological recordings at the neuromuscular junctions of normal and mutant *Drosophila* larvae. *J Neurogenet.* 18:377-402.

Franco, B., L. Bogdanik, Y. Bobinnec, A. Debec, J. Bockaert, M.L. Parmentier, and Y. Grau. 2004. Shaggy, the homolog of glycogen synthase kinase 3, controls neuromuscular junction growth in *Drosophila*. *J Neurosci.* 24:6573-7.

Frangioni, J.V., and B.G. Neel. 1993. Solubilization and purification of enzymatically active glutathione S-transferase (pGEX) fusion proteins. *Anal Biochem.* 210:179-87.

Frost, A., V.M. Unger, and P. De Camilli. 2009. The BAR domain superfamily: membrane-molding macromolecules. *Cell.* 137:191-6.

Fuchs, U., G. Rehkamp, O.A. Haas, R. Slany, M. Konig, S. Bojesen, R.M. Bohle, C. Damm-Welk, W.D. Ludwig, J. Harbott, and A. Borkhardt. 2001. The human formin-binding protein 17 (FBP17) interacts with sorting nexin, SNX2, and is an MLL-fusion partner in acute myelogeneous leukemia. *Proc Natl Acad Sci U S A.* 98:8756-61.

Hanson, B.J., and W. Hong. 2003. Evidence for a role of SNX16 in regulating traffic between the early and later endosomal compartments. *J Biol Chem.* 278:34617-30.

Hoodless, P.A., T. Haerry, S. Abdollah, M. Stapleton, M.B. O'Connor, L. Attisano, and J.L. Wrana. 1996. MADR1, a MAD-related protein that functions in BMP2 signaling pathways. *Cell.* 85:489-500.

Huntwork, S., and J.T. Littleton. 2007. A complexin fusion clamp regulates spontaneous neurotransmitter release and synaptic growth. *Nat Neurosci.* 10:1235-7.

Jia, X.X., M. Gorczyca, and V. Budnik. 1993. Ultrastructure of neuromuscular junctions in *Drosophila*: comparison of wild type and mutants with increased excitability. *J Neurobiol.* 24:1025-44.

Khodosh, R., A. Augsburger, T.L. Schwarz, and P.A. Garrity. 2006. Bchs, a BEACH domain protein, antagonizes Rab11 in synapse morphogenesis and other developmental events. *Development.* 133:4655-65.

Lloyd, T.E., R. Atkinson, M.N. Wu, Y. Zhou, G. Pennetta, and H.J. Bellen. 2002. Hrs regulates endosome membrane invagination and tyrosine kinase receptor signaling in *Drosophila*. *Cell.* 108:261-9.

Macia, E., M. Ehrlich, R. Massol, E. Boucrot, C. Brunner, and T. Kirchhausen. 2006. Dynasore, a cell-permeable inhibitor of dynamin. *Dev Cell.* 10:839-50.

Marques, G., and B. Zhang. 2006. Retrograde signaling that regulates synaptic development and function at the *Drosophila* neuromuscular junction. *Int Rev Neurobiol.* 75:267-85.

McCabe, B.D., G. Marques, A.P. Haghighi, R.D. Fetter, M.L. Crotty, T.E. Haerry, C.S. Goodman, and M.B. O'Connor. 2003. The BMP homolog Gbb provides a retrograde signal that regulates synaptic growth at the *Drosophila* neuromuscular junction. *Neuron.* 39:241-54.

Mettlen, M., T. Pucadyil, R. Ramachandran, and S.L. Schmid. 2009. Dissecting dynamin's role in clathrin-mediated endocytosis. *Biochem Soc Trans.* 37:1022-6.

Miech, C., H.U. Pauer, X. He, and T.L. Schwarz. 2008. Presynaptic local signaling by a canonical wingless pathway regulates development of the *Drosophila* neuromuscular junction. *J Neurosci.* 28:10875-84.

O'Connor-Giles, K.M., L.L. Ho, and B. Ganetzky. 2008. Nervous Wreck interacts with Thickveins and the endocytic machinery to attenuate retrograde BMP signaling during synaptic growth. *Neuron.* 58:507-518.

Packard, M., E.S. Koo, M. Gorczyca, J. Sharpe, S. Cumberledge, and V. Budnik. 2002. The *Drosophila* Wnt, wingless, provides an essential signal for pre- and postsynaptic differentiation. *Cell.* 111:319-30.

Parnas, D., A.P. Haghighi, R.D. Fetter, S.W. Kim, and C.S. Goodman. 2001. Regulation of postsynaptic structure and protein localization by the Rho-type guanine nucleotide exchange factor dPix. *Neuron.* 32:415-24.

Persson, U., H. Izumi, S. Souchelnytskyi, S. Itoh, S. Grimsby, U. Engstrom, C.H. Heldin, K. Funa, and P. ten Dijke. 1998. The L45 loop in type I receptors for TGF-beta family members is a critical determinant in specifying Smad isoform activation. *FEBS Lett.* 434:83-7.

Pylypenko, O., R. Lundmark, E. Rasmuson, S.R. Carlsson, and A. Rak. 2007. The PX-BAR membrane-remodeling unit of sorting nexin 9. *EMBO J.* 26:4788-800.

Raiborg, C., H. Stenmark, and M. 26;. 2009. The ESCRT machinery in endosomal sorting of ubiquitylated membrane proteins. *Nature*. 458:445-52.

Ramaswami, M., K.S. Krishnan, and R.B. Kelly. 1994. Intermediates in synaptic vesicle recycling revealed by optical imaging of *Drosophila* neuromuscular junctions. *Neuron*. 13:363-75.

Rao, Y., Q. Ma, A. Vahedi-Faridi, A. Sundborger, A. Pechstein, D. Puchkov, L. Luo, O. Shupliakov, W. Saenger, and V. Haucke. 2010. Molecular basis for SH3 domain regulation of F-BAR-mediated membrane deformation. *Proc Natl Acad Sci U S A*. 107:8213-8.

Rieckhof, G.E., M. Yoshihara, Z. Guan, and J.T. Littleton. 2003. Presynaptic N-type calcium channels regulate synaptic growth. *J Biol Chem*. 278:41099-108.

Rodal, A.A., R.M. Motola-Barnes, and J.T. Littleton. 2008. Nervous Wreck and Cdc42 cooperate to regulate endocytic actin assembly during synaptic growth. *J. Neurosci*. 28:8316-25.

Rodal AA, Blunk AD, Akbergenova Y, Jorquera RA, Buhl LK, Littleton JT (2011) A presynaptic endosomal trafficking pathway controls synaptic growth signaling. J Cell Biol 193:201–217.

Rogers, S.L., U. Wiedemann, N. Stuurman, and R.D. Vale. 2003. Molecular requirements for actin-based lamella formation in *Drosophila* S2 cells. *J Cell Biol*. 162:1079-88.

Roos, J., and R.B. Kelly. 1998. Dap160, a neural-specific Eps15 homology and multiple SH3 domain-containing protein that interacts with *Drosophila* dynamin. *J Biol Chem*. 273:19108-19.

Roos, J., and R.B. Kelly. 1999. The endocytic machinery in nerve terminals surrounds sites of exocytosis. *Curr Biol*. 9:1411-4.

Sadowski, L., I. Pilecka, and M. Miaczynska. 2008. Signaling from endosomes: Location makes a difference. *Exp Cell Res*. 315:1601-9.

Sone, M., E. Suzuki, M. Hoshino, D. Hou, H. Kuromi, M. Fukata, S. Kuroda, K. Kaibuchi, Y. Nabeshima, and C. Hama. 2000. Synaptic development is controlled in the periactive zones of *Drosophila* synapses. *Development*. 127:4157-68.

Strigini, M., and S. Cohen. 2000. Wingless gradient formation in the *Drosophila* wing. *Current Biology*. 10:293-300.

Sweeney, S.T., and G.W. Davis. 2002. Unrestricted synaptic growth in spinster-a late endosomal protein implicated in TGF-beta-mediated synaptic growth regulation. *Neuron*. 36:403-16.

Van Hoof, D., K.W. Rodenburg, and D.J. Van der Horst. 2005. Receptor-mediated endocytosis and intracellular trafficking of lipoproteins and transferrin in insect cells. *Insect Biochem Mol Biol.* 35:117-28.

Verstreken, P., T. Ohyama, and H.J. Bellen. 2008. FM 1-43 labeling of synaptic vesicle pools at the *Drosophila* neuromuscular junction. *Methods Mol Biol.* 440:349-69.

Wang, Q., H.Y. Kaan, R.N. Hooda, S.L. Goh, and H. Sondermann. 2008a. Structure and plasticity of Endophilin and Sorting Nexin 9. *Structure.* 16:1574-87.

Wang, X., W.R. Shaw, H.T. Tsang, E. Reid, and J. O'Kane C. 2007. *Drosophila* spichthyin inhibits BMP signaling and regulates synaptic growth and axonal microtubules. *Nat Neurosci.* 10:177-85.

Wang, Z., J.G. Edwards, N. Riley, D.W.J. Provance, R. Karcher, X.D. Li, I.G. Davison, M. Ikebe, J.A. Mercer, J.A. Kauer, and M.D. Ehlers. 2008b. Myosin Vb mobilizes recycling endosomes and AMPA receptors for postsynaptic plasticity. *Cell.* 135:535-48.

Wieser, R., J.L. Wrana, and J. Massague. 1995. GS domain mutations that constitutively activate T beta R-I, the downstream signaling component in the TGF-beta receptor complex. *EMBO J.* 14:2199-208.

Wucherpfennig, T., M. Wilsch-Brauninger, and M. Gonzalez-Gaitan. 2003. Role of *Drosophila* Rab5 during endosomal trafficking at the synapse and evoked neurotransmitter release. *J Cell Biol.* 161:609-24.

Yarar, D., M.C. Surka, M.C. Leonard, and S.L. Schmid. 2008. SNX9 activities are regulated by multiple phosphoinositides through both PX and BAR domains. *Traffic.* 9:133-46.

Yoshihara, M., B. Adolfsen, K.T. Galle, and J.T. Littleton. 2005. Retrograde signaling by Syt 4 induces presynaptic release and synapse-specific growth. *Science.* 310:858-63.

Zinsmaier, K.E., K.K. Eberle, E. Buchner, N. Walter, and S. Benzer. 1994. Paralysis and early death in cysteine string protein mutants of *Drosophila*. *Science.* 263:977-80.

CHAPTER 4

Conclusion and Future Directions

Aline Dorret Blunk

The Picower Institute of Learning and Memory, Department of Brain and Cognitive Sciences

Massachusetts Institute for Technology, Cambridge, MA 02139

4.1 Summary

Precise and rapid communication, coupled with the ability of synaptic connections to adapt to changing environmental needs, is essential for functional neuronal circuits. Thus, regulation of synapse development and plasticity is a central question in Neuroscience. In my thesis studies, I have addressed these topics by studying regulation of active zone assembly and synaptic growth using the *Drosophila* neuromuscular junction (NMJ) as a model system.

In an unbiased EMS screen of the second chromosome, we isolated new mutations that disrupt synapse organization at the NMJ. I characterized line 117B, which exhibits striking active zone and morphology phenotypes, in detail to define its role in regulation of synaptic organization. Recombination and deficiency mapping identified a point mutation in actin 57B, one of six actin genes in *Drosophila,* and the main actin of body wall muscles in larvae. PCR screening confirmed a change of the highly conserved amino acid glutamate E84 to a lysine (act^{E84K}). In act^{E84K}, active zone spacing is aberrant and quantification revealed a reduction of synapse density and an increase in unapposed active zones. The organization of the postsynaptic actin cytoskeleton is also disrupted, forming prominent actin swirls concentrating around the NMJ. This phenotype is similar to actin rearrangement observed following loss of postsynaptic β-Spectrin, an actin interactor of the CH domain superfamily. Notably, previous studies have implicated the residue mutated in act^{E84K}, glutamate E84, as part of a binding site mediating actin binding to members of this protein family. This connection,

coupled with the loss of the Spectrin-rich postsynaptic region in act^{E84K}, demonstrates a disruption of the actin-Spectrin postsynaptic cytoskeleton. This is further supported by additional similarities seen in act^{E84K} and muscle-specific β-Spectrin RNAi lines, such as mislocalization of DLG and impaired SSR formation. Functional analysis indicates a postsynaptic defect in neuronal communication, while presynaptic characteristics of neurotransmitter release are unaffected. In summary, we provide evidence that the actin cytoskeleton plays an important role in organizing the postsynaptic protein network, forming the basis for trans-synaptic signaling cascades that coordinate pre- and postsynaptic development.

Modification of synaptic strength can be achieved through regulating the number of synaptic connection at the NMJ. In my thesis work, I have also helped to uncover a key role for endosomal trafficking of activated receptor-ligand complexes as an essential step in regulation of synaptic growth signaling. Loss of proteins regulating endocytosis leads to a distinct overgrowth phenotype characterized by satellite boutons, small varicosities that sprout from the main axis of the synaptic arbor. The F-BAR family member Nervous Wreck (Nwk) is one such protein, localizing to the recycling endosome and acting as a negative regulator of synaptic growth signaling. Nwk has been shown to cooperate with the small GTPase Cdc42 to regulate actin polymerization via WASp/Arp2/3. However, the molecular mechanisms underlying its attenuating function on synaptic growth remain unknown. Using full-length Nwk as bait in a yeast-two-hybrid screen, we isolated the binding partner Sorting Nexin 16 (SNX16) and

mapped their interaction to three glutamate residues of the coiled-coil domain of SNX16 and to the second SH3 domain of Nwk. SNX16 localizes to early endosomes and multivesicular bodies (MVB), and shows transient interaction with Nwk-positive compartments at the NMJ by live imaging. Using genetic approaches, we demonstrate that Nwk negatively regulates SNX16 and that their interaction is required to regulate both BMP and Wnt signaling based synaptic growth. This suggested that upon loss of the Nwk-SNX16 interaction, location of actively signaling receptors might shift from the plasma membrane to early endosomes as their progression through the endosomal system was blocked. Indeed, activated Tkv receptor was primarily localized on endosomes versus the plasma membrane when overexpressing a SNX16 mutant protein that was unable to bind Nwk. Additionally, we provide evidence that SNX16 acts at a branch point between the recycling endosome and the MVB. Disruption of MVB formation upon loss of the ESCRT component Hrs, or trafficking to the recycling endosome via SNX16-Nwk alone does not lead to a significant phenotype. However, loss of both pathways results in synaptic overgrowth. Thus, loss of SNX16 moves trafficking to the MVB, while SNX16-Nwk interaction attenuates signaling upon loss of Hrs. In summary, our results define a presynaptic trafficking pathway mediated by SNX16, NWK and the ESCRT complex that functions to control synaptic growth signaling at the interface between endosomal compartments.

4.2 Future Directions

4.2.1 Mutation of actin 57B impairs presynaptic active zone spacing

We propose that postsynaptic actin is an important organizer of protein networks regulating active zone assembly. Although we present evidence that the phenotypes described in act^{E84K} are due to disruption of postsynaptic actin, we have been unable to definitively exclude a presynaptic contribution. The presynaptic actin cytoskeleton is known to be involved in synaptic vesicle clustering and active zone assembly [reviewed in (Nelson et al., 2013)]. In *C. elegans*, F-actin provides a link between the cell adhesion molecule SYG-1 and Neurabin-1 (NAB-1) (Chia et al., 2012). This interaction is essential for synaptic localization of NAB-1, a key initiator of active zone assembly through its recruitment of SYD-1 and SYD-2/Liprin-α. It is therefore important to show rescue by reintroducing actin 57B in act^{E84K} using muscle-specific overexpression. As discussed in Chapter 2, this has been challenging, as our generated rescue constructs may not express functional protein. However, a GFP-actin 57B transgenic protein has previously been shown to integrate into larval body wall muscle (Roper, 2005). Preliminary analysis shows its integration into the actin cytoskeleton surrounding presynaptic boutons. Tissue-specific overexpression of GFP-actin 57B should therefore rescue phenotypes observed in act^{E84K}. As actin gene expression is tightly regulated, we may not obtain full rescue. Despite this caveat, future rescue experiments will be important to exclude any possible presynaptic contribution.

4.2.2 Mutation of glutamate E84 impairs binding to members of the CH domain superfamily

Based on our results, we hypothesize that multiple protein networks are disrupted in act^{E84K}. As glutamate E84 is part of the CH domain binding site, we expect that, in addition to β-Spectrin, the interaction with α-actinin and dystrophin is disrupted. Co-immunoprecipitation from larval extracts would be ideally suited to test this hypothesis. However the expression of 5 additional, highly similar actin genes could mask loss of binding. Larval lysate will have to be prepared under conditions favoring polymerized actin, as cross-linking proteins preferentially bind F-actin. Therefore, the formation of heterogeneous filaments, containing different actin isoforms, could obscure the effect of E84K mutation. Additionally, since all actin proteins expressed in *Drosophila* only differ in a small number of residues, a specific antibody recognizing actin 57B is unavailable. Functional tagged control and mutant constructs will have to be expressed in mutant background and used for co-immunoprecipitation. Despite these caveats, this approach is favorable to an interaction assay using recombinant proteins, as actin needs multiple chaperones to fold correctly.

4.2.3 Identification of the trans-synaptic pathway affected in act^{E84K}

The most intriguing, unanswered question raised by our characterization of act^{E84K} is the trans-synaptic pathway needed to connect pre and postsynaptic organization. As discussed in Chapter 2, previous studies implicate at least two

different cell adhesion complexes as possible candidates. Teneurins and Neurexin-Neuroligin have been proposed to function in partially overlapping pathways, with Teneurins mainly organizing the pre- and post-synaptic cytoskeleton and Neurexin-Neuroligin coordinating active zone and glutamate receptor assembly (Li et al., 2007; Banovic et al., 2010; Mosca and Schwarz, 2010). As both complexes interact with the actin-spectrin cytoskeleton, actin could provide a link between these pathways. Genetic interaction analysis can reveal their function in a common signaling cascade. Preliminary results show no significant increase in unapposed active zones in heterozygote act^{E84K}/+, *ten-a*/+ and *nrx*/+. If either cell adhesion molecule functions in the same pathway as actin 57B, loss of one copy of Ten-a or Nrx in act^{E84K} mutant background should enhance the apposition phenotype.

4.2.4 Live imaging of actin dynamics during development

Live imaging of fluorescently tagged actin can provide new insights into actin dynamics during development. Regulation of the extent of the actin- and microtubule-rich areas has been shown to influence bouton number and shape (Ruiz-Canada et al., 2004). Simultaneous expression of a presynaptic membrane marker and tagged actin 57B would allow us to study how the actin cytoskeleton assembles and influences presynaptic morphology in live animals during synaptic growth. Here, it would be of special interest to generate a fluorescently tagged

act^{E84K} that yields a functional protein, in order to study whether actin swirls form dynamically and how they influence development of the synaptic arbor.

4.3 Conclusion

This work has provided new insights into regulation of synapse development and plasticity using the *Drosophila* NMJ as a model system. We demonstrate the importance of the actin cytoskeleton in establishing protein networks organizing pre- and post-synaptic specializations. Disruption of a putative binding site in actin 57B leads to aberrant synaptic morphology, as well as impaired active zone spacing and alignment. Additionally, we identify a novel binding partner of Nervous wreck, the sorting nexin SNX16, and illustrate how their interaction regulates synaptic growth signaling at the interface between early and recycling endosomes. Future research will address open questions and strengthen our understanding of regulatory mechanisms ensuring coordinated pre- and post-synaptic development.

References

Banovic D, Khorramshahi O, Owald D, Wichmann C, Riedt T, Fouquet W, Tian R, Sigrist SJ, Aberle H (2010) Drosophila neuroligin 1 promotes growth and postsynaptic differentiation at glutamatergic neuromuscular junctions. Neuron 66:724–738.

Chia PH, Patel MR, Shen K (2012) NAB-1 instructs synapse assembly by linking adhesion molecules and F-actin to active zone proteins. Nat Neurosci.

Li J, Ashley J, Budnik V, Bhat MA (2007) Crucial Role of Drosophila Neurexin in Proper Active Zone Apposition to Postsynaptic Densities, Synaptic Growth, and Synaptic Transmission. Neuron 55:741–755.

Mosca TJ, Schwarz TL (2010) The nuclear import of Frizzled2-C by Importins-β11 and α2 promotes postsynaptic development. Nat Neurosci 13:935–943.

Nelson JC, Stavoe AKH, Colón-Ramos DA (2013) The actin cytoskeleton in presynaptic assembly. celladhesion 7.

Roper K (2005) Contribution of sequence variation in Drosophila actins to their incorporation into actin-based structures in vivo. J Cell Sci 118:3937–3948.

Ruiz-Canada C, Ashley J, Moeckel-Cole S, Drier E, Yin J, Budnik V (2004) New synaptic bouton formation is disrupted by misregulation of microtubule stability in aPKC mutants. Neuron 42:567–580.